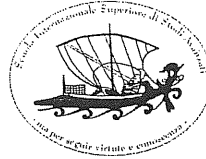




Scuola Internazionale Superiore di Studi Avanzati - Trieste

Scuola Internazionale Superiore di Studi Avanzati



QUARK AND LEPTON MASSES AND MIXING
IN SUPERSYMMETRIC GRAND UNIFIED THEORIES

Thesis submitted for the degree of
Doctor Philosophiæ

Candidate:
Michal Malinský

Supervisor:
Stefano Bertolini

Trieste, October 2005

SISSA – Via Beirut 2-4 – 34014 TRIESTE – ITALY

Contents

Notation, conventions	5
Introduction	6
1 Quark and lepton masses and mixing in Grand unified theories	14
1.1 Quarks and leptons in minimal SUSY $SU(5)$	14
1.1.1 $SU(5)$ matter fields	15
1.1.2 Higgs sector and Yukawa couplings	16
1.1.3 Minimal SUSY $SU(5)$ - parameter counting	17
1.2 Minimal SUSY $SU(5)$ shortcomings	18
1.2.1 Neutrino masses in SUSY $SU(5)$	18
1.2.2 Effective Yukawa sum-rules & quark and lepton masses and mixing	19
1.2.3 Proton decay in SUSY GUTs	20
1.2.4 Proton decay in minimal SUSY $SU(5)$	21
1.3 Quark and lepton masses and mixing in $SO(10)$ models	23
1.3.1 Matter fields in $SO(10)$ GUTs	23
1.3.2 Higgs bosons in $SO(10)$ models	24
1.3.3 Proton decay in SUSY $SO(10)$ models	27
2 Minimal renormalizable SUSY $SO(10)$ model	30
2.1 The model	30
2.1.1 The matter content	31
2.1.2 The Higgs sector	31
2.1.3 The symmetry breaking pattern	33
2.2 Basic features of the minimal SUSY $SO(10)$	33
2.2.1 Gauge coupling unification and intermediate scales	33
2.2.2 R-parity conservation	34
2.2.3 $SU(2)_L \otimes SU(2)_R$ triplets and Majorana masses of neutrinos	35
2.2.4 Electroweak Higgs doublets and Dirac masses of matter fermions	36

2.3	Minimal SUSY $SO(10)$ GUT - summary	36
2.3.1	Minimal SUSY $SO(10)$ - parameter counting	37
3	Quark and lepton masses and mixing in minimal SUSY $SO(10)$	39
3.1	Minimal SUSY $SO(10)$ Yukawa sum-rules	39
3.1.1	Light neutrino masses	40
3.1.2	Partial diagonalization and phasecounting	41
3.1.3	Number of real parameters	43
3.2	Large atmospheric mixing and $b - \tau$ unification in case of triplet dominated seesaw	45
3.3	Quark and lepton mass and mixing correlations in minimal SUSY $SO(10)$ with dominant triplet seesaw	45
3.3.1	Partial semianalytic treatment - real case	46
3.3.2	Constraints on the lepton mixing with dominant triplet seesaw	47
3.4	Numerical analysis - general prerequisites	50
3.4.1	GUT scale input parameters	50
3.4.2	Running neutrino spectrum and PMNS mixing angles	52
3.4.3	χ^2 versus direct scan	52
3.5	Numerical analysis - CP conserving Yukawa sector	53
3.6	Additional phases and CP violation	55
3.6.1	Electron mass formula and δ_{CKM} - the leading terms	56
3.6.2	Electron mass formula and δ_{CKM} - the effects of subleading terms	57
3.6.3	Comments on smallness of the Dirac CP-violating phase in the lepton sector with triplet-dominated seesaw	58
3.7	Numerical analysis - CP violating Yukawa sector	62
4	Quark and lepton masses and mixing in extensions of minimal renormalizable SUSY $SO(10)$	80
4.1	Minimal extension of minimal Yukawa sector	81
4.1.1	Effects of an additional antisymmetric Yukawa contribution	81
4.2	Adding a small Y_{120} to the minimal Yukawa sum-rules	82
4.2.1	Group-theory properties of 120_H	82
4.2.2	The model	83
4.3	Effective Yukawa sum-rules	85
4.3.1	Phasecounting	86
4.3.2	Counting all real parameters	86
4.4	Quark and lepton mass and mixing correlations	87
4.4.1	Effective sum-rules - real setup	87

4.4.2	Right-handed quark mixing matrix	88
4.4.3	Effective sum-rules - complex case	90
4.4.4	Screening effects of CKM CP violating phase in the electron mass formula	91
4.4.5	GUT scale input parameters	92
4.5	Numerical analysis - CP conserving Yukawa sector	92
4.6	Numerical analysis - CP violating Yukawa sector	94
5	$SO(10)$ models with $16_H \oplus \overline{16}_H$	98
5.1	Net effects of $16_H \oplus \overline{16}_H$	99
5.1.1	$d = 4$ proton decay	99
5.1.2	R-parity	100
5.1.3	Quark and lepton masses and mixing	100
5.2	Witten's mechanism in $SO(10)$ GUTs	101
5.2.1	Witten's mechanism in split-SUSY $SO(10)$	101
5.2.2	Problems of the split-SUSY $SO(10)$ model with pair of 10_H only - a call for 120_H	103
5.3	Cascade seesaw in models with matter singlets	105
5.4	The inverse seesaw mechanism	106
5.5	Inverse seesaw scheme in SUSY GUTs	108
5.5.1	The seesaw structure	109
5.6	Minimally finetuned SUSY $SO(10)$ inverse seesaw model	110
5.6.1	The symmetry breaking pattern	110
5.6.2	Structure of the Higgs sector	111
5.6.3	One-loop gauge coupling unification	112
5.6.4	Other physical implications	114
	Conclusions and outlook	116
	A PMNS lepton mixing matrix	119
	B $SO(10)$ group theory	121
B.1	The $SO(10)$ group	121
B.2	The $SO(10)$ spinors	121
B.3	The $SO(10)$ tensors	123
B.3.1	$SO(10)$ tensor products	123
B.4	The $SO(10)$ subgroups	124
B.4.1	Pati-Salam decomposition of basic $SO(10)$ irreps	125
B.4.2	$SU(3)_c \otimes U(1)_{B-L}$ decompositions of basic $SU(4)$ irreps	125

B.5	Origin of the -3 factors of $\overline{126}_H$ doublets	127
B.5.1	Direct decomposition of the relevant $SO(10)$ invariants	127
B.5.2	Pati-Salam approach	129
C	Antisymmetric perturbations of symmetric matrices	132
C.1	Real case	132
C.2	Complex case	133
D	Illustration of effects of 120_H on the leptonic mixing	135

Notation, conventions

Masses and couplings:

$M_\nu^s, M_\nu^t, M_M \dots$	singlet and triplet (type-I and type-II) neutrino Majorana masses
$m_\nu, M_\nu \dots$	light neutrino masses and mass matrices
m_1, m_2, m_3	light neutrino masses
$\Delta m_\odot^2, \Delta m_A^2$	neutrino oscillation solar and atmospheric mass differences
v_u, v_d	VEVs of the MSSM light Higgs doublets; $v_u/v_d \equiv \tan \beta$
$\alpha_3, \alpha_L, \alpha_R, \alpha_{B-L}$	$SU(3)_c \otimes SU(2)_L \otimes SU(2)_R \otimes U(1)_{B-L}$ couplings $\alpha \equiv g^2/4\pi$
Y_{10}, Y_{126}, Y_{120}	$SO(10)$ Yukawa couplings
$Y_5, Y_{\bar{5}}$	$SU(5)$ Yukawa couplings
$Y_{u,d,l,\nu}$	effective MSSM Yukawa couplings
$M_{10}, M_{126}, M_{120} \dots$	heavy Higgs masses
$M_G, M_R, M_{B-L} \dots$	GUT and intermediate symmetry breaking scales

Parameters:

U_{PMNS}	Pontecorvo-Maki-Nakagawa-Sakata mixing matrix
V_{CKM}	Cabibbo-Cobayashi-Maskawa mixing matrix
$\theta_{12}, \theta_{23}, \theta_{13}$	PMNS mixing angles in the lepton sector
$\delta_{PMNS}, \phi_1, \phi_2$	leptonic Dirac and Majorana CP-phases
$\phi_{12}, \phi_{23}, \phi_{13}$	quark sector mixing angles
δ_{CKM}	CKM CP-phase
J, J_{CP}	Jarlskog invariant
λ, A, ρ, η	Wolfenstein CKM parameters
$\alpha_1, \alpha_2, \alpha_3, \beta_1, \beta_2$	additional $SO(10)$ phase parameters.
$F_d, F_s, F_c \dots$	quark masses normalized to powers of λ
$c_{L,R}^{ijkl}$	Wilson coefficients of d=5 proton decay operators
$\varepsilon_{u,d,l}, \varepsilon$	perturbative parameters

Unless specified otherwise, summation over repeated greek and latin indices is always understood. The Standard Model hypercharge is normalized so that $Q = T^3 + \frac{1}{2}Y_W$. The normalization of the $U(1)_{B-L}$ charge follows the ‘‘physical’’ convention $B(\text{quark}) = 1/3$. In canonical units, $(B - L)' = \sqrt{\frac{3}{8}}(B - L)$.

Introduction

The status of the particle physics during the last thirty years could be regarded as a golden age of the Standard Model [1, 2, 3, 4]. The experimental evidence accumulated over this period, be it the the discovery of charm [5, 6] or neutral current interactions[7, 8, 9] in seventies, the direct production of the intermediate vector bosons in the middle of eighties [10, 11] and a decade of extensive precision tests in nineties [12, 13, 14] crowned by the full completion of the third matter family[15, 16, 17], confirmed the relevance of the simple $SU(3)_c \otimes SU(2)_L \otimes U(1)_Y$ spontaneously broken gauge theory to such an extend that nowadays it is often called the *Standard Theory* of elementary particle interactions rather than just a “model”.

It is rather impressive that though having originally arisen from the need to overcome the issues of the Feynman and Gell-Mann model of weak interactions [18] formulated as a description of physics in the hundred MeV range, the validity of the simple $SU(3)_c \otimes SU(2)_L \otimes U(1)_Y$ gauge scheme was not compromised even stretching the probed energy span up to the hundred GeV scale. Despite of its success it is widely believed that Standard Model can hardly be the final milestone of the road towards the complete description of all microscopic phenomena, see e.g. [19] and references therein. The theory suffers from drawbacks that can be tackled only in suitable generalizations of the minimal framework.

Perhaps the strongest motivation to go beyond the Standard Model stems from the neutrino physics. In the last decade, a significant amount of experimental information about neutrino masses and lepton mixing was accumulated. The solar and atmospheric neutrino anomalies found a successful theoretical description within the framework of the neutrino oscillations tracing back to the end of the fifties [20]. It is based on the effects of mixing among the different neutrino flavor states due to the misalignment of the mass and flavour bases that can occur when the light neutrino masses are not degenerate. Apart from the results of the LSND experiment that are still a subject of discussions, the whole plethora of the neutrino oscillation phenomena can be described in terms of 6 parameters: two mass-squared differences ($\Delta m_{\odot}^2 \equiv \Delta m_{12}^2 \equiv m_2^2 - m_1^2$

and $\Delta m_A^2 \equiv \Delta m_{23}^2 \equiv m_3^2 - m_2^2$ that give rise to the solar and atmospheric oscillation patterns respectively) and three mixing angles θ_{12} , θ_{23} and θ_{13} plus a Dirac CP phase δ_{PMNS} residing in the so called Pontecorvo-Maki-Nakagawa-Sakata (PMNS) mixing matrix U_{PMNS} , the analogue of the Cabibbo-Kobayashi-Maskawa (CKM) mixing matrix parametrizing the charged current interactions of the quarks.

The solar neutrino deficit, as well as the results of various reactor experiments like KamLAND or SNO [21, 22], are naturally understood in terms of the $\nu_e \leftrightarrow \nu_\mu$ oscillations driven by the Δm_\odot^2 and θ_{12} parameters while the atmospheric neutrino phenomena observed in the Super-Kamiokande results [23] fit the $\nu_\mu \leftrightarrow \nu_\tau$ conversion picture governed by Δm_A^2 and θ_{23} . The recent extractions from the experimental data yield at 1- σ [24]:

$$\tan^2 \theta_{12} = 0.45 \pm 0.05 \quad \sin^2 2\theta_{23} = 1.02 \pm 0.04 \quad \sin^2 2\theta_{13} < 0.05 \quad (1)$$

$$\Delta m_\odot^2 = (8.0 \pm 0.3) \times 10^{-5} \text{ eV}^2 \quad |\Delta m_A^2| = (2.5 \pm 0.3) \times 10^{-3} \text{ eV}^2$$

Unfortunately, the Dirac CP phase δ_{PMNS} is so far beyond the reach of the current experiments and the sign of the atmospheric mass-square difference is unknown. Therefore, two distinct shapes of the neutrino spectra are compatible with the recent bounds - the “normal hierarchy” case in which the state with the “minimal amount of the e -flavor” is the heaviest one, and the “inverted hierarchy” setup where such a state plays the role of the lightest one. Moreover, also the absolute scale of the neutrino masses (as well as the two additional Majorana CP phases) can not be determined by the oscillation experiments and in this respect we have only a limited information coming from the neutrinoless double beta decay experiments [25] and various cosmological bounds.

From the theoretical point of view, the neutrinos are strictly massless in the Standard Model (at the renormalizable level) due to the absence of the right-handed components that would allow for a neutrino Dirac mass term alike the case of the other matter fermions. To some extent, this can be viewed as a tautology because nothing really forbids us to add a full gauge singlet field to the SM spectrum while tuning its mass above the experimental bounds. On the other hand, such a singlet should be given a mass that is not protected by the gauge symmetry. This, of course, brings another (in principle large) scale to the SM and the model calls strongly for a generalization.

It is remarkable that this approach also provides a natural explanation for the smallness of the “active” (i.e. coupled to the Z -boson in the SM-fashion) neutrino masses. Note that the spectrum of the SM fermions spans the range from fractions of electronvolt up to almost two hundred GeV, covering more than 11 orders of magnitude. Approaching the problem of neutrino masses along the same line as the masses

of the other matter SM fermions, the relevant Yukawa couplings must be extremely hierarchical.

On the other hand, adding a singlet Majorana mass term for the right-handed neutrinos, the neutrino bilinears occupy a 6×6 matrix of the form¹

$$\mathcal{L} \ni \left(\nu_L^T, \nu_L^c \right) C^{-1} \begin{pmatrix} 0 & Y_\nu^T v \\ Y_\nu v & M_M \end{pmatrix} \begin{pmatrix} \nu_L \\ \nu_L^c \end{pmatrix} \quad (2)$$

and the renowned “seesaw” formula arising upon its diagonalization yields

$$m_\nu \sim -Y_\nu^T M^{-1} Y_\nu v^2 \quad (3)$$

To get the proper range for the light neutrino masses one can infer $M \sim 10^{12-15}$ GeV provided the neutrino Yukawa couplings are of size similar to the other Yukawas of the Standard Model. Therefore, to understand the smallness of the neutrino masses in terms of this attractive mechanism² a large new physical scale close to the 10^{12-15} GeV range appears.

Another hint about a new large fundamental scale comes from the observed phenomenon of the SM gauge coupling convergence. Remarkably enough, the effective gauge couplings subject to the renormalization scaling³ evolve in such a way to approach each other at roughly 10^{16} GeV, suspiciously close to the seesaw scale above.

It is interesting that this coincidence becomes almost perfect once another important theoretical concept, namely the idea of low-energy supersymmetry (SUSY) is taken into account. This framework, in which the fermionic and bosonic degrees of freedom as two facets of one fundamental object - superfield - is very attractive not only for the philosophically appealing “unification” of the concepts of matter and force but also for the capability to resolve other issues of the Standard Model.

¹Here the left chiral components of the charge-conjugated fields instead of the right-handed ones are used.

²Perhaps a short point is worth making here. Unless there is a symmetry that prevents the zero on the 11 position of the mass matrix from receiving radiative corrections, there is a small but nonzero entry generated at the loop level. Denoting this (the so called type-II) term by m the seesaw formula changes into

$$m_\nu \sim m - Y_\nu^T M^{-1} Y_\nu v^2.$$

In unified frameworks such a term arises naturally even at the tree-level from the Yukawa interactions with heavy $SU(2)_L$ triplets and m is therefore often called a “triplet” seesaw term.

³In particular those of $SU(3)_c$ and $SU(2)_L$; since there is an ambiguity in defining the abelian charges at the SM level let us for a moment set aside the gauge coupling associated with the $U(1)_Y$ factor. It is intriguing that normalizing the abelian charge in accordance with the unification schemes like for instance $SU(5)$, *all tree* gauge couplings meet almost at a point !

One of them is the so called hierarchy problem stemming from the fact that the mass of the Higgs scalar is not protected by the gauge symmetry from receiving large radiative corrections from the physics at very high energies. This calls for a tremendous fine-tuning order-by-order in perturbation theory to prevent destabilization of the Higgs mass and the electroweak symmetry breaking scale. If supersymmetry is present (or softly broken [26, 27]), each fermionic (bosonic) field is accompanied by a bosonic (fermionic) partner with equal mass (or shifted by finite amount if soft terms are present) that leads to cancellations of divergences between the fermionic and bosonic loop factors.

Moreover, within a class of supersymmetrized extensions of SM like for instance the Minimal supersymmetric Standard Model (MSSM) [28, 29] we may understand the phenomenon of spontaneous breakdown of the $SU(3)_c \otimes SU(2)_L \otimes U(1)_Y$ gauge symmetry at the electroweak scale. It can be shown that evolving the MSSM parameters from a high scale at which the soft-SUSY breaking terms are generated down to the low energies, one of the mass parameters in the Higgs potential may switch sign driving the vacuum of the theory out of the gauge symmetric point.

Coming back to the gauge coupling unification in a supersymmetric framework, the new states living around the TeV scale, in particular the gauginos and higgsinos (the superpartners of the intermediate gauge bosons and Higgs scalars) affect the relevant beta-functions in such a way that all the three effective SM gauge couplings meet at roughly 2×10^{16} GeV.

These hints strongly suggest that many aspects of the “new physics” beyond the Standard Model could be naturally accommodated within the so-called grand unified theories, GUTs. In this class of models, the $SU(3)_c \otimes SU(2)_L \otimes U(1)_Y$ gauge group of the SM is embedded into a simple or a semisimple Lie group and the transformation properties of the SM fields are realized by fitting the SM multiplets ⁴ into just few irreducible representations of the larger group. Notice that, as a consequence, in GUTs there naturally exist transitions among quarks and leptons leading to baryon and lepton number violating processes such as proton decay and neutron-antineutron oscillations.

The most popular GUT schemes are based on the simple Lie groups $SU(5)$, $SO(10)$, E_6 while partial unification can be achieved imposing for instance the Pati-Salam symmetry $SU(4)_{PS} \otimes SU(2)_L \otimes SU(2)_R$ that allows for treating the lepton number as a “fourth color”, or via $SU(3)_c \otimes SU(2)_L \otimes SU(2)_R \otimes U(1)_{B-L}$ or the $SU(5) \otimes U(1)$

⁴This usually concerns the multiplets of each generation separately. However, there are attempts to construct schemes like for instance $SO(16)$ [30] in which an irreducible representation accommodates more than one generation of the SM fermions with nontrivial consequences for the flavor structure of such models.

intermediate symmetries. In general, the choice of the unified gauge group is driven by the requirements of minimality⁵ and by the need of complex representations to account for fermion chirality. As we shall see, the hypercharges of the SM multiplets fit precisely the low-dimensional multiplets of these groups⁶ ($\bar{5} \oplus 10 \oplus 1$ in case of $SU(5)$, 16 of $SO(10)$ or 27 (with a slight redundancy of the vector-like fermions) of E_6). In case of an anomaly-free GUT group, this assignment also sheds light on the “miraculous” anomaly cancellations in Standard Model.

Another interesting consequence of the embedding of the SM gauge group into a unified structure is a natural explanation of the fractional quark charges. Indeed, the electric charge operator is identified with a combination of generators in the Cartan algebra of the unified group. However, the eigenvalues of such operators are subject to strong constraints arising from the nonabelian nature of the GUT group. As for the simplest $SU(5)$ GUT (c.f. section 1.1) the electric charge operator must be traceless over any of its unitary representations and thus the charges of the quarks and leptons residing in $\bar{5}$ must sum up to zero. Consequently, the three down-type antiquarks of different colour equilibrate the electron charge only if $Q_{\bar{d}}/Q_{e^-} = 1/3$.

Another issue that can be addressed by GUTs is the so called flavor problem of the Standard Model. In particular, without additional ad-hoc assumptions the minimal $SU(3)_c \otimes SU(2)_L \otimes U(1)_Y$ framework does not provide any understanding of the peculiar Yukawa textures giving rise to the observed quark and lepton mixing patterns. This stems from the fact that the symmetry of the model does not impose any constraints on the flavor structure of these couplings and thus there is no way to correlate the 13 relevant parameters⁷ from first principles. Another aspect of this difficulty is the peculiar pattern of the weak hypercharges of the SM fermions that, while fitting neatly the $SU(3)_c \otimes SU(2)_L \otimes U(1)_Y$ gauge structure, remains unexplained. The flavor problem is generally boosted once the idea of softly-broken supersymmetry is invoked and the supersymmetric versions of the SM with a plethora of flavor-dependent soft-SY SY breaking terms are considered.

Both these aspects of the flavor problem can be partially traced back to the relatively complicated structure of the SM gauge group. Indeed, the families of quarks and leptons reside in 5 distinct multiplets of $SU(3)_c \otimes SU(2)_L \otimes U(1)_Y$ (6 if the right-

⁵Naturally, there are many Lie groups containing $SU(3)_c \otimes SU(2)_L \otimes U(1)_Y$ as a subgroup; to avoid proliferation of new particles only the few of them such as those mentioned above seem a reasonable choice.

⁶In fact, this very observation points strongly to the concept of a unified gauge group even without the need for other hints like the experimental convergence of the gauge couplings or the large scale in the seesaw formula for neutrinos!

⁷6 quark masses, 3 angles and one phase in the CKM mixing matrix and 3 charged lepton masses

handed neutrinos are taken into account) and up to 4 independent Yukawa structures are needed to construct (Dirac) masses for all of the matter fields, namely:

$$\mathcal{L}_Y = \overline{Q}_L Y_u \langle \Phi_u \rangle U_R + \overline{Q}_L Y_d \langle \Phi_d \rangle D_R + \overline{L}_L Y_\nu \langle \Phi_\nu \rangle N_R + \overline{L}_L Y_l \langle \Phi_l \rangle E_R + h.c.$$

The way this issue can be (at least partially) addressed in unified theories is clear. Since the number of independent “building blocks” is reduced considerably once the SM multiplets are accommodated within irreducible representations of the higher symmetry group, the number of independent contractions needed to generate the appropriate mass terms is smaller.

Remarkably enough, though enhancing the communication among the multiplets in the “vertical” direction (i.e. within generations of the SM matter), the GUTs can also lead to valuable clues on the flavour textures “across the families” that is usually the domain of models with the so-called horizontal symmetries, c.f. [31, 32, 33] and references therein. Such correlations can arise for example consequence of various permutation symmetries acting on the family indices of fermionic bilinears; a typical example could be the symmetry property of the up-quark Yukawa matrix Y_u in the $SU(5)$ model, see section 1.1.

Extending this argument to the neutrino fields accompanying quarks and charged leptons in the GUT multiplets, one may attempt studying the “internal” structure of the seesaw formula (3) as well, that is smeared out in the low-energy data by the degeneracy and nonlinearities therein. For instance, the tight correlations among the effective Yukawa couplings of quarks and leptons arising from the same GUT origin can give rise to nontrivial constraints on the structure of leptonic Dirac (and Majorana) mass matrices which can subsequently shed a light on the patterns of the parameters governing the neutrino physics.

The advent of the “precision measurements” of the neutrino oscillation parameters inspired a proliferation of this type of studies in the last few years. As a matter of fact, for the first time we are able to test some of the GUT models using neutrino experimental data. As we shall see later, of particular interest are the models based on the $SO(10)$ gauge symmetry. In the minimal version [34], this scheme is very restrictive in the Yukawa sector and can lead to testable constraints on some of the neutrino oscillation parameters.

As a matter of fact, the results are quite interesting. Some of the recent year’s analyses [35, 36, 37, 38] claimed that the large PMNS mixing angles in $SO(10)$ models with dominant type-I term in the seesaw formula could be hardly accommodated. This brought some attention to those setups where the triplet (type-II) term is assumed to screen the type-I contribution. Bajc, Senjanović and Vissani [39] pointed out that

in such class of models there is a nice correlation among the apparent convergence of the b -quark and τ -lepton Yukawa couplings at the GUT scale and the large 2-3 mixing angle in the neutrino sector in such class of models. In the same framework, Mohapatra, Goh and Ng [40] demonstrated that the almost bimaximal leptonic mixing could be accommodated even in setups with only real Yukawa couplings and mixing parameters. In a subsequent paper [41], the same authors attempted to generalize the numerical analysis for the realistic (complex) case and claimed that the stringent minimal SUSY $SO(10)$ Yukawa sum-rules force the CKM CP-phase to fall in the second or third quadrant, in contradiction with the experimental values $\delta_{CKM} \sim \frac{\pi}{3}$. The option of generating the Majorana mass entries radiatively making use of the so-called Witten's mechanism [42] in the split-SUSY $SO(10)$ model was studied recently by Bajc and Senjanović [43]. It was shown that in this scheme the neutrino masses are always dominated by the type-I seesaw formula.

In this respect, the present work could be understood as an attempt to clarify some issues raised in the recent surveys and to add another little piece into the mosaic of this type of studies of $SO(10)$ grand unified models. In particular, the stringent lower bound on the 1-3 mixing in the leptonic sector $|U_{e3}| > 0.16$ [40] emerging in the minimal SUSY $SO(10)$ with dominant triplet seesaw contribution is reexamined in detail paying particular attention to the quality of the numerical fit and the experimental uncertainties in the input parameters [44]. It is shown that in the simplified scenario with real Yukawa couplings there is an overall tension among the predicted correlations of the neutrino oscillation parameters and the latest experimental data [24]. As demonstrated subsequently, in the physical (complex) setup this problem can be partially avoided by adjusting the additional phases entering the GUT-scale Yukawa sum-rules but discrepancies still persist [45].

In order to address the raising tension between the minimal setups and neutrino data, a slight extension of the minimal framework containing a subleading antisymmetric Yukawa texture is proposed and a possible role of contributions stemming from such a class of effective operators is studied⁸. It is demonstrated that even a per-mille contribution can affect the 1-3 mixing angle by tens of percent. Though slightly relaxed, the stringent $|U_{e3}|$ lower bound does not vanish and can tell the model in future experiments.

As for the CKM CP violation, the qualitative argument driving the CKM phase into the second or third quadrant [41] is questioned and subject to a detailed analysis.

⁸Such a correction can be generated by giving a small VEV to a specific $SO(10)$ Higgs multiplet, see section 4. The antisymmetry is important for the stability of the perturbative method developed for this purpose.

Indeed, it is argued that the CKM phase is obtained in the first quadrant via a minor “conspiracy” among the input parameters. The regions of parametric space for which this can happen are shown to be non-negligible confirming the semianalytic expectations. It is shown that this issue is naturally resolved in the extension of the minimal setup with a quasidecoupled 120_H in the Higgs sector.

The remarkable preference of small values of the Dirac CP-phase in the leptonic sector obtained in the numerical studies [40, 45] of the minimal setting is justified by a detailed inspection of the relevant mass matrices. It is claimed that this prediction, though in general subject to large effects of running, remains stable for the physically interesting regions of the parametric space.

The second part of the work is devoted to a class of $SO(10)$ models in which the Majorana masses for neutrinos do not arise from the Yukawa interaction with the “standard” 126-dimensional multiplet. It is argued that in order to implement the Witten’s mechanism[42] in a split-SUSY $SO(10)$ GUT one should (in minimal versions) employ a 120-dimensional Higgs representation. A class of “inverse” cascade seesaw models is considered and a potentially realistic SUSY $SO(10)$ implementation of this setup is constructed. It is argued that the $B - L$ breaking scale can be in general decoupled from the scale of the neutrino masses. The potential smallness of the $B - L$ breaking scale is shown to be fully compatible with both the neutrino physics and the gauge-coupling unification constraints.

The material is organized as follows: the first chapter is devoted to several remarks on the two basic supersymmetric GUTs – first the minimal SUSY $SU(5)$ is considered and the main shortcomings are pointed-out in brief, and in the second part these issues are addressed concerning a general class of $SO(10)$ models. This provides a natural motivation to approach and describe shortly the minimal SUSY $SO(10)$ scheme in the second chapter. The third chapter is dedicated to a detailed study of the correlations among the quark and lepton masses and mixing within the framework with dominant triplet seesaw contribution. An extended framework, a setup with an additional, quasidecoupled Higgs multiplet transforming as 120 of $SO(10)$, is introduced and studied in detail in chapter 4. Chapter 5 is devoted to a class of alternative seesaw schemes emerging in theories with a spinorial 16 in the Higgs sector of SUSY and split-SUSY $SO(10)$ GUTs. Finally, a set of Appendices is added to comment on technical points in the main text.

Chapter 1

Quark and lepton masses and mixing in Grand unified theories

Let us start by introducing in brief the basic SUSY GUTs and making several remarks on their salient features in view of the possible predictive power in the Yukawa sector providing the key for understanding the correlations among the quark and lepton masses and mixing studied in the subsequent chapters.

1.1 Quarks and leptons in minimal SUSY $SU(5)$

One of the first realistic attempts to embed the three distinct sectors of the Standard Model in a unified framework dates back to 1974 when a simple scheme based on $SU(5)$ gauge symmetry was proposed by Georgi and Glashow [46]. Concerning the main achievements, the theory was capable to provide for a partial understanding of the electric charge quantization and predicted the value of the weak mixing angle in rough agreement with the contemporary experimental data. On top of that, the 5 irreducible representations accommodating the matter fields of each SM generation (assuming purely left-handed neutrinos) were embedded into just two irreps – the antifundamental $\bar{5}_F$ and the two-index antisymmetric tensor 10_F . Since in such a scheme the quarks and leptons transform among each other under the gauge symmetry, the baryon and lepton numbers are violated in the interactions of the matter currents with the gauge bosons associated to the coset $SU(5)/SU(3)_c \otimes SU(2)_L \otimes U(1)_Y$. This gives rise to a variety of new phenomena, as for instance the proton decay or the neutron-antineutron oscillations.

Remarkably enough, the theory turned out to be so robust and compelling that it did not require any drastic revision for almost 30 years. Up to few necessary “up-

grades” motivated by further theoretical and phenomenological development – in particular, supersymmetry[28] was invoked [47, 48] to solve the gauge hierarchy problem and cure the mismatch of the running gauge couplings at the GUT scale – the minimal SUSY $SU(5)$ [47] is still considered a prototype of a potentially realistic grand unified framework.

To appreciate the power of the unification idea and explain the motivation to concerning even larger GUT groups such as $SO(10)$ in subsequent chapters, let us discuss briefly some of the salient features of the minimal SUSY $SU(5)$ paying particular attention to the mass and mixing patterns arising in the quark and lepton sectors.

1.1.1 $SU(5)$ matter fields

Under the $SU(3)_c \otimes SU(2)_L \otimes U(1)_Y$ subgroup, the $\bar{5}$ and 10 irreps of $SU(5)$ accommodating the SM matter multiplets decompose as

$$\bar{5} = (\bar{3}, 1, +1/3) \oplus (1, \bar{2}, -1/2) \quad \text{and} \quad 10 = (\bar{3}, 1, -2/3) \oplus (3, 2, +1/6) \oplus (1, 1, +1) \quad (1.1)$$

In a self-explanatory notation, the embedding of the SM matter fields in these representations can be depicted as¹

$$\bar{5}_i \equiv \begin{pmatrix} d_1^c \\ d_2^c \\ d_3^c \\ e^- \\ -\nu \end{pmatrix}_L \quad 10^{[ij]} \equiv \begin{pmatrix} 0 & u_3^c & -u_2^c & u^1 & d^1 \\ \cdot & 0 & u_1^c & u^2 & d^2 \\ \cdot & \cdot & 0 & u^3 & d^3 \\ \cdot & \cdot & \cdot & 0 & e^c \\ \cdot & \cdot & \cdot & \cdot & 0 \end{pmatrix}_L \quad (1.2)$$

The positions of various entries are dictated by the way the fundamental triplet of $SU(3)_c$ and the doublet of $SU(2)_L$ are placed in the fundamental pentaplet of $SU(5)$. In our notation the triplet is spanned over the first three indices of 5 while the doublet resides at the position of the remaining pair². The structure of 10_F is then obtained by inspecting the “distribution” of the SM quantum numbers in the antisymmetric subspace of $5 \otimes 5$.

In SUSY context, these multiplets become chiral superfields hosting also the MSSM squark and slepton fields that are pushed above the experimental thresholds by the effects of the soft SUSY-breaking terms. This gives rise to several effects with direct phenomenological consequences:

¹We utilize the standard trick of putting the left-handed components of a charge-conjugated field instead of the right-handed ones.

²The doublet and the “antidoublet” of $SU(2)$ are equivalent representations. From now on the bar of $\bar{2}$ is going to be omitted.

- The additional scalars arising at the SUSY breaking scale (in the so called low-energy SUSY scenarios this scale is usually put in the TeV range) do not affect the position of the unification scale at the one-loop level because they fall into full $SU(5)$ multiplets. As a consequence, their contributions to the various b -coefficients are equal (at one-loop order) and the slopes of the curves corresponding to the three running gauge couplings change by the same amount. However, the value of the GUT-scale (universal) gauge coupling $\alpha_G = \frac{g^2}{4\pi}$ is affected.
- The presence of the charged scalars close to the SM physics opens a Pandora shell of $d = 5$ effective operators overwhelming in most cases the traditional $d = 6$ ones of the non-SUSY setups. Moreover, since the chiral superfields obey the Bose-Einstein statistics, supersymmetry puts further constraints on the flavor structure of these operators.

The latter observation leads to a class of typical experimental signatures of SUSY, like for instance the dominance of the kaon decay channels in proton decay experiments, c.f. section 1.2.4.

1.1.2 Higgs sector and Yukawa couplings

Let us first write down the $SU(5)$ decompositions of the three different matter bilinears that can be constructed from $\bar{5}$ and 10 :

$$\begin{aligned}
\bar{5} \otimes \bar{5} &= \bar{10} \oplus \bar{15} & \begin{array}{|c|} \hline \square \\ \hline \square \\ \hline \square \\ \hline \end{array} \otimes \begin{array}{|c|} \hline \square \\ \hline \square \\ \hline \square \\ \hline \end{array} &= \begin{array}{|c|} \hline \square \\ \hline \square \\ \hline \square \\ \hline \end{array} \oplus \begin{array}{|c|c|} \hline \square & \square \\ \hline \square & \square \\ \hline \square & \square \\ \hline \end{array} \\
\bar{5} \otimes 10 &= 5 \oplus \bar{45} & \begin{array}{|c|} \hline \square \\ \hline \square \\ \hline \square \\ \hline \end{array} \otimes \begin{array}{|c|c|} \hline \square & \square \\ \hline \square & \square \\ \hline \square & \square \\ \hline \end{array} &= \begin{array}{|c|} \hline \square \\ \hline \square \\ \hline \square \\ \hline \end{array} \oplus \begin{array}{|c|c|} \hline \square & \square \\ \hline \square & \square \\ \hline \square & \square \\ \hline \end{array} \\
10 \otimes 10 &= \bar{5} \oplus 45 \oplus 50 & \begin{array}{|c|} \hline \square \\ \hline \square \\ \hline \square \\ \hline \end{array} \otimes \begin{array}{|c|c|} \hline \square & \square \\ \hline \square & \square \\ \hline \square & \square \\ \hline \end{array} &= \begin{array}{|c|} \hline \square \\ \hline \square \\ \hline \square \\ \hline \end{array} \oplus \begin{array}{|c|c|} \hline \square & \square \\ \hline \square & \square \\ \hline \square & \square \\ \hline \end{array} \oplus \begin{array}{|c|c|} \hline \square & \square \\ \hline \square & \square \\ \hline \square & \square \\ \hline \end{array}
\end{aligned} \tag{1.3}$$

As expected, there is no singlet in eq. (1.3) and all the fermion masses in minimal $SU(5)$ must be generated by the Higgs mechanism as in the Standard Model case. Notice that the first matter bilinear ($\bar{5}_F \otimes \bar{5}_F$) can not provide for quark and lepton Dirac masses as it contains only one chiral component of each of these fields, see (1.2). However, it can be used to generate Majorana mass for neutrinos if the $SU(2)_L$ -triplet of 15_H (if present) acquires a VEV [19]. The second structure ($\bar{5}_F \otimes 10_F$) contains both chiral components of down quarks and charged leptons and thus can be used to generate the Yukawa vertices for these fields, while the last bilinear ($10_F \otimes 10_F$) can do the same for the up-type quarks (again, due to the absence of the opposite chirality it can not do this for the other matter fermions).

The structure of the minimal SUSY $SU(5)$ Yukawa sector becomes clear: the Dirac masses of all quarks and charged leptons can be generated by a pair of 5-dimensional Higgs representations $\bar{5}_H \oplus 5_H$, the former³ giving rise to the masses of charged leptons and down-type quarks while the latter to the up-quarks⁴. The relevant Yukawa superpotential can be written in the form

$$\mathcal{W}_Y = Y_{\bar{5}}^{ij} \bar{5}_F^i 10_F^j \bar{5}_H + Y_5^{ij} 10_F^i 10_F^j 5_H \quad (1.4)$$

The mass matrices generated by the VEVs of the $SU(2)_L$ doublets in $\bar{5}_H \oplus 5_H$ then read

$$M_d = M_l = Y_{\bar{5}} \langle \bar{5}_H \rangle, \quad M_u = Y_5 \langle 5_H \rangle \quad (1.5)$$

Note that due to the symmetry properties of the $10_F^i 10_F^j$ bilinear the up-quark Yukawa couplings are symmetric in the generation indices: $M_u = M_u^T$.

However, it is obvious that the Higgs multiplets used so far are not sufficient to break the $SU(5)$ symmetry down to the $SU(3)_c \otimes SU(2)_L \otimes U(1)_Y$ of SM as there is no SM singlet in 5 nor $\bar{5}$. Equivalently, since both $SU(5)$ and $SU(3)_c \otimes SU(2)_L \otimes U(1)_Y$ are rank 4 groups, the adjoint of $SU(5)$ – a 24 dimensional multiplet – is the smallest Higgs representation that can be used for this purpose⁵. Indeed, under $SU(3)_c \otimes SU(2)_L \otimes U(1)_Y$

$$24_H = (1, 1, 0) \oplus (8, 1, 0) \oplus (1, 3, 0) \oplus (3, 2, -5/6) \oplus (\bar{3}, 2, +5/6) \quad (1.6)$$

and the $(1, 1, 0)$ component can acquire a GUT-scale VEV provided the parameters of the Higgs superpotential

$$\mathcal{W}_H = m_5 \bar{5}_{H_i} 5_H^i + m_{24} 24_{H_i}^j 24_{H_j}^i + \lambda 24_{H_i}^j 24_{H_j}^k 24_{H_k}^i + \eta \bar{5}_{H_i} 24_{H_j}^i 5_H^j \quad (1.7)$$

are tuned properly. Note that once the necessary fine-tuning is performed at the tree-level, the SUSY no-renormalization theorem of Grisaru, Roček and Siegel [50] ensures that it is not compromised by the radiative effects.

1.1.3 Minimal SUSY $SU(5)$ - parameter counting

For sake of comparison with the other models considered later in this work let us count the number of free parameters of minimal SUSY $SU(5)$. There are 4 complex couplings in the Higgs superpotential, that (upon redefinition of two of the Higgs fields) leave 6

³upon the spontaneous breakdown of $SU(2)_L \otimes U(1)_Y \rightarrow U(1)_Q$

⁴The situation is quite similar to the MSSM where two doublets of opposite hypercharges were also needed to preserve supersymmetry and cancel the anomalies generated by higgsinos.

⁵Another option is for instance the 75-dimensional Higgs multiplet that allows for an implementation of the so-called “missing partner mechanism” addressing the generic doublet-triplet splitting problem of unified schemes [49].

real parameters. In the Yukawa sector, there are 6 complex entries of the symmetric Y_u and 9 complex entries in $Y_d = Y_l$. Obviously, not all of them are physical and one can diagonalize Y_d to end up with just three real numbers in the down quark and charged lepton sector. Having done that there is no more freedom in the up-quark coupling up to the phase redefinition of 5_H ⁶. Together with the gauge coupling g , there are in total 21 independent real parameters in the minimal SUSY $SU(5)$ model. The soft SUSY terms are universal for all the potentially realistic models and as such are not counted here.

1.2 Minimal SUSY $SU(5)$ shortcomings

Though the minimal SUSY $SU(5)$ model briefly described in the previous section seems to be a promising candidate for the simplets potentially realistic GUT theory, it suffers from several drawbacks that require additional assumptions and model building. Apart of the problem with the neutrino masses that can be generated at the level of effective operators, but only for the price of nonzero R -parity violating couplings like $\bar{5}_F 5_H 24_H$ (see [34] and references therein), the predicted relation for the Yukawa couplings $y_d^i = y_l^i$ (that works well for the third generation giving a hint for the observed convergence of running y_b and y_τ around the GUT-scale) fails for the first and the second generation. Moreover, as we shall see in the subsequent part, the minimal model is plagued by rather fast proton decay.

1.2.1 Neutrino masses in SUSY $SU(5)$

Concerning the neutrino mass problem, the most straightforward solution consists in adding an $SU(5)$ singlet containing the right-handed neutrino component and invoking the standard Yukawa interaction and the singlet Majorana mass term for ν_L^c ⁷

$$\mathcal{W}_\nu^{SU(5)} \ni Y_\nu^{ij} \bar{5}_F^i 1_F^j 5_H + M_\nu^{ij} 1_F^i 1_F^j \quad (1.8)$$

However, also this construction suffers of several unpleasant features :

- The number of parameters one has to add to give masses to the three neutrinos is enormous - after rotation into the basis in which M_ν^{ij} is diagonal⁸ we are left with 3 real eigenvalues of M_ν and in general 9 complex entries of Y_ν^{ij} - 21 additional parameters in total, i.e. double of the original minimal $SU(5)$ number!

⁶Note that the phase of 10_F is fixed upon diagonalization of $M_{d,l}$.

⁷The Lorenz structure of the Majorana mass term is suppressed.

⁸Such a basis always exists as the Majorana mass matrix is symmetric in generation indices.

- Since M_ν^{ij} are gauge-singlet mass parameters, without additional assumptions their overall scale remains undetermined in the SUSY $SU(5)$ framework.

Therefore, the predictive power of a realistic SUSY $SU(5)$ in the leptonic sector (and in particular for neutrinos) is very constrained.

On the other hand, there is an interesting hint in favor of this scheme. It stems from the observation that although $SU(5)$ is not anomaly free, the anomalies generated by the minimal model fermionic content ($\bar{5}_F$ and 10_F) exactly cancel [51], pretty much like in the SM case. This is of course highly welcome for the consistency of the theory, but calls for deeper understanding. Remarkably enough, this feature can be explained if $SU(5)$ is considered as a subgroup of $SO(10)$ that is automatically anomaly free. In such a case the additional matter singlet is a must since the $SU(5)$ matter multiplets are embedded into the 16-dimensional spinorial representation of $SO(10)$ as

$$16 = \bar{5} \oplus 10 \oplus 1 \quad (1.9)$$

Therefore, from the $SO(10)$ point of view the extended $SU(5)$ matter spectrum is very natural.

Alternatively, since the SM neutrino masses are strongly suppressed with respect to the masses of the other matter fermions, a natural option could be to generate them at the nonrenormalizable level by means of appropriate effective operators, for instance

$$\mathcal{W}_\nu^{SU(5)} \ni \lambda_{ij} \frac{1}{M} \bar{5}_F^i \bar{5}_F^j 5_H 5_H \quad (1.10)$$

in a complete analogy with the SM effective structure [19]

$$\mathcal{L}^{SM} \ni \lambda_{ij} \frac{1}{M} \psi_L^{Ti} C^{-1} \tau_2 \bar{\tau} \psi_L^j \cdot H^T \tau_2 \bar{\tau} H \quad (1.11)$$

Unfortunately, neither this approach is satisfactory, although the number of new real parameters is reduced to just 12. The reason is that for the natural cut-off scale M above M_G the neutrino masses are too small to account for the mass-squared ratios measured in oscillation experiments.

1.2.2 Effective Yukawa sum-rules & quark and lepton masses and mixing

As we saw in section 1.1.2 the $SU(5)$ gauge symmetry and the minimal Higgs content yields at the renormalizable level

$$Y_u = Y_u^T \quad \text{and} \quad Y_d = Y_l \quad (1.12)$$

There are therefore two independent Yukawa matrices in the quark sector, one of them (Y_u) symmetric. This is welcome, because this structure can accommodate the CKM mixing easily. On the other hand $Y_d = Y_l$ is a *nontrivial prediction* that the down quark and the charged lepton spectra are equal at the GUT-scale. In case of the third generation this relation is nicely satisfied in terms of the mentioned $y_b - y_\tau$ (or shortly $b - \tau$) unification acquired around the GUT scale⁹. However, to get the right prediction for y_s and y_μ one would rather need roughly $y_\mu \sim 3y_s$ at M_G while for the first generation $3y_e \sim y_d$. Therefore, though very successful for the heavy flavors, the light fermion masses call for an extension of the minimal $SU(5)$, either by coupling additional Higgs multiplets to the matter bilinears or emphasizing the role of the effective operators.

Another serious issue of the minimal SUSY $SU(5)$ model comes from the predictions for the proton lifetime. Prior discussing this problem in more detail let us shortly comment on general features of proton decay in SUSY GUTs.

1.2.3 Proton decay in SUSY GUTs

The proton decay scenario in the supersymmetric grand unified models differs from the nonsupersymmetric case in several aspects.

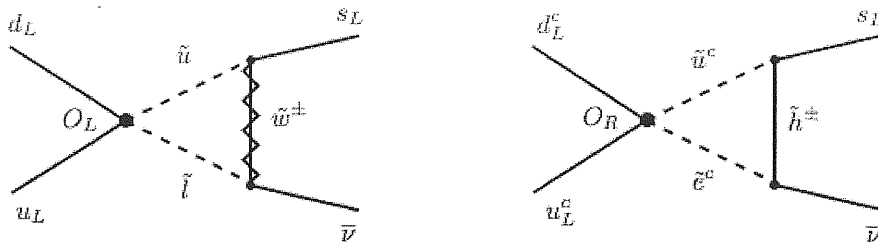
- The new coloured scalars required by supersymmetry give rise to a new set of $d = 5$ (and sometimes even $d = 4$, c.f. section 5.1.1) baryon and lepton number violating operators. This usually leads to a strong enhancement of the proton decay amplitudes in comparison to the nonsupersymmetric models where such operators, generated by the exchanges of the leptoquark gauge bosons, appear at $d = 6$ level.
- The dominant nucleon decay modes in supersymmetric models (e.g. $p^+ \rightarrow K^+ \bar{\nu}_\mu$, $n \rightarrow K^0 \bar{\nu}$) differ from the non-SUSY ones (mostly $p^+ \rightarrow \pi^+ \bar{\nu}_e$, $p^+ \rightarrow \pi^0 e^+$, $n \rightarrow \pi^- e^+$). The reason for this stems from the bosonic nature of the superfields. Indeed, writing the relevant “LLLL” and “RRRR” operators in “full glory” (with i, j, k, l being the family indices while α, β, γ and r, s, t, u standing for colour and $SU(2)_L$ indices respectively and omitting all the Lorenz patterns):

$$\begin{aligned}
O_L &\propto c_L^{ijkl} \varepsilon^{\tau s} \varepsilon^{tu} \varepsilon^{\alpha\beta\gamma} Q_{L\alpha r}^i Q_{L\beta s}^j Q_{L\gamma t}^k L_{L\mu}^l \\
O_R &\propto c_R^{ijkl} \varepsilon^{\alpha\beta\gamma} u_{L\alpha}^i u_{L\beta}^j d_{L\gamma}^k e_L^l
\end{aligned} \tag{1.13}$$

⁹Due to the different RGE evolution (b is coloured while τ is not) this leads to roughly $3y_\tau \sim y_b$ around the electroweak scale, in good agreement with the experimental data.

The structure of the Wilson coefficients c_L^{ijkl} and c_R^{ijkl} stems from the Feynman diagrams with the heavy coloured Higgs triplet exchanges. Apart from the Yukawa entries they contain (rotating the quark fields into the mass basis) combinations of the various CKM entries. Since this product must be symmetric with respect to the interchange of the superfields Q (and also u^c), the relevant family indices must be antisymmetrized as well – one gets $i \neq j \neq k$ for the “LLLL” type while $i \neq j$ for the “RRRR” operators. Therefore, the $d = 5$ operators must be spanned over more than one generation. Converting these structures to the four-fermion operators by the wino and higgsino dressing¹⁰ depicted at Fig. 1.1, the dominant proton decay mode in most supersymmetric models is shown to be $p^+ \rightarrow K^+ \bar{\nu}_\mu$, c.f. [52] and references therein. This feature can in principle tell SUSY in the proton decay experiments.

Figure 1.1: The basic structure of the $d = 5$ operators driving the proton decay in SUSY models. The diagrams with gluino, bino and neutral higgsino dressings are often strongly suppressed by the first and second generation Yukawa couplings arising in the Wilson coefficients of the O_L and O_R effective operators. The dominant decay channel is usually $p^+ \rightarrow K^+ \bar{\nu}_\mu$.



1.2.4 Proton decay in minimal SUSY $SU(5)$

Let us now inspect in brief the structure of the effective operators (1.13) in the minimal SUSY $SU(5)$ model. They are generated upon integrating out the heavy coloured triplets $H_C \equiv (3, 1, -2/3)$ and $\bar{H}_C \equiv (\bar{3}, 1, +2/3)$ residing in 5_H and $\bar{5}_H$. The structure

¹⁰The gluino, bino and neutral higgsino dressed diagrams are strongly suppressed by the Yukawa couplings of the first and second generation governing the relevant effective $d = 5$ vertices (note that this dressing is flavour-diagonal and only relatively light mesons up to kaons are allowed by kinematic reasons). Moreover, the charged higgsino dressings of the “RRRR” operators are also usually suppressed unless there are relatively large Yukawa couplings corresponding to the third generation squarks propagating in the loops.

of the Wilson coefficients c_L^{ijkl} and c_R^{ijkl} is dictated by the the Yukawa interactions of H_C and \bar{H}_C with matter fermions encoded in formula (1.4), namely

$$\mathcal{W}_Y \ni Y_d^{ij} d_L^i u_L^j \bar{H}_C + Y_d^{ij} Q_L^i L_L^j \bar{H}_C + Y_u^{ij} u_L^i e_L^j H_C + Y_u^{ij} Q_L^i Q_L^j H_C + \dots \quad (1.14)$$

From this expression it is easy to infer¹¹

$$c_L^{ijkl} \sim c_R^{ijkl} \sim \frac{1}{M_{H_C}} Y_u^{ij} Y_d^{kl} \quad (1.15)$$

Therefore, in the minimal SUSY $SU(5)$ the structure of the effective operators (1.13) is very rigid and the model is highly predictive. Concerning the physical implications of relation (1.15) one can see for instance that in most cases the “LLLL” contribution dominates over the “RRRR” ones because of the Yukawa suppressions in the higgsino-squark couplings. On the other hand, the “RRRR” contributions can play a significant role if c_R is accidentally enhanced, like for instance in the very large $\tan\beta$ limit (due to the blow-up of the bottom Yukawa coupling [52, 53]) or in case of $p^+ \rightarrow K^+ \bar{\nu}_\tau$ (as a consequence of the Yukawas associated with the third generation sparticles propagating in the loop).

As regards to the numerical results, this type of analysis gives a stringent lower bound on the proton decay width of roughly¹² $\Gamma_{p^+} \sim (10^{32} \text{ years})^{-1}$, see for instance [53, 54] and references therein. This should be compared to the SuperKamiokande experimental bounds [55, 56] of roughly $\Gamma_{p^+} < (2.2 \times 10^{33} \text{ years})^{-1}$. This observation often leads to the claims that the minimal SUSY $SU(5)$ is excluded [54, 57]

However, it was pointed out recently that there still can exist areas in the parametric space that remain compatible with experimental limits if for instance the effective operators are invoked [58, 59] and/or the effects of GUT-scale “Yukawa mismatch” are taken into account [53, 60]. Therefore, though minimal SUSY $SU(5)$ is clearly in troubles with proton decay it still can not be definitely excluded.

The remainder of this chapter is devoted to a similar analysis of the other very popular class of the unified schemes, the $SO(10)$ GUTs.

¹¹For sake of simplicity the two additional phases arising upon redefinitions of 5_F , 10_F , 5_H and $\bar{5}_H$ (making the quark and lepton masses real and positive, c.f. section 1.1.3) are suppressed in relations (1.15). Note also that these formulae fix the structure of c_L^{ijkl} and c_R^{ijkl} at the GUT scale. In precise quantitative analysis the effects of running of these operators down to the hadronization scale must be taken into account. For more detail see [52, 53] and references therein.

¹²This result corresponds to the masses of all sfermions at 1 TeV, maximal negative interference among the relative phases of the “LLLL” and “RRRR” contributions and an “optimal” value of $\tan\beta \sim 4$.

1.3 Quark and lepton masses and mixing in $SO(10)$ models

As we have seen case of the simplest unified model based on the $SU(5)$ gauge symmetry, grouping the SM multiplets within few irreducible representations of a GUT group leads to correlations among the various Yukawa couplings arising at the level of the low-energy effective theory. This can be viewed as one of the major achievements of the grand unified scenarios as it, at least in principle, provides for a possible way of addressing the flavor problem of SM without additional ad-hoc assumptions, like for instance in models equipped by horizontal symmetries [32, 31, 33]. Since the number of multiplets accommodating the matter fermion is further reduced in the $SO(10)$ case one can expect stronger communication among the various flavors giving rise to even more constrained sum-rules for the effective Yukawa couplings at low energies.

1.3.1 Matter fields in $SO(10)$ GUTs

One of the strongest motivation for the $SO(10)$ gauge symmetry comes from the observation that all the standard model multiplets of one generation fit neatly a single 16-dimensional chiral spinor of $SO(10) \supset SU(3)_c \otimes SU(2)_L \otimes U(1)_Y$:

$$16_F = (3, 2, +1/3) \oplus (1, 2, -1) \oplus (\bar{3}, 1, -4/3) \oplus (\bar{3}, 1, +2/3) \oplus (1, 1, 0) \oplus (1, 1, +2) \quad (1.16)$$

or, equivalently, $16 = \bar{5} \oplus 10 \oplus 1$ at the $SU(5)$ level. This immediately brings several benefits for general model-building:

- The right-handed neutrinos are automatically present and (since $16_F \otimes 16_F$ does not contain a gauge singlet) the structure and scale of the Majorana masses are dictated by the Yukawa couplings, spontaneous symmetry breaking pattern and the requirements of gauge-coupling unification.
- Since the gauge symmetry does not distinguish among the components of the decomposition (1.16) there are tight correlations among the effective Yukawa couplings that originate from a common source. As a consequence, the number of independent parameters determining the $SO(10)$ textures of the effective quark and lepton mass and mixing matrices can be reduced considerably.

On the other hand, oversimplifying the Yukawa sector one can easily end up with similar problems as in the minimal $SU(5)$ case. However, using a “reasonable” number of “active” Higgs representations, the generalized Yukawa sum-rules remain under control and need not lead to a complete loss of predictivity. Indeed, in realistic versions of $SO(10)$ GUTs one usually employs 2 distinct Yukawa couplings with definite generation

symmetries that give rise to all the 5 Yukawa structures of “standard” MSSM-like effective theories¹³. Thus, the structure remains rigid enough to provide for nontrivial and testable correlations among the quark and lepton masses and mixing subject of the next chapters. This brings us to the question of the Higgs sectors of $SO(10)$ models.

1.3.2 Higgs bosons in $SO(10)$ models

As in any realistic grand unified framework the Higgs sector of a general $SO(10)$ GUT must satisfy two basic requirements:

- The flavour structure of the Yukawa interactions of the matter fermions with the effective MSSM doublets should be compatible with the current data on quark and lepton masses and mixing
- It must allow for a proper spontaneous symmetry breaking of $SO(10)$ gauge symmetry down to the $SU(3)_c \otimes SU(2)_L \otimes U(1)_Y$ of the MSSM.

Of particular interest are representations of $SO(10)$ that are capable to act in both these roles. In such a case the number of free parameters can be reduced considerably.

Concerning the first requirement, the dimensions of the Higgs representations that can couple to the matter fermions of the MSSM are given by the group-theoretical properties of the bilinear [61]

$$16 \otimes 16 = 10 \oplus 126 \oplus 120 \tag{1.17}$$

Thus, at the renormalizable level there are only three types of $SO(10)$ Higgs multiplets that can give masses to the matter fermions: the 10-dimensional fundamental (vector) representation 10_H , the 126-dimensional anti-selfdual 5-index antisymmetric tensor $\overline{126}_H$ and the 120-dimensional three-index antisymmetric tensor 120_H , see Appendix B.3.1.

However, at the level of effective operators, any combination of Higgs representation containing at least one of these three structures as a part of its decomposition, can be used. For example, typical choices are the 10- or 120-dimensional components of $16_H \otimes 16_H$ or any of the three factors arising from $\overline{16}_H \otimes \overline{16}_H$ coupled in an appropriate way to $16_F \otimes 16_F$ in models with low dimensionality of the Higgs sector representations.

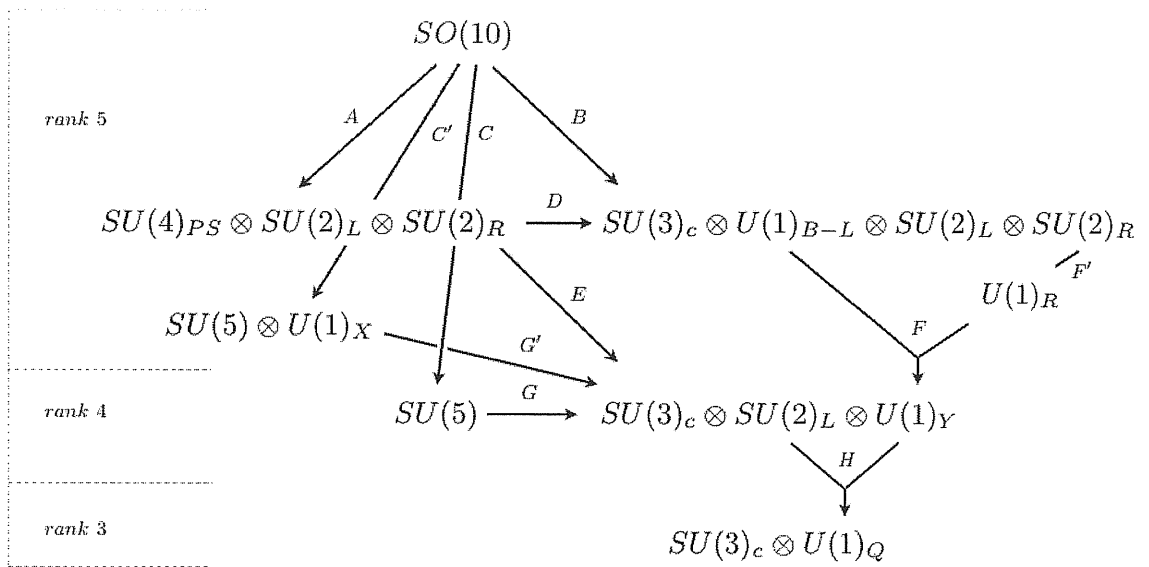
As regards to the spontaneous symmetry breaking chains, the important difference with respect to the minimal $SU(5)$ case stems from the fact that $SO(10)$ is a rank-5 group. Therefore, there are many different symmetry breaking “chains” leading to the

¹³2+2 quark and lepton Dirac mass matrices and, optionally, the Majorana mass matrix for neutrinos.

rank-4 $SU(3)_c \otimes SU(2)_L \otimes U(1)_Y$ of SM. To break $SO(10)$ properly along the desired chain one must make sure that at each intermediate scale there live Higgs multiplets capable to break the considered symmetry down to a subsequent one. In order to do this, the components acquiring VEVs must be completely neutral with respect to the desired lower intermediate symmetry groups and there must exist a scalar potential (encoded in the superpotential of the SUSY models) that can develop negative signs of the appropriate mass terms driving the symmetry breakdown.

Looking at the decomposition of the basic $SO(10)$ representations with respect to the physically interesting subgroups (c.f. [61] and Appendix B.4), in particular $SU(5)$, the Pati-Salam left-right symmetric group $SU(4)_{PS} \otimes SU(2)_L \otimes SU(2)_R$ or $SU(3)_c \otimes SU(2)_L \otimes SU(2)_R \otimes U(1)_{B-L}$, it is easy to see that only some combinations of the $SO(10)$ irreps are suitable for such purposes. The most common $SO(10)$ breaking chains¹⁴ and the representations that can be used to break the intermediate symmetries at each step are given at Fig. 1.1 and in Table 1.1.

Figure 1.2: The most common $SO(10)$ breaking chains of $SO(10)$ down to the $SU(3)_c \otimes U(1)_Q$ gauge symmetry at low energies. The Higgs multiplets usually chosen to break the intermediate symmetries are given in Table 1.1.



¹⁴For simplicity reasons, all subgroups that differ only by an additional discrete symmetry factors are omitted. For details, c.f. [61] and [30].

It is worth stressing that also the multiplets that do not couple directly to the fermionic bilinears can play an important role in the effective quark and lepton Yukawa relations. After the GUT-scale symmetry breaking, all the $SU(2)_L$ -doublet components with equal SM quantum numbers coming from different $SO(10)$ representations can mix and enter the formulae for the effective SM light Higgs doublets acquiring the electroweak VEVs, c.f. section 2.2.4. The same mechanism applies also to the other multiplets. For instance, the $SU(2)_R$ triplets¹⁵ in 45_H and 210_H mix at the $SU(3)_c \otimes SU(2)_L \otimes SU(2)_R \otimes U(1)_{B-L}$ stage giving rise to the relatively light triplet responsible for a $SU(2)_R \rightarrow U(1)_R$ breaking discussed in chapter 5.

Remarkably enough, inspecting Table 1.1 one can see that at least two (and three in the SUSY case) Higgs representations acquiring VEVs are needed to break $SO(10)$ down to the low energy $SU(3)_c \otimes U(1)_Q$ gauge group¹⁶.

Concerning for instance the breaking of the $SU(2)_L \otimes SU(2)_R$ subgroup of $SO(10)$ there are only two multiplets (up to the complex conjugated ones) that contain SM singlets capable to break this intermediate symmetry - 16_H (and/or $\overline{16}_H$) or 126_H (and/or $\overline{16}_H$)¹⁷. However, the SM singlet components of none of these multiplets can break the $SU(5)$ subgroup of $SO(10)$ ¹⁸. This can be seen easily in the case of $16_H/\overline{16}_H$ - only the $SU(5)$ singlet is also a singlet under $SU(3)_c \otimes SU(2)_L \otimes U(1)_Y$. Concerning the properties of the SM singlets of 126 , one can use the embedding of 5^i (and $\overline{5}_j$) into the $SO(10)$ vector 10_H . The pair of $SU(5)$ singlets coming from the full antisymmetric contractions of five 5^i (and $\overline{5}_j$) reside in the five index antisymmetric tensor of $SO(10)$ that is nothing but $126 \oplus \overline{126}$, see Appendix B.3. Since there is just one SM singlet direction in each of these multiplets [61] it must be the one we constructed and thus the SM singlets in 126_H and $\overline{126}_H$ are also $SU(5)$ singlets.

Therefore, to break $SO(10)$ through the left-right subgroups avoiding the $SU(5)$ intermediate step, additional Higgs representations are needed on top of either $\overline{126}_H$

¹⁵(1,3,1) with respect to the Pati-Salam group $SU(4)_{PS} \otimes SU(2)_L \otimes SU(2)_R$.

¹⁶Moreover, there is always at least one representation that can not couple to the fermionic bilinear, right as 24_H in the $SU(5)$ case. This is needed to avoid a GUT-scale VEV entering the matter fermion masses at tree-level. The only exception is $\overline{126}_H$ that (if present) typically contains a $B - L$ breaking VEV giving rise to the Majorana masses of right-handed neutrinos. Thus, in $SO(10)$ the seesaw scale is usually not free like in the simplest $SU(5)$ scenario.

¹⁷Since both these are complex representations, acquiring VEVs they generate a nontrivial contribution to the corresponding D -terms in SUSY scenarios. To keep supersymmetry unbroken below the GUT scale one must add also the complex conjugate representation and tune also the relevant VEVs to be complex conjugate of each other. On the other hand, one usually needs a complex conjugated representation anyway to form a superpotential mass term for these multiplets.

¹⁸The requirement of avoiding an intermediate $SU(5)$ symmetry is usually added to preserve the consistency with the proton decay limits, c.f. section 1.2.4.

or 16_H (and conjugated). The adjoint 45_H is not sufficient because alone it does not develop a SUSY-preserving VEV [62] and so the usual choice is $45_H \oplus 54_H$. Another option to break the GUT symmetries down to $SU(4)_{PS} \otimes SU(2)_L \otimes SU(2)_R$ of Pati-Salam or $SU(3)_c \otimes SU(2)_L \otimes SU(2)_R \otimes U(1)_{B-L}$ is to use the 4-index antisymmetric tensor 210_H ¹⁹, c.f. Appendix B.3.

Finally, one should look for a representation that breaks the $SU(3)_c \otimes SU(2)_L \otimes U(1)_Y$ of SM down to $SU(3)_c \otimes U(1)_Q$. Although there are already submultiplets that can do this once 16 or 126-dimensional irreps are used, usually (due to the obvious lack of Yukawa couplings) an additional multiplet is added. In most cases, the 10_H vector representation and/or the three-index antisymmetric tensor 120_H is added to account for this.

One can see that the overlap of the sets of the multiplets equipped by the renormalizable Yukawa couplings - 10_H , $\overline{126}_H$ and 120_H - and those capable to break GUT-scale symmetries (see Table 1.1) is actually very small - apart of 10_H that can not play any role in the high scale symmetry breaking mechanism, only $\overline{126}_H$ contains colorless $SU(2)_L$ doublets that (upon $SU(2)_L \otimes U(1)_Y$ breaking) can give rise to the Dirac masses of the matter fermions, and an $SU(2)_R$ triplet capable to participate at the breaking of $SO(10)$ and/or the left-right symmetric subgroups at intermediate scales. From this point of view, $\overline{126}$ can be viewed as a “multi-purpose building block” that singles out a class of economical $SO(10)$ models. An important representative of this set - the minimal renormalizable SUSY $SO(10)$ model - is the subject of the next chapters.

An “orthogonal” option, a class of models in which the intermediate breaking steps are driven by 16-dimensional representations, are briefly discussed in chapter 5.

1.3.3 Proton decay in SUSY $SO(10)$ models

Let us finally comment on proton decay in SUSY $SO(10)$ models. The situation is technically quite similar to that of the minimal SUSY $SU(5)$ discussed in brief in section 1.2.4 . However, the structure of the effective operators (1.13) that was very constrained in the $SU(5)$ case can be relaxed and the lower bound on Γ_{p^+} can be in some situations pushed well below the experimental limits. This stems from the fact that the $SU(3)_c \otimes SU(2)_L \otimes U(1)_Y$ colored Higgs triplets governing the rise of the relevant $d = 5$ effective operators can be found in different $SO(10)$ irreps and mix once the GUT-scale symmetries are broken. Therefore, the relevant expressions for the Wilson coefficients c_L^{ijkl} and c_R^{ijkl} (dominated by the contribution of the lightest triplet)

¹⁹Clearly, as an antisymmetric representation of $SO(10)$ with even number of indices 210_H contains an $SU(5)$ singlet. However, here the relevant components are $(1, 1, 1)_{210}$ and $(15, 1, 1)_{210}$ of $SU(4)_{PS} \otimes SU(2)_L \otimes SU(2)_R$ that obviously break $SU(5)$.

typically contain elements of the mixing matrix parametrizing the projections of the $SO(10)$ basis on the triplet mass eigenstates. As a consequence, adjusting properly the color-triplet mixing, one can often suppress the proton decay rate below the observable limit. On the other hand, a proliferation of the Higgs multiplets can affect the gauge coupling unification pattern. Moreover, in order to accommodate the characteristic Yukawa textures arising from the quark and lepton masses and mixing data studied in the subsequent chapters, the Wilson coefficients (1.13) can not be made arbitrarily small and there are still rather stringent limits on the proton decay in realistic SUSY $SO(10)$ models, see for example [63, 64, 65, 66].

Table 1.1: The basic properties of $SO(10)$ irreps up to dimension 210. The quantum numbers of the submultiplets correspond to the Pati-Salam subgroup $SU(4)_{PS} \otimes SU(2)_L \otimes SU(2)_R$. The letters denoting the different breaking steps are those used at Fig.1.2. Notice that various components of some of these representations can participate at many different symmetry breaking steps. (The Pati-Salam notation is particularly suitable for the left-right symmetric breaking chains but slightly misleading in case of the breaking steps C , C' , G and G' , c.f. Fig.1.2 with intermediate $SU(5)$ symmetries. The relevant decompositions in such a case can be found for instance in [61].)

irrep	PS multiplet	breaking steps	typical scales	Yukawa
10_H	$(1, 2, 2)_{10}$	H	M_Z	+
16_H	$(4, 2, 1)_{16}$	H	M_Z	-
	$(\bar{4}, 1, 2)_{16}$	$C', G'; E, F$	$M_G; B - L$	-
$\bar{16}_H$	$(\bar{4}, 2, 1)_{\bar{16}}$	H	M_Z	-
	$(4, 1, 2)_{\bar{16}}$	$C', G'; E, F$	$M_G; B - L$	-
45_H	$(1, 3, 1)_{45}$	$C, G'; F'$	$M_G; SU(2)_R$	-
	$(15, 1, 1)_{45}$	$B, C; D$	$M_G; PS$	-
54_H	$(1, 1, 1)_{54}$	A, G	M_G	-
120_H	$(1, 2, 2)_{120}$	$G'; H$	$M_G; M_Z$	+
	$(15, 2, 2)_{120}$	$G'; H$	$M_G; M_Z$	+
126_H	$(15, 2, 2)_{126}$	H	M_Z	-
	$(10, 1, 3)_{126}$	$E, F; G'$	$B - L; M_G$	-
$\bar{126}_H$	$(15, 2, 2)_{\bar{126}}$	H	M_Z	+
	$(\bar{10}, 1, 3)_{\bar{126}}$	$E, F; G'$	$B - L$	+
144_H	$(4, 2, 1)_{144}$	H	M_Z	-
	$(\bar{4}, 1, 2)_{144}$	$C', G, G'; E, F$	$M_G; B - L$	-
$\bar{144}_H$	$(\bar{4}, 2, 1)_{\bar{144}}$	H	M_Z	-
	$(4, 1, 2)_{\bar{144}}$	$C', G, G'; E, F$	$M_G; B - L$	-
210_H	$(1, 1, 1)_{210}$	$A; C', G, G'$	M_G	-
	$(15, 1, 1)_{210}$	$B, D; C', G, G'$	PS, M_G	-
	$(10, 2, 2)_{210}$	H	M_Z	-
	$(\bar{10}, 2, 2)_{210}$	H	M_Z	-

Chapter 2

Minimal renormalizable SUSY $SO(10)$ model

Among the variety of unified Standard Model extensions, a particular attention should be naturally paid to the simplest schemes with the maximal level of predictive power. Only in scenarios unbiased by additional assumptions (up to those that are needed for the very consistency of the model ¹), the idea of grand unification and the “GUT desert” can be tested up to “the bitter end” [34]. Only in such a conservative approach, though often hardly tractable in practise, one can hope for a clear-cut evidence in favor or against the very concept of unification and/or its embeddings within schemes based on conventional field theory models, strings or whatever even more general. On quantitative level, it is always the amount of predictivity that qualifies a particular scheme (and the assumptions behind it) as experimentally testable and capable to draw conclusions about the “beyond Standard Model physics”.

The minimal renormalizable SUSY $SO(10)$ model that is the subject of this chapter is not only a very interesting example of such a concise framework, but in a certain sense even the most predictive (potentially realistic) renormalizable GUT model ever formulated [34].

2.1 The model

The basic structure of the minimal $SO(10)$ was first considered at the beginning of eighties in papers by Clark, Kuo and Nakagawa [67] and Aulakh and Mohapatra [68]. The main feature that singles it out from the other simple unified theories is the partic-

¹as for example the structure of the symmetry breaking chain or the high-scale gauge coupling coincidence.

ular choice of the Higgs sector that allows² for only a small number of free parameters and thus makes the model very predictive. Though the requirement of renormalizability is more a technical prerequisite that could be avoided once the scheme is examined in detail, it can be viewed as a very convenient guideline that identifies the basic building blocks of the theory responsible for most of its key features. Supersymmetry enters the game to achieve the proper gauge unification pattern and to address the gauge hierarchy problem that often plagues theories highly different symmetry breaking scales.

2.1.1 The matter content

As in most of the GUTs based on the $SO(10)$ gauge group the Standard Model matter fields reside in three copies of the 16-dimensional spinorial irrep denoted from now on by 16_F^i , see Appendix B.2. Schematically, it can be written as

$$16_F = (\overset{Q_L}{3}, \overset{L_L}{2}, \overset{u_L^c}{+1/3}) \oplus (\overset{L_L}{1}, \overset{d_L^c}{2}, \overset{e_L^c}{-1}) \oplus (\overline{3}, 1, -4/3) \oplus (\overline{3}, 1, +2/3) \oplus (1, 1, 0) \oplus (1, 1, +2) \quad (2.1)$$

where the quantum numbers on the right-hand side are those of the SM $SU(3)_c \otimes SU(2)_L \otimes U(1)_Y$ symmetry.

2.1.2 The Higgs sector

The structure of the minimal SUSY $SO(10)$ Higgs sector is strongly constrained by the requirements of minimality, renormalizability and supersymmetry. As far as minimality is concerned, the 126-dimensional representation is used (in particular, the anti-selfdual component $\overline{126}_H$ of 252) and plays a twofold role - it can participate on the breaking of a “portion” of the unified gauge symmetry and also couple to the fermionic bilinear to take part on the mechanism generating the masses of the SM matter fermions. The point is that under the Pati-Salam subgroup $SU(4)_{PS} \otimes SU(2)_L \otimes SU(2)_R$, $\overline{126}_H$ decays into

$$\overline{126}_H \ni (15, 2, 2)_{\overline{126}} \oplus (\overline{10}, 1, 3)_{\overline{126}} \oplus \dots \quad (2.2)$$

Since there is an $SU(3)_c$ singlet in $\overline{10}$ of $SU(4)_{PS}$ with even $B - L$ quantum number giving rise to a zero weak hypercharge $Y_W = 2T_R^3 + (B - L)$, the first component in eq. (2.2) can receive a large VEV capable to break the $SU(2)_R \otimes U(1)_{B-L}$ down to the $U(1)_Y$ of the Standard Model. Since this VEV is an $SU(2)_L$ singlet, it can also give rise to the singlet Majorana mass of the neutrino through the Yukawa coupling of $\overline{126}_H$ to the matter bilinear $16_F 16_F$.

²even without imposing other symmetries than just the $SO(10)$ gauge

However, given a GUT-scale VEV to the $\overline{126}_H$ multiplet, a nontrivial D -term driving the SUSY breakdown is generated. To maintain supersymmetry unbroken up to the TeV range, this contribution must be canceled by adding the conjugate representation 126_H with a conjugated VEV $\langle \overline{126}_H \rangle = \langle \overline{126}_H \rangle$. This term also gives rise to an explicit mass term $M_{126} \overline{126}_H 126_H$ that (as a consequence of the minimization conditions) drives all the dangerous coloured Higgs states to live naturally around the GUT scale.

As we have already seen, there must be other Higgs multiplets to account for the proper symmetry breaking (recall that the VEVs of $126_H \oplus \overline{126}_H$ do not break the $SU(5)$ subgroup of $SO(10)$). Moreover, the effective SM Yukawa structure descending from $\overline{126}_H$ only can not be sufficient to generate the CKM mixing in the quark sector. Therefore, another ‘‘Yukawa-active’’ multiplet should be added. Last, but not least, to ensure enough freedom to make a pair of the $SU(2)_L$ doublets light enough to play the role of H_u and H_d of the MSSM, one should mix the $126_H \oplus \overline{126}_H$ bidoublets with other components coming from other sectors of the model.

From this respect, the role of a source of additional SM Higgs doublets could be played for instance by the vectorial 10_H or the three-index antisymmetric tensor 120_H , c.f. Appendix B.3. In $SO(10)$ model building the former option is usually used. However, to mix the doublets of 10_H with those of $126_H \oplus \overline{126}_H$ and to break properly the $SU(5)$ subgroup (neither 10_H or 120_H can do the job, see Appendix B.3), additional Higgs multiplets are needed. The usual choice is $45_H \oplus 54_H$ (both of them are needed [62] for the proper $SO(10)$ breaking and the desired doublet mixing appears at the level of nonrenormalizable operators). The former statement can be inferred from Table 1.1 while the latter becomes evident from the following decompositions of the relevant tensor products:

$$\begin{aligned} 10 \otimes \overline{126} &= 210 \oplus 1050 \\ 45 \otimes 45 &= 1 \oplus 45 \oplus 54 \oplus 210 \oplus 770 \oplus 945 \end{aligned}$$

Remarkably enough, it is possible to provide a solution of both these problems at once yet at the renormalizable level! [34] The trick consists in using the 210-dimensional 4-index antisymmetric tensor (the ‘‘messenger’’ multiplet in the decompositions above) as an elementary field instead. Indeed, under the Pati-Salam $SU(4)_{PS} \otimes SU(2)_L \otimes SU(2)_R$ symmetry:

$$210 = (15, 1, 3) \oplus (15, 3, 1) \oplus (10, 2, 2) \oplus (\overline{10}, 2, 2) \oplus (6, 2, 2) \oplus (15, 1, 1) \oplus (1, 1, 1)$$

As a matter of fact, there are even 3 different $SU(3)_c \otimes SU(2)_L \otimes U(1)_Y$ singlets within 210_H that are nonsinglets under $SU(5)$ - $(15, 1, 1)_{210} \oplus (15, 1, 3)_{210} \oplus (1, 1, 1)_{210}$ can trigger the breaking of $SO(10)$ to a left-right symmetric intermediate stage (to

$SU(3)_c \otimes SU(2)_L \otimes SU(2)_R \otimes U(1)_{B-L}$ in case of $\langle(15, 1, 1)_{210}\rangle \neq 0$ while to $SU(4)_{PS} \otimes SU(2)_L \otimes SU(2)_R$ if $\langle(1, 1, 1)_{210}\rangle \neq 0$ or to $SU(3)_c \otimes SU(2)_L \otimes U(1)_R \otimes U(1)_{B-L}$ (if $\langle(15, 1, 3)_{210}\rangle \neq 0$).

The desired doublet mixing is provided by the vertex $10_H \overline{126}_H 210_H$ (plus the conjugated term) and it is even enhanced as the doublet mixing matrices become 4×4 due to additional doublet contributions coming from $(10, 2, 2)_{210} \oplus (\overline{10}, 2, 2)_{210}$. Indeed, upon $SU(4)_{PS} \rightarrow SU(3)_c \otimes U(1)_{B-L}$ breaking, under which $10 \rightarrow (1, -2) \oplus (3, -2/3) \oplus (6, +2/3)$. Thus, in general, for each SM hypercharge there are 4 different multiplets that mix to give rise to the light Higgs doublets denoted from now on $H_{u,d}$. These are identified with the “standard” MSSM doublets triggering the electroweak symmetry breaking, see section 2.2.4.

2.1.3 The symmetry breaking pattern

With all this information at hand, one can draw a rough picture of the viable symmetry breaking chains in the minimal SUSY $SO(10)$ model, see Fig. 2.1. In total, there are 5 different types of VEVs triggering the intermediate symmetry breaking steps [34]:

$$\begin{aligned} \langle(1, 1, 1)_{210}\rangle &\equiv p & \langle(15, 1, 1)_{210}\rangle &\equiv a & \langle(15, 1, 3)_{210}\rangle &\equiv \omega \\ \langle(10, 1, 3)_{\overline{126}}\rangle &\equiv \bar{\sigma} & \langle(\overline{10}, 1, 3)_{126}\rangle &\equiv \sigma & & \\ \langle H_{u,d}\rangle &\equiv v_{u,d} & & & & \end{aligned} \quad (2.3)$$

To obtain the set of supersymmetric vacua, one must solve the flatness conditions for the F and D-terms and find solutions that obey the desired intermediate symmetry properties. This tedium was worked out in great detail in [69].

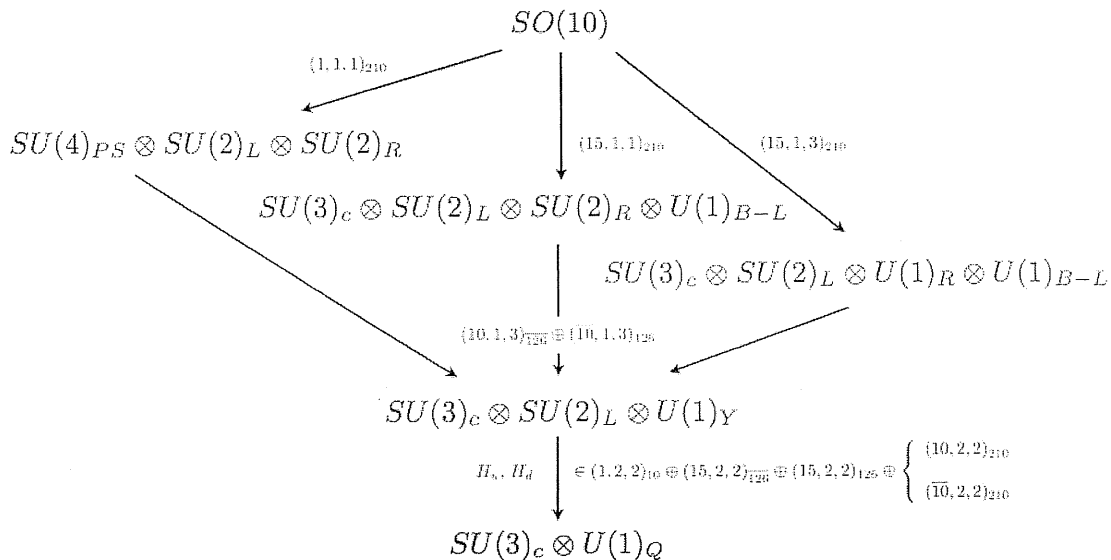
2.2 Basic features of the minimal SUSY $SO(10)$

Let us give a brief list of the main achievements of the simple structure discussed in the previous section paying particular attention on the physical consequences of the particular choice of the Higgs sector of the minimal SUSY $SO(10)$ model

2.2.1 Gauge coupling unification and intermediate scales

Remarkably enough, concerning the gauge coupling unification constraints it can be shown [69] that all the rank-5 subgroups in the symmetry groups depicted at Fig. 2.1 should be broken very close to the GUT scale, i.e. $p \propto a \propto \omega \propto \sigma(\bar{\sigma}) \sim M_G$. The reason is the large number of Higgs fields populating the would-be intermediate scale

Figure 2.1: The basic breaking chains driving the minimal SUSY $SO(10)$ model down to the $SU(3)_c \otimes U(1)_Q$. The quantum numbers of the Higgs multiplets responsible for the intermediate breakings are those of the Pati-Salam subgroup $SU(4)_{PS} \otimes SU(2)_L \otimes SU(2)_R$. If the VEVs of the 210_H components are spread enough, there could be a cascade of intermediate steps (the up-left to right-down diagonal). However, the gauge coupling unification strongly prefers one-step breaking with all the rank-5 subgroups broken at around $\mu \sim M_G$, c.f. [69].



driving the $U(1)_{B-L}$ coupling to blow³ so fast that the unification point is achieved well before 2×10^{16} GeV, in contradiction with the proton lifetime bounds.

2.2.2 R-parity conservation

Another remarkable feature of the minimal SUSY $SO(10)$ model is the automatic R-parity conservation along all the symmetry breaking chains, up to the low energies. It stems from the fact that the intermediate $B - L$ symmetry breakdown is achieved by the VEVs of the $(10, 1, 3)$ components of $\overline{126}_H$ (plus the conjugate ones) and therefore $B - L$ changes always by 2 units. Thus the R-parity defined as

$$R = (-1)^{3(B-L)+2S} \quad (2.4)$$

³One usually expects a new type of strongly coupled dynamics to resolve the problem of the Landau pole appearing rather close above the unification scale.

remains a good symmetry and the lightest neutralino is automatically stable providing for a viable cold dark matter candidate.

2.2.3 $SU(2)_L \otimes SU(2)_R$ triplets and Majorana masses of neutrinos

The situation in the Majorana part of the neutrino sector is governed by the VEVs of the $\overline{126}_H$ -components. In particular, the nonzero value of $\langle (10, 1, 3)_{\overline{126}} \rangle = \bar{\sigma} \equiv v^s$ propagates to the effective type-I ($SU(2)_L$ -singlet) Majorana neutrino entry of the form⁴

$$Y_{126}(\overline{4}, 1, 2)_{16}(\overline{4}, 1, 2)_{16} \langle (10, 1, 3)_{\overline{126}} \rangle \rightarrow Y_{126}(1, 1, 0)_{16}(1, 1, 0)_{16} \langle (1, 1, 0)_{\overline{126}} \rangle \quad (2.5)$$

$$\ni (Y_{126}v^s)N_L^{cT}C^{-1}N_L^c + h.c.$$

Moreover, one can see that there is also a small VEV induced on the left-right ‘‘mirror’’ component of this triplet, namely $\langle (\overline{10}, 3, 1)_{\overline{126}} \rangle$. Indeed, using the F-term identities coming from the $10_H 126_H 210_H$ and $M_{126} \overline{126}_H 126_H$ terms in the Higgs superpotential

$$\mathcal{W}_H \ni \mathcal{O}(1)(10, 3, 1)_{126}(1, 2, 2)_{10}(\overline{10}, 2, 2)_{210} + \mathcal{O}(1)(\overline{10}, 1, 3)_{126}(1, 2, 2)_{10}(\overline{10}, 2, 2)_{210} +$$

$$+ M_{126}(10, 3, 1)_{126}(\overline{10}, 3, 1)_{\overline{126}} + M_{210}(10, 2, 2)_{210}(\overline{10}, 2, 2)_{210} \dots$$

one infers

$$F_{(10,3,1)_{126}}^\dagger \sim M_{126}(\overline{10}, 3, 1)_{\overline{126}} + (1, 2, 2)_{10}(\overline{10}, 2, 2)_{210} + \dots \quad (2.6)$$

$$F_{(10,2,2)_{210}}^\dagger \sim M_{210}(\overline{10}, 2, 2)_{210} + (1, 2, 2)_{10}(\overline{10}, 1, 3)_{126} + \dots$$

This yields

$$\langle (\overline{10}, 2, 2)_{210} \rangle \sim \frac{\langle (1, 2, 2)_{10} \rangle \langle (\overline{10}, 1, 3)_{126} \rangle}{M_{210}} = \frac{\sigma}{M_{210}} \langle (1, 2, 2)_{10} \rangle$$

and as a consequence

$$\langle (\overline{10}, 3, 1)_{\overline{126}} \rangle \sim \frac{\langle (1, 2, 2)_{10} \rangle \langle (\overline{10}, 2, 2)_{210} \rangle}{M_{126}} \sim \frac{\sigma}{M_{126} M_{210}} \langle (1, 2, 2)_{10} \rangle^2 \equiv v^T$$

is naturally strongly suppressed. Since the $SU(2)_R$ -breaking VEVs $\sigma(\bar{\sigma})$ must be close to the GUT-scale, (c.f. section 2.2.1), the $SU(2)_L$ triplet VEV v^T giving rise to the type-II Majorana entry

$$Y_{126}(\overline{4}, 1, 2)_{16}(\overline{4}, 1, 2)_{16} \langle (\overline{10}, 3, 1)_{\overline{126}} \rangle \rightarrow Y_{126}(1, 2, -1)_{16}(1, 2, -1)_{16} \langle (1, 1, +2)_{\overline{126}} \rangle \quad (2.7)$$

$$\ni (Y_{126}v^T)L_L^T C^{-1}L_L + h.c.$$

falls approximately to the right range to provide a significant correction to the traditional (singlet) seesaw formula for the light neutrinos. Notice that, in agreement with expectations, both the Majorana mass matrices are symmetric in the generation indices because of the symmetry properties of the Y_{126} matrix [30].

⁴Here the right-hand side quantum numbers are those of the $SU(3)_c \otimes SU(2)_L \otimes U(1)_Y$ group.

2.2.4 Electroweak Higgs doublets and Dirac masses of matter fermions

As we have seen in section 2.1.2. after the GUT-scale SSB there are in general 4 multiplets with the quantum numbers of the MSSM Higgs doublets. In the $SU(4)_{PS} \otimes SU(2)_L \otimes SU(2)_R \rightarrow SU(3)_c \otimes SU(2)_L \otimes U(1)_Y$ notation, they are

$$\begin{aligned}
(1, 2, 2)_{10} &\rightarrow (1, 2, -1)_{10} \oplus (1, 2, +1)_{10} \\
(15, 2, 2)_{\overline{126}} &\rightarrow (1, 2, -1)_{\overline{126}} \oplus (1, 2, +1)_{\overline{126}} \oplus \dots \\
(15, 2, 2)_{126} &\rightarrow (1, 2, -1)_{126} \oplus (1, 2, +1)_{126} \oplus \dots \\
(10, 2, 2)_{210} &\rightarrow (1, 2, -1)_{210} \oplus \dots \\
(\overline{10}, 2, 2)_{210} &\rightarrow (1, 2, +1)_{210} \oplus \dots
\end{aligned}$$

Therefore, the spectrum of each of the $Y_W = \pm 1$ components is encoded in a 4×4 mass matrix M_{\pm} . By minimal finetuning (enforcing $\det M_{\pm} = 0$) one obtains a pair of the light electroweak Higgs doublets as an admixture of all these components⁵

$$H_{\pm} = V_{\pm}^{1j} \phi_{\pm}^j \quad (2.8)$$

where ϕ is a vector with components

$$\phi_{\pm} \equiv [(1, 2, \pm 1)_{10}, (1, 2, \pm 1)_{\overline{126}}, (1, 2, \pm 1)_{126}, (1, 2, \pm 1)_{210}],$$

and V_{\pm} are unitary mixing matrices. When the light Higgs doublets receive electroweak VEVs, due to the mixing in eq. (2.8) the following effective VEVs are generated on the relevant $SO(10)$ components:

$$\begin{aligned}
\langle (1, 2, \pm 1)_{10} \rangle &= (V_{\pm}^{\dagger})^{11} \langle H_{\pm} \rangle \equiv v_{u,d}^{10} \\
\langle (1, 2, \pm 1)_{\overline{126}} \rangle &= (V_{\pm}^{\dagger})^{21} \langle H_{\pm} \rangle \equiv v_{u,d}^{126}
\end{aligned}$$

Thus, in general, there are 4 distinct (in general complex) VEV parameters entering the effective mass matrices in the minimal SUSY $SO(10)$ model, see section 3.1.

2.3 Minimal SUSY $SO(10)$ GUT - summary

As was argued in previous sections, there should be at least two distinct Higgs multiplets in a potentially realistic $SO(10)$ framework to drive the proper spontaneous symmetry breaking chain down to the $SU(3)_c \otimes U(1)_Q$ level (a typical example is $\overline{126}_H$ and 210_H of the minimal model, plus 126_H in the SUSY context to preserve D-flatness at the GUT scale). On top of that, at least one additional Higgs representation (either 10_H ,

⁵Without loss of generality the lightest state in the mass basis is placed to the 1st position.

$\overline{126}_H$ (if not already present) or 120_H) must be put in to get a potentially realistic flavour structure (the traditional choice is 10_H). The minimal SUSY $SO(10)$ model is *by definition* equipped by one 10_H , one pair of $\overline{126}_H \oplus 126_H$ and one copy of 210_H in the Higgs sector. The Higgs part of the superpotential reads

$$\begin{aligned} \mathcal{W}_H = & M_{10} 10_H^2 + M_{126} 126_H \overline{126}_H + M_{210} 210_H^2 + \\ & + \lambda 210_H^3 + \eta 210_H 126_H \overline{126}_H + \alpha 10_H 126_H 210_H + \beta 10_H \overline{126}_H 210_H \end{aligned} \quad (2.9)$$

The effective matter fermion masses and mixings are driven by the doublets (the Dirac entries) contained in all these three irreps and $SU(2)_L \otimes SU(2)_R$ triplets (the Majorana entries for neutrinos) residing in $\overline{126}_H$. After the GUT-scale SSB all the doublets mix to give rise to the light (MS)SM-like effective Higgs doublets that receive the electroweak VEVs. The direction of these VEVs in the space of the various doublet components is “distributed” among all the relevant $SO(10)$ components. Subsequently, two of them (10_H and $\overline{126}_H$) transmit this information into the effective Yukawa vertices descending from the Yukawa part of the superpotential

$$\mathcal{W}_Y = Y_{10} 16_F 16_F 10_H + Y_{126} 16_F 16_F \overline{126}_H \quad (2.10)$$

giving rise to the typical effective Yukawa pattern [67]

$$\begin{aligned} Y_u v_u &= Y_{10} v_u^{10} + Y_{126} v_u^{126} \\ Y_d v_d &= Y_{10} v_d^{10} + Y_{126} v_d^{126} \\ Y_\nu v_u &= Y_{10} v_u^{10} - 3Y_{126} v_u^{126} \\ Y_l v_d &= Y_{10} v_d^{10} - 3Y_{126} v_d^{126} \end{aligned} \quad (2.11)$$

As far as the left-right triplets of $\overline{126}_H \oplus 126_H$ are concerned, upon the $U(1)_{B-L}$ breaking they generate Majorana entries for neutrinos

$$\begin{aligned} M_\nu^s &= Y_{126} \langle (1, 1, 0)_{\overline{126}} \rangle \\ M_\nu^t &= Y_{126} \langle (1, 3, +2)_{\overline{126}} \rangle \end{aligned} \quad (2.12)$$

giving rise to the general (type-II) seesaw pattern, c.f. page 8. Both these contributions are proportional to a single (symmetric) Yukawa matrix Y_{126} . These 6 relations are the main subject of a detailed analysis given in the next chapter.

2.3.1 Minimal SUSY $SO(10)$ - parameter counting

It is very instructive to compare the predictive potential of the two basic minimal GUTs – the minimal SUSY $SU(5)$ and $SO(10)$ models– by means of a simple parameter

counting. In section 1.1.3 the 21 parameters of minimal SUSY $SU(5)$ were identified [34]. To make the model potentially realistic, the neutrino Majorana masses should be added, as discussed in brief in section 1.2.1. This exactly doubles the freedom, i.e. in the realistic version of SUSY $SU(5)$ we are left with 42 free parameters (plus soft terms) [34]. In contrast to this, the minimal SUSY $SO(10)$ contains only 26 parameters : there are 15 independent real quantities in the Yukawa sector (one of the symmetric matrices Y_{10} and Y_{126} can be made diagonal and real while the other one remains symmetric and complex), 10 others in the Higgs potential (four of the 7 complex parameters can be made real upon redefining the Higgs fields) and one gauge coupling. That is why the minimal SUSY $SO(10)$ is often concerned the simplest realistic grand unified framework [34].

For more details on other interesting features and issues that must have been avoided in this brief description of the minimal SUSY $SO(10)$ scenario, the interested reader is deferred to the wealth of comprehensive studies and reviews given in the literature, for instance [34, 40, 41, 44, 63, 64, 65, 66, 69, 70, 71, 72, 73, 74, 75, 76] and in references therein.

Chapter 3

Quark and lepton masses and mixing in minimal SUSY $SO(10)$

As it was argued in the previous chapter, the minimal SUSY $SO(10)$ model is constructed in such a way to account for a potentially realistic description of the quark and lepton spectra and mixing patterns. With two Higgs multiplets 10_H and $\overline{126}_H$ coupled to the fermionic bilinear $16_F 16_F$ there are only two (in general complex) symmetric Yukawa matrices [30] parametrizing all the effective (Dirac and Majorana) mass matrices of the MSSM, the effective low-energy limit of this scheme. Recall that standard approach to tackle the correlations among the quark and lepton masses and mixing parameters in general schemes consists in imposing additional assumptions on the flavor structure of the Yukawa couplings descending usually from a class of horizontal symmetries.

On the other hand, the scope of this chapter is a detailed analysis of the correlations arising in the minimal SUSY $SO(10)$ GUT scheme without any such additional constraints. Though not as sharp in predictions as the simplified setups, there are still interesting correlations coming from the Higgs structure of the model, that could lead to valuable clues for better understanding some of the peculiarities in the quark and lepton mass and mixing pattern.

3.1 Minimal SUSY $SO(10)$ Yukawa sum-rules

Using the shorthand notation for the VEVs of various Higgs doublets in the game

$$v_u^{10} \equiv \langle (1, 2, +1)_{10} \rangle, \quad v_u^{126} \equiv \langle (1, 2, +1)_{\overline{126}} \rangle, \quad v_d^{10} \equiv \langle (1, 2, -1)_{10} \rangle, \quad v_d^{126} \equiv \langle (1, 2, -1)_{\overline{126}} \rangle$$

and similarly for the physical MSSM neutral light Higgs doublets $H_{u,d}$ ¹

$$v_u \equiv \langle H_u \rangle, \quad v_d \equiv \langle H_d \rangle \quad (3.1)$$

one arrives to the traditional set of equalities for the effective quark and lepton Dirac Yukawa couplings [68]

$$\begin{aligned} Y_u v_u &= Y_{10} v_u^{10} + Y_{126} v_u^{126} && \equiv M_u \\ Y_d v_d &= Y_{10} v_d^{10} + Y_{126} v_d^{126} && \equiv M_d \\ Y_\nu v_u &= Y_{10} v_u^{10} - 3Y_{126} v_u^{126} && \equiv M_\nu^d \\ Y_l v_d &= Y_{10} v_d^{10} - 3Y_{126} v_d^{126} && \equiv M_l \end{aligned} \quad (3.2)$$

On top of that, the $SU(2)_R$ breaking VEV of the neutral component of the right-handed triplet (denoted by its SM quantum numbers $(1, 1, 0)_{\overline{126}}$) and the induced VEV of the $SU(2)_L$ triplet $(1, 3, +2)_{\overline{126}}$ give rise to the following relations for the Majorana entries in of the neutrino mass matrix ([39]):

$$\begin{aligned} M_\nu^s &= Y_{126} \langle (1, 1, 0)_{\overline{126}} \rangle \sim M_R \\ M_\nu^t &= Y_{126} \langle (1, 3, +2)_{\overline{126}} \rangle \sim \frac{v^2}{M_R} \end{aligned} \quad (3.3)$$

The important “−3” factor in relations (3.2) is a Clebsch-Gordon coefficient coming from the fact that the weak-scale VEV in $\overline{126}_H$ points in the $(1, 1, 1, -3)$ direction in the Pati-Salam subgroup [77]. More details and comments on this key feature of $\overline{126}_H$ can be found in Appendix B.5.

3.1.1 Light neutrino masses

The light physical neutrino masses descend from the 6×6 Dirac-Majorana mixing matrix of the form

$$M = \begin{pmatrix} M_\nu^t & M_\nu^{dT} \\ M_\nu^d & M_\nu^s \end{pmatrix} \quad (3.4)$$

If $|M_\nu^d| \ll |M_\nu^s|$ the relevant effective neutrino mass matrix is given by the renowned seesaw formula [78, 79, 80, 81, 82, 83, 84]

$$M_\nu \sim M_\nu^t - M_\nu^{dT} (M_\nu^s)^{-1} M_\nu^d \quad (3.5)$$

Recall that, unlike in the Standard Model, all the physical Yukawa and light neutrino mass matrices are given in terms of just two complex *symmetric* matrices and few

¹The quantum numbers correspond to the decomposition of the considered multiplets under the $SU(3)_c \otimes SU(2)_L \otimes U(1)_Y$ subgroup of $SO(10)$.

additional parameters. However, not all these parameters are independent² and, as a matter of fact, the number of physically relevant entries is so small that putting into eqs. (3.2)–(3.3) all information about the quark and lepton spectra and CKM mixing the system becomes overconstrained and the other parameters could be, at least in principle, predicted. To see this more explicitly, recall the beautiful formula for the neutrino mass matrix in case of the triplet component dominating in eq. (3.5)

$$M_\nu = M_\nu^t \propto M_d - M_l. \quad (3.6)$$

It is easy to see that once the charged lepton masses are reconstructed fitting the quark sector by means of the first two relations in 3.2, the type-II neutrino mass matrix is fully reconstructed!

3.1.2 Partial diagonalization and phasecounting

In general, all entries in relations (3.2) and (3.3) are complex as Y_{10} and Y_{126} are generic 3×3 symmetric matrices in the generation space³. However, it is easy to see that not all 32 parameters giving rise to these structures are independent.

First, one can always consider only the *combinations* of Y_x and v_x as the basic building blocks and shuffle freely their internal phases so that the overall ones remain untouched. In other words, by redefining properly the global phases of Y_{10} and Y_{126} we can forget about the phases of one of v_u^{10} and v_d^{10} and one of v_u^{126} and v_d^{126} . Second, one can always perform a rotation into a basis in which one of Y_{10} and Y_{126} (or a suitable combination) is real and diagonal. Therefore, in the most general case we are left with 8 phases. However, if one of the type-I or type-II contributions in the seesaw formula (3.5) becomes irrelevant, an additional phase drops out.

To be more explicit let us look at the effective structure of the quark and lepton mass matrices arising from the effective Yukawa interactions

$$\mathcal{L}_Y = \overline{Q}_L Y_u U_R H_u + \overline{Q}_L Y_d D_R H_d + \overline{L}_L Y_\nu N_R H_u + \overline{L}_L Y_l E_R H_d + h.c. \quad (3.7)$$

Inverting the sum-rules (3.2) one can rewrite the leptonic Yukawas in terms of the quark ones as

$$Y_l = \alpha Y_u + \beta Y_d \quad \text{and} \quad Y_\nu = \alpha' Y_u + \beta' Y_d \quad (3.8)$$

where α , β , α' and β' are meromorphic functions of $v_{u,d}^{10,126}$. In the next step one can use the symmetry property of the matrices under consideration and diagonalize each

²For instance, one can get rid of off-diagonal entries in one of these matrices by choosing a proper basis etc., for more details see section 3.1.2.

³Recall that also the induced VEVs $v_{u,d}^{10,126}$ arise from the light MSSM Higgs doublets by means of unitary transformations parametrizing the misalignment of the $SO(10)$ and the mass bases.

of them by means of a unitary transformation

$$Y_x = U_x^T Y_x^D U_x \quad (3.9)$$

fixing the diagonal elements of Y_x^D to be real and positive.⁴ Redefining the quark fields

$$\bar{Q}'_L \equiv \bar{Q}_L U_d^T, \quad U'_R \equiv U_u U_R \quad \text{and} \quad D'_R \equiv U_d D_R$$

one arrives to

$$\begin{aligned} \mathcal{L}_Y &= \bar{Q}'_L V^T Y_u^D U'_R H_u + \bar{Q}'_L Y_d^D D'_R H_d + \bar{L}_L U_d^T (\alpha' V^T Y_u^D V + \beta' Y_d^D) U_d N_R H_u + \\ &+ \bar{L}_L U_d^T (\alpha V^T Y_u^D V + \beta Y_d^D) U_d E_R H_d + h.c. \end{aligned} \quad (3.10)$$

where $V \equiv U_u U_d^\dagger$ is the “raw” Cabibbo-Kobayashi-Maskawa matrix, that (as any general unitary matrix) can be decomposed in terms of the “standard form” V_{CKM} and five additional phases

$$V = P_L V_{CKM} P_R$$

where

$$V_{CKM} = \begin{pmatrix} c_{12}c_{13} & s_{12}c_{13} & s_{13}e^{-i\delta} \\ -c_{23}s_{12} - s_{23}s_{13}c_{12}e^{i\delta} & c_{23}c_{12} - s_{23}s_{13}s_{12}e^{i\delta} & s_{23}c_{13} \\ s_{23}s_{12} - c_{23}s_{13}c_{12}e^{i\delta} & -s_{23}c_{12} - c_{23}s_{13}s_{12}e^{i\delta} & c_{23}c_{13} \end{pmatrix}$$

and

$$P_L \equiv \begin{pmatrix} e^{i\delta_1} & & \\ & e^{i\delta_2} & \\ & & e^{i\delta_3} \end{pmatrix}, \quad P_R \equiv \begin{pmatrix} e^{i\delta_4} & & \\ & e^{i\delta_5} & \\ & & 1 \end{pmatrix} \quad (3.11)$$

The lepton Yukawa matrices can be then written in the form (redefinig $\bar{L}'_L \equiv \bar{L}_L U_d^T$, $N'_R \equiv U_u N_R$ and $E'_R \equiv U_d E_R$)

$$\begin{aligned} Y'_l &= |\alpha| e^{i\phi_\alpha} P_R V_{CKM}^T P_L^2 Y_u^D V_{CKM} P_R + |\beta| e^{i\phi_\beta} Y_d^D \\ Y'_\nu &= |\alpha'| e^{i\phi_{\alpha'}} P_R V_{CKM}^T P_L^2 Y_u^D V_{CKM} P_R + |\beta'| e^{i\phi_{\beta'}} Y_d^D \end{aligned} \quad (3.12)$$

Finally, one can divide these equalities by $e^{i\phi_\beta}$ and $e^{i\phi_{\beta'}}$ respectively and absorb one of the relative phases of α and β parameters, say $e^{i(\phi_\alpha - \phi_\beta)}$, in the redefinition of P_L . However, the remaining $e^{i(\phi_{\alpha'} - \phi_{\beta'})}$ factor persists and acts as an additional phase factor to be taken into account whenever both Y_l and Y_ν enter one formula, as for instance if none of the type-I nor type-II seesaw contributions are neglected.

⁴This can always be done by “distributing” the would-be phases of the diagonal elements into the unitary matrices U_x .

To conclude, there are always 6 phases to deal with (the CKM phase δ_{CKM} and 5 phases $\delta_{1,2,\dots,5}$ in P_L and P_R) fitting the charged lepton masses (in such a case the overall $e^{-i\phi_\beta}$ does not play any role). If, subsequently, this information is passed to seesaw formula, the “ $e^{-i\phi_\beta}$ ambiguity” reappears and must be taken into account as the 7th phase. On top of that, the 8th phase ($e^{i(\phi_{\alpha'} - \phi_{\beta'})}$) starts to play a role if both the type-I and type-II terms in the neutrino mass formula (3.5) are considered. This confirms the expectations drawn at beginning of this section.

3.1.3 Number of real parameters

Apart from the 8 phases identified in the previous section there are additional 13 real parameters on the right hand side of eq. (3.12): 3+3 diagonal quark Yukawa entries, 3 CKM mixing angles and 4 absolute values of the α , α' and β , β' parameters. On top of that one must add two unknown values of singlet and triplet VEVs parametrizing the overall scale of the Majorana entries in eq. (3.5) (though, in principle, there could be constraints on M_R from the gauge running and the triplet VEV is computable once we fix the superpotential). Altogether, 23 real parameters.

In general, there are 22 independent measurable quantities in the quark and lepton sector : 6 quark masses, 3 CKM angles and 1 CKM phase, 6 lepton masses, 3 PMNS mixing angles and 3 phases (1 Dirac and 2 Majorana). In reality, there are only upper bounds on absolute light neutrino mass scale and from oscillation experiments we are able to deduce only the neutrino mass-squared differences and the PMNS mixing angles. Moreover, so far we have practically no information on the 3 phases in the leptonic sector. Thus, the relatively “reliable” set of input data consists of 18 experimental results.

At the first glance this looks like a “no-go” for any strong correlations among the quark and lepton sector of the minimal SUSY SO(10) as there are 5 pending variables. Despite this, as we shall see, performing a careful and detailed analysis with reasonable constraints imposed on some of the parameters, one can obtain interesting results that can be experimentally tested. This is namely because of the particular structure of the sum-rules (3.2) and (3.3).

As an example consider the possible role of the 5 unconstrained phases in the charged lepton sum rule (3.12) rewritten in a convenient form [40, 44, 70]

$$\tilde{M}'_l \propto V_{CKM}^T \tilde{D}_u V_{CKM} + r \tilde{D}_d. \quad (3.13)$$

Here the $\delta_{1,2,\dots,5}$ phases of eq. (3.11) were reshuffled into the matrices $\tilde{D}_{u,d}$ that are diagonal and normalized so that $\|[\tilde{D}_{u,d}]_{33}\| = 1$, r is a function of the α and β parameters in eq. (3.12) and the ratio of the $b-$ and $\tau-$ Yukawa couplings. Since the overall normal-

ization of the left hand side remains undetermined, only the charged lepton ratios can be fitted from this relation. But, remarkably enough, this can turn impossible despite the 5 phases ($\delta_{1,2,\dots,5}$) one has at hand if for example r , for whatever reason, becomes small enough so that the second term is not able to modify substantially the wrong charged lepton hierarchy descending from the first term, regardless the values of the 5 phases therein. Another example of irrelevance of some big regions of the parametric space can be observed in the strong suppression of the effects of the δ_1 phase (sometimes called δ_u [45]) that is always accompanied by a factor of 10^{-5} order stemming from the hierarchy of the up-quark diagonal Yukawa entries.

Another important source of possible suppressions of the sensitivity on the input parameters refers to the highly nonlinear nature of the relations among the free parameters and the quantities of our interest ⁵. Alternatively, a serendipity of accidental cancellations can make some of the relevant relations exceptionally simple. A particular realization of the first option shall be identified in the peculiar behaviour of the electron mass formula, see section 3.6.1, while the second plot can be observed in the simplicity and a robustness of the relation for the $|U_{e3}|$ PMNS mixing parameter, c.f. section 3.3.2.

In any case, it is very difficult to draw a general conclusion on the predictive power of the minimal renormalizable SUSY SO(10) in the Yukawa sector and only a careful numerical (or within more constrained setups even semianalytical) treatment can give us a definite answer to this profound question.

Prior approaching the general case in full complexity let us try to digest several limiting cases obtained under few simplifying (though well motivated) assumptions. In particular, in the first part of this chapter we shall stick to the setup where all the relevant phases become real. Remarkably enough, even such a constrained scheme (up to the obvious lack of capability to describe the effects of CP-violation in the quark and lepton sector in the CKM manner⁶) still poses very good fits of all 17 relevant physical measurables ⁷ though the number of input parameters does not exceed 15 in case of a general seesaw formula with both singlet and triplet contributions of comparable sizes, and even 14 if one of them is neglected. Thus, in such a case the scheme is highly overconstrained and predicts rather sharp correlations among the quark and lepton masses and mixings.

⁵For instance the diagonalization procedure giving rise to the fermionic spectra and mixing angles, the presence of the inverse singlet Majorana mass matrix in the type-I seesaw formula etc.

⁶Let us assume that in such a case the CP-violation originates entirely from other sectors of the model.

⁷6 quark and 3 charged lepton masses, 2 neutrino mass square differences, 3 CKM and 3 PMNS mixings.

3.2 Large atmospheric mixing and $b - \tau$ unification in case of triplet dominated seesaw

Another assumption leading to major simplification and rise of the predictive power of the scheme is the case of a dominant triplet seesaw contribution in the light neutrino mass matrix (3.5). In such a case there is a nice link [39, 72] between the large atmospheric mixing in the leptonic sector and the convergence of the b -quark and τ -lepton Yukawa couplings around the GUT-scale ($b - \tau$ unification). As a matter of fact, eq. (3.13) together with (3.6) imply that in the basis fixed by eq. (3.13), the charged lepton mass matrix becomes almost diagonal and the PMNS mixings are encoded predominantly in M_ν . The 2-3 block of the neutrino mass matrix in such a case reads (up to the phases)

$$M_\nu \propto m_\tau \begin{pmatrix} \mathcal{O}(\lambda^2) & \mathcal{O}(\lambda^2) \\ \mathcal{O}(\lambda^2) & 1 - \frac{m_b}{m_\tau} \end{pmatrix}$$

where λ is the Wolfenstein symbol for $\sin \theta_C$. Clearly, large atmospheric mixing requires $\mathcal{O}(\lambda^2)$ cancellation between m_b and m_τ . On more formal grounds, the interplay among the quark and lepton 2-3 mixing angles and the 3rd generation down-type Yukawa couplings fits nicely the semianalytic formula derived in [39]⁸:

$$\tan 2\theta_{23} \doteq \frac{2 \sin \phi_{23}}{2 \sin^2 \phi_{23} - \frac{m_b - m_\tau}{m_b}}$$

It is remarkable (though far from obvious) that this neat interplay is only softly affected if one takes into account the effects of the first generation [72]. Moreover, there are strong hints that the type-I contribution in eq. (3.5) (at least in the real case) can not account for the dominant source of the neutrino masses and mixing [72, 37, 38]. This provides an interesting option to reduce the number of free parameters entering the subsequent numerical analysis as two of them (the relative phase and magnitude of the two terms in the seesaw formula) drop out. Moreover, the analytical structure of the triplet dominated neutrino mass matrix (3.6) is much simpler than in general or in the singlet dominated case.

3.3 Quark and lepton mass and mixing correlations in minimal SUSY SO(10) with dominant triplet seesaw

However, even adopting these simplifying assumptions, the number of the remaining free parameters remains such that a general analysis is very involved and any additional

⁸Here ϕ_{23} stands for the 2-3 mixing angle in the quark sector.

information originating from an analytic treatment is highly welcome. Unfortunately, as we shall see, there are only few such clues and the major part of the information can be obtained only in a detailed numerical survey.

Let us start by specifying the set of input parameters and outputs of our interest. As usual, the input consists of measurables on which we have a relatively detailed information – the quark and charged lepton masses (or, equivalently the entries of the corresponding diagonalized Yukawa mass matrix) and the CKM mixing angles (plus the CKM CP-violating phase δ_{CKM} in the complex case). So far 12 parameters (or 13 if CP is violated in the quark sector) . All these input data are known with certain accuracy that must be taken into account in any quantitative analysis. The outputs of our major interest is the shape of the neutrino spectrum (in terms of the relevant mass-square differences) and mixing angles in the leptonic sector, in total 5 quantities⁹ (and 8 if the Dirac and Majorana CP-phases are concerned).

Finally, notice that all the physical parameters are determined at around the electroweak scale while the effective sum-rules (3.2) are valid at the scale of the $SO(10)$ breakdown. Thus, all the input parameters must be evolved from low energies up to the GUT scale subject to the standard MSSM renormalization group equations¹⁰. Similarly, any results obtained at the GUT-scale must be run down prior being compared with the experimental data.

3.3.1 Partial semianalytic treatment - real case

It is remarkable, that in the CP conserving case (using the quark sector data as the input) there are only 2 additional parameters in the sum-rule for the charged lepton mass matrix, namely (in the “standard” notation of refs. [40, 41, 44])

$$k\tilde{M}'_l = V_{CKM}^T \tilde{D}_u V_{CKM} + r\tilde{D}_d \quad (3.14)$$

Here r and k are functions of the third generation quark and charged lepton masses and the α and β parameters of eq. (3.8). Each of the tilded matrices is normalized to its maximal eigenvalue

$$\tilde{D}_u = \text{diag} \left(\frac{m_u}{m_t}, \frac{m_c}{m_t}, 1 \right) S_u, \quad \tilde{D}_d = \text{diag} \left(\frac{m_d}{m_b}, \frac{m_s}{m_b}, 1 \right) S_d$$

⁹However, there is nothing fundamental about this choice; we might have as well chosen the lepton data as the input (plus some additional set of parameters either from the quark sector and/or the ones that do not have physical interpretation at the level of the SM – the $\delta_{1,2,\dots,5}$ phases or α_i and β_j) and study the correlations in the quark sector. On the other hand, the information from the quark sector is particularly suitable as an input as it brings only a relatively small amount of experimental uncertainty and allows to draw immediate conclusions on the lepton mixing.

¹⁰Since the minimal SUSY $SO(10)$ strongly prefers one-step breaking scenarios, MSSM is a valid effective theory up to the GUT scale.

Notice that even if CP is conserved there is still a freedom in 6 signs descending from $\delta_{1,2,\dots,5}, \delta_{CKM} = 0, \pi$. This freedom is encoded in the “sign matrices” $S_u \equiv \text{diag}(\delta_1, \delta_2, \delta_3) = (\pm 1, \pm 1, \pm 1)$ and $S_d = \text{diag}(\delta_4, \delta_5, 1) = (\pm 1, \pm 1, \pm 1)$.

In spite of this freedom the system (3.14) is overconstrained and the fit becomes nontrivial [37]. The parameters k and r must be tuned to fit the charged lepton masses in eq. (3.14). The equality of LHS and RHS traces implies $k = 1 + r + \mathcal{O}(\lambda^2)$. It turns out (see e-print of ref. [40]) that a better fit of the atmospheric mixing is obtained for $\delta_5 = \pi$ (i.e. “effectively” $m_s < 0$) and $\delta_1 = 0$ (i.e. $m_\mu > 0$). In this case, the requirement of reproducing the correct value of m_μ/m_τ leads to $k \sim 0.25$ and $r \sim -0.75$.

3.3.2 Constraints on the lepton mixing with dominant triplet seesaw

In the same basis, the triplet dominated light neutrino mass matrix receives the following form:

$$M'_\nu = m_0 \left(\tilde{M}'_l - \frac{m_b}{m_\tau} \tilde{D}_d \right) \quad (3.15)$$

where m_0 is an overall neutrino mass scale possibly determined from the analysis of the Higgs potential. Given r, k for a given choice of S_u and S_d ¹¹, the right-hand side of eq. (3.15) is completely determined and defines the neutrino mass matrix up to an overall mass scale.

In order to provide a simple analytical understanding of the predictions in the lepton sector, let us assume for the time being $k = 0.25$ and $r = -0.75$ exactly¹². Using the Wolfenstein parametrization of V_{CKM} and neglecting $\mathcal{O}(\lambda^4)$ terms the charged lepton mass matrix exhibits a hierarchical structure

$$\tilde{M}'_l = \begin{pmatrix} 0 & 0 & 4V_{td} \\ \dots & -3\frac{m_s}{m_b} & 4V_{ts} \\ \dots & \dots & 1 \end{pmatrix} \quad (3.16)$$

while the hierarchy in the neutrino mass matrix is broken by the $b - \tau$ unification¹³:

$$M'_\nu = m_0 \begin{pmatrix} 0 & 0 & 4V_{td} \\ \dots & -\left(\frac{m_b}{m_\tau} + 3\right) \frac{m_s}{m_b} & 4V_{ts} \\ \dots & \dots & 1 - \frac{m_b}{m_\tau} \end{pmatrix} \quad (3.17)$$

¹¹As a matter of fact, for general choice of S_u and S_d a pair of r and k giving rise to a good fit of formula (3.14) need not exist at all.

¹²Detailed variations in k and r shall be taken into account in the numerical fit discussed in section 3.5.

¹³Here we use the convention in which V_{ts} and m_s are negative while V_{td}, m_b and m_τ positive.

It is impressive that the structure of these matrices reflects qualitatively all the basic features of lepton masses and mixings. In this basis, the contributions to the leptonic mixing angles generated by diagonalization of \tilde{M}'_l are small and

$$\left| \frac{m_\mu}{m_\tau} \right| \approx 3 \frac{m_s}{m_b} + 16 V_{ts}^2 .$$

Therefore, both large 1-2 and 2-3 mixing should be contained in M'_ν . Indeed, this is the case since the elements in the 2-3 block of M'_ν can be taken of the same order (dominant $\mu - \tau$ block) and the 1-3 element is automatically smaller. As a consequence [85], the spectrum of neutrinos is predicted to be with *normal hierarchy*.

Another important point can be made on the approximate value of the 1-3 mixing in the neutrino sector. Due to the particular texture of the neutrino mass matrix (3.17) one can write approximately¹⁴ [41]

$$\sin \theta'_{13} \sim \frac{(M'_\nu)_{13}}{(M'_\nu)_{33} - (M'_\nu)_{11}} \sim \frac{4V_{td}}{1 - \frac{m_b}{m_\tau}} \quad (3.18)$$

Clearly, there is an anticorrelation between the the $b - \tau$ unification precision and the smallness of the U_{e3} entry of the neutrino mixing matrix.

In ref. [72] an exact computation of the leptonic 2-3 mixing is performed for the present model in the case of two generations. The authors find two classes of solutions with large atmospheric mixing: one corresponds to the scenario described above: \tilde{M}'_l hierarchical and $b - \tau$ unification inducing large 2-3 mixing in M'_ν . The second solution corresponds to $r \approx -1$ (and $|k| \ll 1$), leading to a cancellation in the 33-entry of \tilde{M}'_l . However, it can be easily shown that this possibility is spoiled by a three generation analysis. In fact, one finds that in this case the charged lepton mass matrix has the form

$$\tilde{M}'_l|_{r \approx -1} = -\frac{m_b}{m_s a} \begin{pmatrix} 0 & 0 & V_{td} \\ \dots & -\frac{m_s}{m_b} & V_{ts} \\ \dots & \dots & -\frac{V_{ts}^2 m_b}{m_s} \end{pmatrix} + \mathcal{O}(\lambda^4) , \quad (3.19)$$

where $a \approx (1 + V_{ts}^2 m_b^2 / m_s^2)$ is of order unity. This structure can be suitable to generate a small m_μ / m_τ in the case of two generations, but since the determinant of \tilde{M}'_l is of order λ^2 , it is clear that the hierarchy $m_e \div m_\mu \div m_\tau \approx \lambda^5 \div \lambda^2 \div 1$ cannot be reproduced.

Let us analyze in some detail eqs. (3.16)–(3.17). The matrices \tilde{M}'_l and M'_ν depend (in this approximation) only on four quark parameters (V_{td} , V_{ts} , m_s/m_b , m_b/m_τ) that

¹⁴The superscript ν denotes quantities derived from M'_ν only. Though they corresponds to large extend to the physical PMNS mixing angles, the corrections coming from the mixing contained in \tilde{M}'_l can be important, c.f. formula (3.22).

are required to reproduce five parameters in the leptonic sector (m_μ/m_τ , $\Delta m_\odot^2/\Delta m_A^2$, θ_{12} , θ_{13} and θ_{23}). The first generation masses m_e and m_1 are sensitive also to sub-leading terms neglected in eqs. (3.16)–(3.17). Since the quark parameters are known with small uncertainties, there is very small freedom to fit lepton data. Notice that, in good approximation, one can compare directly the neutrino masses and mixing angles obtained from eq. (3.17) at the GUT scale with the experimental values at the electroweak scale. As a matter of fact, in the case of normal hierarchy, the RGE running of the neutrino mass matrix has a negligible effect on mass squared differences and mixings [86, 87, 88].

Concerning the contributions to the mixing angles arising from \tilde{M}'_l and M'_ν , since $4|m_s/m_b| \sim 4|V_{ts}| \lesssim \lambda$, the 2-3 mixing in M'_ν is generically of order unity if $b - \tau$ unification is realized to $\mathcal{O}(\lambda^2)$ accuracy. Moreover, the deviation from maximal mixing tends to increase with $\Delta m_\odot^2/\Delta m_A^2$. The 1-3 mixing in M'_ν is given roughly by [85]

$$\sin 2\theta_{12}^\nu \sim \frac{8V_{td}}{1 - \frac{m_b}{m_\tau}} \left(\frac{\Delta m_\odot^2}{\Delta m_A^2} \right)^{-\frac{1}{2}} \sin \theta_{23}^\nu \cos^2 \theta_{23}^\nu = \mathcal{O}(1) \quad (3.20)$$

It is remarkable that if one neglects the small mixing in \tilde{M}'_l , all oscillation data can be reproduced. For example, taking $m_b/m_\tau = 0.89$, $V_{ts} = -0.035$, $V_{td} = 0.011$, $m_s/m_b = -0.028$, one obtains $s_{13}^\nu \approx 0.12$, $\tan \theta_{23}^\nu \approx 0.97$, $\tan^2 \theta_{12}^\nu \approx 0.43$ and $\Delta m_\odot^2/\Delta m_A^2 \approx 0.038$. However, it turns out that the small mixing angles in \tilde{M}'_l add up to those in M'_ν in such a way to spoil the agreement with data. In fact, one can find [44]

$$\begin{aligned} \theta_{23}^l &\doteq 4V_{ts} \approx -0.14 \sim -\lambda \\ \theta_{13}^l &\doteq 4V_{td} \approx 0.04 \sim \lambda^2 \\ \theta_{12}^l &\doteq -\frac{16}{3} \frac{m_\tau}{m_\mu} V_{ts} V_{td} \approx 0.10 \sim \lambda \end{aligned}$$

The effect of the two $\mathcal{O}(\lambda)$ rotations in U_l modifies the physical mixing angles in U_{PMNS} ($\equiv U_l^T U_\nu$ in the real case) as follows:

$$\begin{aligned} \theta_{23} &\doteq \theta_{23}^\nu + \theta_{23}^l \\ \sin \theta_{13} &\doteq \sin \theta_{13}^\nu + \sin \theta_{12}^l \sin \theta_{23}^\nu \\ \sin 2\theta_{12} &\doteq \sin 2\theta_{12}^\nu \left(1 + \frac{2 \cos \theta_{23}^\nu}{\tan 2\theta_{12}^\nu} \sin \theta_{12}^l \right) \end{aligned} \quad (3.21)$$

As a consequence, to reproduce data one needs θ_{23}^ν larger than $\pi/4$, $\sin \theta_{13}^\nu$ significantly below the experimental upper bound and $\sin 2\theta_{12}^\nu$ smaller than the solar mixing value. However, both the deviation from $\theta_{23}^\nu = \pi/4$ and the suppression of $\sin 2\theta_{12}^\nu$ tend to increase the ratio $\Delta m_\odot^2/\Delta m_A^2$ above the allowed range, producing a tension between predictions and experimental data, as confirmed by the numerical study in the following sections.

3.4 Numerical analysis - general prerequisites

Prior entering the machinery of a numerical analysis the GUT-scale input data used therein should be specified. Indeed, the running effects could be rather strong, in particular for the light quark masses. For large values of $\tan\beta$ the down-quark Yukawa coupling are enhanced and their running becomes also strongly nonlinear.

3.4.1 GUT scale input parameters

Concerning the GUT-scale input values of the quark and lepton masses (or, equivalently, the corresponding Yukawa couplings) [89] we shall use the results of the analyses of Fusaoka and Koide [90, 91] and Das and Parida [92] given in Table 3.2. However, since the up-to-date experimental data in some cases (in particular for the light quarks) differ considerably from the inputs used in these studies it is worth pointing out at least the net effects of these changes on the GUT-scale parameters under consideration.

Light quark masses - $m_s(M_G)$

The latest experimental results based on better input data and perturbation methods indicate slightly smaller $m_s(2\text{GeV})$ than the older extractions. The same happens also for the recent improved lattice simulations. The current ranges are [93]:

$$\begin{aligned} \text{Experiment :} & \quad 80 \text{ MeV} \lesssim m_s(2\text{GeV}) \lesssim 155 \text{ MeV} \\ \text{Lattice :} & \quad m_s(2\text{GeV}) \sim 105 \pm 25 \text{ MeV} \end{aligned}$$

We shall use a combination of these results corresponding to roughly

$$m_s(2\text{GeV}) \sim 110 \pm 20 \text{ MeV}.$$

Evolved to the weak scale this value corresponds to $m_s(M_Z) \sim 73 \pm 20 \text{ MeV}$ that should be used as a boundary condition for an improved analysis à la Das & Parida [92]. Doing that one predicts the following approximate range for $m_s(M_G)$:

$$m_s(M_G) \sim 23 \pm 6 \text{ MeV}.$$

Light quark masses - $m_{u,d}(M_G)$

There are similar (though not so dramatic) effects arising in the recent u and d quark mass extractions [94, 95, 96] supported further by lattice studies [97, 98]. However, the net effect usually does not exceed ten percent level. Moreover, m_u and m_d , being the smallest parameters in the game, are often screened in the formulae of our interest¹⁵.

¹⁵However, there is an important exception from this rule. As we shall see in section 3.6.1, the minimal SUSY SO(10) relation for the electron mass is dominated by the down-quark mass.

Heavy quark masses - $m_{c,b,t}(M_G)$

Concerning the recent experimental heavy quark masses defined at $\mu = M_q^{pole}$ the central values did not depart much from those used in [90]. However, the errors in m_c and m_b [90] seem slightly underestimated and we take this into account in the corresponding values at the GUT-scale¹⁶.

Evolution of the CKM mixing angles

Concerning the running of the quark masses one has to take into account also the effects stemming from misalignment of the two bases in which the quark Yukawa matrices are diagonal that are encoded in the Cabibbo-Kobayashi-Maskawa mixing angles and the CKM CP-phase. The running of these parameters is usually very mild [90, 92] and the only CKM entries encountering considerable changes are those corresponding to the heaviest quarks, i.e. V_{ub} , V_{cb} , V_{tb} and V_{ts} . However, even for these parameters the corrections due to the running from M_Z to M_G never exceed roughly 15% level.

Charged lepton masses - $m_{e,\mu,\tau}(M_G)$

In comparison with quarks the situation in the leptonic sector is quite simple. The ambiguities descending from the quark thresholds enter only at higher loop level so that the evolution within the SM stage as well as in the “desert” from M_S to M_G is relatively pure. Moreover, the weak scale initial conditions are defined with a very good accuracy. Thus the main source of uncertainties affecting the predictions for $m_{e,\mu,\tau}(M_G)$ are the SUSY thresholds and running of the weak scale VEVs. Nevertheless, the errors at the GUT scale are so small that one can almost always neglect them¹⁷.

Effective GUT-scale input parameters - summary

Let us summarize the information given in the previous paragraphs. The updated values of the effective quark and lepton masses used in the numerical analysis are given in Tables 3.3 and 3.5. For sake of comparison, the 2000 data by Fusaoka & Koide and Das & Parida are presented in Table 3.2. The evolved CKM mixing angles are specified in Table 3.4.

¹⁶In case of the heavy quark errors we do not perform the full two-loop analysis; since the central values are practically untouched in the first approximation we just rescale the relevant error bars and keep only 2 significant digits for m_b in the $\tan\beta = 55$ case that is particularly sensitive to the changes of the initial conditions.

¹⁷Unless a complete χ^2 -analysis is performed.

3.4.2 Running neutrino spectrum and PMNS mixing angles

The effects of MSSM running of neutrino masses and the mixing parameters were analyzed in detail in many studies, see e.g. [86, 88] and references therein. Let us mention here just the points that are relevant for the discussions of the numerical results obtained in the subsequent parts of this work.

Running of PMNS mixing and CP phases

As we argued in the discussion following eq. (3.17), the neutrino spectrum in minimal SUSY $SO(10)$ with triplet dominated seesaw formula is always hierarchical. As a consequence, the effects of running on the leptonic mixing angles are usually very mild [88]. In particular, $|U_{e3}|$ is stable, with corrections below 1% for the whole range of $\tan\beta$ considered. The variation of the atmospheric angle is small as well, remaining below one percent for $\tan\beta = 10$ and at one percent level for $\tan\beta = 55$. The largest corrections arise for the solar angle in case of large $\tan\beta$; however, even for $\tan\beta = 55$ it does not exceed several percent level. In any case, the solar and atmospheric mixing angles tend to grow towards the weak scale.

Concerning the fate of the three CP phases in the leptonic sector the situation is more complicated and in some cases the effects of running can be substantial. In particular, the Dirac CP-phase can be quite unstable if $|U_{e3}|$ is very small. Moreover, the correlation among the Majorana phases entering here can affect the results considerably. For more information see for instance [88] and comments at the end of section 3.6.3.

Running of the neutrino spectrum

Unlike the evolution of the PMNS mixing angles, the running effects on the neutrino spectrum (in particular, the mass-squared differences) can be rather significant. However, since the overall neutrino mass scale is not specified, the relevant quantity becomes the mass-squared ratio $\Delta m_{\odot}^2/\Delta m_{\text{A}}^2$. Due to the normal hierarchy in the quark sector, running effects in the numerator and the denominator cancel to large extent and $\Delta m_{\odot}^2/\Delta m_{\text{A}}^2$ is almost constant [88].

3.4.3 χ^2 versus direct scan

Concerning the numerical methods used to inspect the correlations arising from relations (3.14) and (3.15), the traditional χ^2 -fit becomes quite nontrivial. It is namely due to the highly nonlinear nature of the formulae for the physical observables that lead to a very complicated landscape of the χ^2 minima. To make sure that none of

the potentially interesting areas is missed it is better to perform (at least in the first stage) an extensive overall scan that reveals all suspect regions and, if necessary, use the output of this method as an input for a second stage optimization.

3.5 Numerical analysis - CP conserving Yukawa sector

Let us finally approach the results of the extensive numerical survey performed at the first stage for real (CP conserving) parameters in eq. (3.2). The existing numerical analyses [40, 41] find a tension between lepton mixings and quark parameters, in agreement with the simple expectations discussed in section 3.3.2. In particular, $|U_{e3}|$ turns out to be close to the present upper bound (~ 0.15 at 90% C.L.), the atmospheric mixing can be hardly close enough to maximal ($\sin^2 2\theta_{23} \lesssim 0.9$) and the solar mixing is too large to fit the LMA MSW solution ($\sin^2 2\theta_{12} \gtrsim 0.9$). The last drawback is claimed to be relaxed tuning CP violating phases, but in disagreement with the known value of the CKM phase [41, 73].

However, the existing results were usually obtained without taking into account the uncertainties in the CKM sector of the model, or under simplifying assumptions. We performed an independent fit of the experimental data paying particular attention to the uncertainties in the input parameters [44, 45]. As a matter of fact, it is crucial to determine how far the minimal $SO(10)$ scenario can be pushed in reproducing the known fermion spectrum and mixings. Due to the complexity of the numerical analysis, we have taken advantage of the analytical results derived in the previous section to elaborate an efficient approach to the fit, while obtaining a rationale for the emerging patterns.

Up to the partial freedom in permuting the signs coming from the relevant phases, there are only 12 independent continuous parameters sufficient to specify completely the masses and mixing in the quark and lepton sector, c.f. formulae (3.14) and (3.15). Since the overall light neutrino mass scale is unknown one can omit m_0 in eq. (3.15) and fit only the mass-squared ratio in the neutrino sector.

Using the GUT-scale values of quark masses given in ref. [92] for two typical values of $\tan \beta$, namely $\tan \beta = 10$ and $\tan \beta = 55$, and considering both 1- and 2- σ ranges, our numerical fit [44] confirms the results of ref. [41] for the central values of the quark mixing angles and $\Delta m_{\odot}^2/\Delta m_A^2 \lesssim 0.05$ there considered. In this case we find $\sin^2 2\theta_{23} \lesssim 0.93$, $|U_{e3}| \sim 0.16$ and $\sin^2 2\theta_{12} \gtrsim 0.92$, the latter being excluded at 90% C.L. When the 1- σ uncertainties in the V_{CKM} entries [99] are included and we allow for $0.019 \leq \Delta m_{\odot}^2/\Delta m_A^2 \leq 0.069$ (the 90% C.L. experimental range [100, 101, 102] in 2003) we did not find any major deviation due to the V_{CKM} entries, the largest

effects being related to the extended $\Delta m_{\odot}^2/\Delta m_A^2$ range, c.f. Figures 3.4 and 3.6. For $\tan\beta = 10$ larger values (albeit not maximal) of the atmospheric neutrino mixing angle are allowed, the upper bound being $\sin^2 2\theta_{23} \lesssim 0.97$, together with a reduced solar mixing, namely $\sin^2 2\theta_{12} \gtrsim 0.85$ (the extreme values are obtained for $\Delta m_{\odot}^2/\Delta m_A^2$ close to the 90% C.L. upper bound). The predictions for $|U_{e3}|$ is not significantly modified: $|U_{e3}| \gtrsim 0.16$. For $\tan\beta = 55$ the results are quite similar: the upper bound for the atmospheric mixing is reduced to $\sin^2 2\theta_{23} \lesssim 0.95$, while the solar angle lower bound is relaxed to $\sin^2 2\theta_{12} \gtrsim 0.82$. The $|U_{e3}|$ parameter is bound to be about 0.15. Only when the scan is performed over the $2\text{-}\sigma$ ranges of the quark sector parameters, maximal atmospheric mixing is allowed, while the lower bound for $|U_{e3}|$ can be at most reduced to about 0.12 and the solar mixing angle can be lowered to 0.75 (such values are reached for large $\tan\beta$ and for $\Delta m_{\odot}^2/\Delta m_A^2$ close to the 90% C.L. upper bound).

However, using the recent update of the lepton mixing parameters [24], the tension becomes strong. Due to the lower bound on $|U_{e3}|$ and strongly reduced uncertainty on $\Delta m_{\odot}^2/\Delta m_A^2$ there is no longer a good solution within the $1\text{-}\sigma$ ranges for the input parameters for any value of $\tan\beta$, see Figures 3.5 and 3.7. Even at $2\text{-}\sigma$ level there are only small regions in the parametric space that are compatible with all lepton data.

As pointed out in ref. [72], the two neutrino analysis suggests the possible relevance of the parameter region characterized by $r \approx -1$ (c.f. section 3.3.2) (corresponding to the solution $\sigma = +1$ in the notation of ref. [72]), where the atmospheric mixing may be *naturally* large. However, we have checked that in this domain one can not recover a good fit of the electron mass, in full agreement with the argument following eq. (3.19).

In conclusion, the numerical analysis confirmed the patterns found by previous authors and analytically discussed in the previous section. The minimal renormalizable SUSY $SO(10)$ model with the CP conserving Yukawa sector, while providing a suggestive and appealing framework for understanding the main features of the quark and lepton spectra¹⁸, fails in reproducing the recent neutrino [24] data at the present $1\text{-}\sigma$ experimental accuracy. When considering the $2\text{-}\sigma$ experimental ranges, partial agreement with the data is obtained in limited regions of the parameter space¹⁹.

It is natural to expect some of these strict bounds to be relaxed once the additional freedom in the various phase parameters is taken into account performing an extended analysis in the CP violating (i.e. realistic) setups.

¹⁸in terms of triplet dominated seesaw formula connecting the unification of the b and τ Yukawa couplings with large values of the leptonic 2-3 mixing

¹⁹However, there are no solutions obeying all the phenomenological constraints simultaneously, c.f. Figures 3.5 and 3.7.

3.6 Additional phases and CP violation

The additional 8 phases make the numerical analysis much more involved. Even if one sticks to the triplet dominated seesaw case to take the advantage of obtaining large atmospheric mixing easily from the GUT-scale b - τ unification²⁰, the number of free continuous parameters entering the numerical analysis is still rather large. Counting them, let us first note that the Yukawa structures Y_{10} and Y_{126} entering the sumrules (3.2) and (3.3) become *complex symmetric* matrices. This leads to the following form of the relevant sum-rules:

$$\begin{aligned} k\tilde{M}'_l &= (P_L V_{CKM} P_R)^T \tilde{D}_u (P_L V_{CKM} P_R) + r\tilde{D}_d \\ M'_\nu &\propto M'_l - M_d \end{aligned} \quad (3.22)$$

The k and r parameters become also *complex*²¹ $\mathcal{O}(1)$ functions of $v_{u,d}^{10,126}$. The primed matrices in eq. (3.22) are given by

$$M'_x \equiv U_d^* M_x U_d^\dagger$$

where U_d is a unitary matrix that brings M_d into the diagonal form and all the tilded matrices are again normalized to their maximal eigenvalue. One can always rescale eq. (3.22) by a global phase such that r becomes real ($r = -|r|e^{i\phi_r}$) and define $k' = k e^{-i\phi_r}$. Since all the masses are symmetric they can be diagonalized by means of unitary transformations $M_x = U_x^T D_x U_x$. Taking into account that $U_u^T U_d^* \equiv V_{CKM}^0 = P_L V_{CKM} P_R$, where $P_L = \text{diag}(e^{\frac{1}{2}i\alpha_1}, e^{\frac{1}{2}i\alpha_2}, e^{\frac{1}{2}i\alpha_3})$ and $P_R = \text{diag}(e^{\frac{1}{2}i\beta_1}, e^{\frac{1}{2}i\beta_2}, 1)$ parametrize the re-phasing of the quark mass matrices necessary to bring the CKM matrix in the standard form (denoted by V_{CKM} with one CP-violating phase, δ_{CKM}) and lead to positive eigenvalues, the sum-rules in the M_d -diagonal basis can be rewritten as follows

$$\begin{aligned} k'\tilde{M}'_l &= V_{CKM}^0{}^T \tilde{D}_u V_{CKM}^0 - |r|\tilde{D}_d \\ k'\tilde{M}'_\nu &\propto V_{CKM}^0{}^T \tilde{D}_u V_{CKM}^0 - |r|\tilde{D}_d - e^{i\omega} \left| k' \frac{m_b}{m_\tau} \right| \tilde{D}_d \end{aligned} \quad (3.23)$$

The factor $e^{i\omega}$ accounts for the phase of k' and the sign of m_b/m_τ . The factors $\frac{1}{2}$ in definitions of phases of $P_{L,R}$ are chosen to maintain compatibility with the notation used in ref. [41, 45]. Counting the total number of parameters we are left with 7 phases and 9 real parameters on the right-hand side of equations (3.23), in agreement with the general estimations in section 3.1.3.

²⁰Recall that in the triplet dominated seesaw case, one also gets rid of the relative phases and magnitude of the singlet and triplet contribution.

²¹In general, the effective light doublet mixing, c.f. formula (2.8) is governed by a pair of unitary matrices.

As before, one can attempt to exploit the information contained in eq. (3.23) by plugging into the charged lepton mass formula all the parameters that are known (by running the data up to the GUT scale), namely the ratios of quark masses in $\tilde{D}_u \equiv \text{diag}(|m_u/m_t|, |m_c/m_t|, 1)$, $\tilde{D}_d \equiv \text{diag}(|m_d/m_b|, |m_s/m_b|, 1)$, the CKM mixing angles and the CP-violating phase δ_{CKM} and vary them within their experimental ranges. The remaining 8 real parameters $|r|$, $|k'|$, $\text{Arg}(k')$, α_i , β_j , that appear in the first mass sum-rule, in principle arbitrary are varied over their allowed domains. In spite of the many pending parameters, the constraints imposed on charged lepton mass sum rule (3.23) in order to reproduce the electron and muon masses are so strong that it is rather nontrivial to achieve a good fit which needs an intricate interplay of many different parameters.

Having obtained an allowed solution of the charged lepton mass sum rule, the neutrino masses and mixings are then sensitive to the sign of m_b/m_τ and the phase ω . Since a negative interference between the 3-3 entries of the M_l and M_d matrices is needed to obtain a large atmospheric mixing angle²², the phase ω becomes strongly correlated to quark phases, in particular to α_3 , see section 3.6.3. As a consequence this framework is still highly constrained and capable to determine characteristic correlations among the neutrino parameters.

Before proceeding to the discussion of numerical results let us review some issues related to the fit of the fermion spectrum in the case of complex Yukawa couplings.

3.6.1 Electron mass formula and δ_{CKM} - the leading terms

When complex Yukawa couplings are considered, it is claimed that a successful fit of the electron mass forces the CKM phase to take values in the second or third quadrant [41, 73, 74], thus requiring an extension of the model to recover the measured amount of CKM CP-violation.

The argument that supports the numerical outcome is based on the approximated formula for the electron mass eigenvalue that can be obtained from (3.23) using the hierarchical properties of the quark mass matrices on the right-hand side:

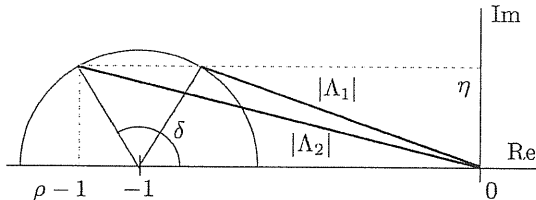
$$|k' \tilde{m}_e| e^{i\phi_1} = -|r| e^{i\beta_1} F_d \lambda^4 + e^{i\alpha_2} F_c \lambda^6 - A^2 \Lambda^2 e^{i\alpha_3} \lambda^6 \frac{|r|}{e^{i\alpha_3} - |r|} + \mathcal{O}(\lambda^7) \quad (3.24)$$

Here $\Lambda \equiv (1 - \rho - i\eta)$ where ρ and η are the Wolfenstein CKM parameters, while $F_d \equiv \frac{m_d}{m_b}/\lambda^4$, $F_c \equiv \frac{m_c}{m_t}/\lambda^4$ are $\mathcal{O}(1)$ factors. Fitting the normalized electron mass (with a typical magnitude of the order of $\mathcal{O}(\lambda^5)$) amounts to compensating the dominant λ^4 term on the right-hand side of eq. (3.24) by other terms therein, the only possible one

²²c.f. formulae (3.23) and (3.17)

at the given order of expansion being that proportional to Λ^2 . In turn this amounts

Figure 3.1: The magnitude of $|\Lambda| = \sqrt{(1 - \rho)^2 + \eta^2}$ as a function of the CKM CP-phase δ . The proper fit of the electron mass favors large values $|\Lambda|$ that calls for $\rho < 0$ driving δ into the second or third quadrant.



to constraining the size of the CKM phase. The CKM phase is encoded in ρ and η as $e^{i\delta_{CKM}} \sin\theta_{13} = A\lambda^3(\rho + i\eta)$. The typical values of ρ and η for δ_{CKM} in the physical region are centered around $\rho \sim 0.21$ and $\eta \sim 0.34$ [93]. Since the parameter $|\Lambda|^2 = (1 - \rho)^2 + \eta^2$ is maximized for $\rho < 0$, c.f. Fig. 3.1²³, the fit of the electron mass in formula (3.24) seems to strongly disfavor the CKM phase in the first quadrant [41].

3.6.2 Electron mass formula and δ_{CKM} - the effects of subleading terms

On the other hand, one should be careful in claiming the relevance of “subleading” terms in a truncated expansion. A detailed inspection of the $O(\lambda^7)$ terms in eq. (3.24) shows that λ is not a faithful expansion parameter, in that some cofactors, not necessarily dependent on Λ , can become accidentally large (a small denominator in the λ^6 term is an example). Therefore a larger number of “subleading” terms in eq. (3.24) may contribute on top of the $O(\lambda^6)$ term, and the scan over the complex phases must be very detailed not to miss such solutions. As an example let us consider the $O(\lambda^7)$ term

$$\mathcal{O}(\lambda^7) \sim + \frac{A^4 |r| \Lambda^2 e^{i(2\alpha_3 - \beta_2)}}{F_s (e^{i\alpha_3} - |r|)^2} \lambda^7 + \dots, \quad (3.25)$$

where $F_s \equiv \frac{m_s}{m_b} / \lambda^3$. Since for typical values of r one obtains $(1 - |r|)^2 \approx \lambda^2$, the denominator can be small enough to lead to an important correction to the $O(\lambda^6)$ term provided α_3 is close enough to 0. Notice that a small m_s together with β_2 around π favors as well the needed destructive interference in eq. (3.24), as emphasized in ref. [73].

In the numerical analysis, a particular attention is paid to the quality of the parameter scan in those regions that may lead to departures from the expectations based

²³In refs. [40, 44] the CP conserving case $\eta = 0$ was considered.

on the estimate of size of Λ in eq. (3.24). Once an approximate solution of the charged lepton mass sum-rule (3.23) is found, a detailed analysis is performed in the neighbor parameter space by linearizing the mass relations. Such a procedure improves dramatically the convergence of the numerical code, revealing solutions that would escape the original scan, unless one performs it with extremely high granularity and huge demand of computing power. Indeed, such an improved numerical analysis shows many solutions of the charged lepton mass formula emerging in parts of the parameter space where the cancelation among the leading terms in eq. (3.24) is not as effective. Let us discuss the numerical results in the next section.

The sensitivity of the electron mass fit to subleading terms in eq. (3.24) is going to be crucial in the case of the extended model with an additional 120-dimensional chiral super-multiplet [44] discussed in section 4.2. As we shall see ²⁴, even for typical magnitudes of the 120_H Yukawa contributions to fermion masses as low as per-mille of those coming from the 10_H and $\overline{126}_H$, the role of the Λ^2 term in eq. (3.24) is easily screened by the 120_H induced terms, thus lifting the bias on the CKM phase.

3.6.3 Comments on smallness of the Dirac CP-violating phase in the lepton sector with triplet-dominated seesaw

Concerning the amount of CP violation in the leptonic sector there is a semianalytical argument in favor of smallness of the PMNS Dirac CP-violation. It differs considerably from the one given in [41] that seems to work under the conditions specified therein but becomes obscure in realistic setups.

Let us start with the observation that the charged lepton mass matrix in the M_d diagonal basis is strongly hierarchical while at the same time the triplet dominated neutrino mass matrix poses a particular phase structure. To see this, consider the approximate form of M_ν up to the λ^3 order

$$M_\nu \propto \begin{pmatrix} 0 & 0 & A\lambda^3(1 - \rho - i\eta) \\ \cdot & -e^{-i\beta_2} F_s x & A\lambda^2 \\ \cdot & \cdot & 1 - x \end{pmatrix} \quad (3.26)$$

where

$$x \equiv \left(e^{i\omega} \left| k' \frac{m_b}{m_\tau} \right| + |r| \right) e^{-i\alpha_3} \quad (3.27)$$

Since $\alpha_3 \sim 0$ is preferred by the charged lepton mass fit and x should be real and maximal to make the $b - \tau$ unification produce the large atmospheric mixing angle, we also get a preference of $\omega \sim 0$.

²⁴c.f. formula (4.25)

Let us show now that the amount of CP-violation in the leptonic sector is small compared to the CKM case. The PMNS mixing matrix can be written in the particular form

$$U_{PMNS} = U_l^T U_\nu^* \doteq \tilde{V}_{CKM} \begin{pmatrix} e^{i\gamma_1} & \cdot & \cdot \\ \cdot & e^{i\gamma_2} & \cdot \\ \cdot & \cdot & e^{i\gamma_3} \end{pmatrix} \tilde{U}_\nu^* \quad (3.28)$$

Here

$$\tilde{V}_{CKM} \equiv \begin{pmatrix} V_{11} & V_{12} & V_{13} \\ V_{21} & V_{22} & V_{23} \\ V_{31} & V_{32} & V_{33} \end{pmatrix} \quad (3.29)$$

is the standard form of the unitary matrix diagonalizing the charged lepton masses (due to the large hierarchy in the charged lepton sector it is close to V_{CKM}) while

$$\tilde{U}_\nu^* \equiv \begin{pmatrix} U_{11} & U_{12} & U_{13} \\ U_{21} & U_{22} & U_{23} \\ U_{31} & U_{32} & U_{33} \end{pmatrix} \quad (3.30)$$

denotes the unitary matrix diagonalizing the neutrino masses (3.26)²⁵. Since the mixing in \tilde{V}_{CKM} is small, the \tilde{U}_ν^* matrix is the predominant source of the PMNS mixing angles.

Concerning the phases $\gamma_{1,2,3}$ arising upon bringing these two matrices into the standard form, they play only a subleading role. Indeed, passing the phase matrix in eq. (3.28) through \tilde{V}_{CKM} , only the relative phase of the \tilde{V}_{CKM} entries can change. Due to the strong hierarchy of \tilde{V}_{CKM} , this does not bring substantial changes to the formulae of our interest.

Let us start by estimating the magnitude of the Dirac CP phase δ_ν of the \tilde{U}_ν^* matrix. Plugging in the experimental information on A , λ , F_s , ρ and η and assuming $x \sim 1 - A\lambda^2$ as required by the large atmospheric mixing and $b - \tau$ unification correspondence, it is easy to see that regardless the value of β_2 the phase angle δ_ν never exceeds roughly 10 degrees, c.f. Figure 3.2.

To infer the order of magnitude of the PMNS Dirac phase one can look at the Jarlskog invariant (of particular interest for our purposes is the combination of the 1-3 elements denoted by X_{ij}) of the full PMNS matrix (c.f. Appendix A) [103]

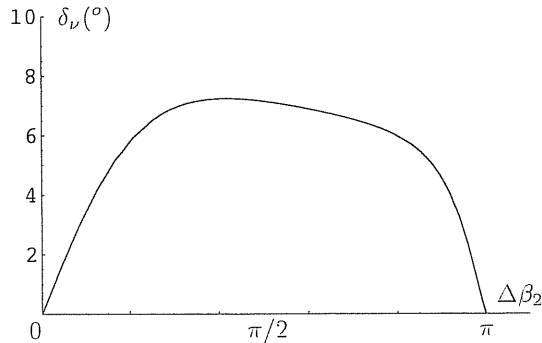
$$J_{CP} = \frac{1}{2} |\text{Im}(X_{11}^* X_{13} X_{31} X_{33}^*)| \quad (3.31)$$

and use the identity

$$J_{CP} = \frac{1}{2} |c_{12} c_{13}^2 c_{23} s_{12} s_{13} s_{23} \sin \delta_{PMNS}| \quad (3.32)$$

²⁵again in the standard form with 11,12,23 and 33 entries real

Figure 3.2: The magnitude of the δ_ν phase angle of the unitary matrix \tilde{U}_ν^* diagonalizing the neutrino mass matrix (3.26). For any value of the quark phase $\beta_2 = \pi \pm \Delta\beta$ associated with the strange-quark mass it does not exceed roughly 10° . Recall that $\beta_2 \sim \pi$ is preferred by the required ‘‘conspiracy’’ in the electron mass formulae (3.24) and (3.25). It is assumed that the numerical structure of M_ν is such that it leads to the proper almost bimaximal mixing in \tilde{U}_ν^* .



To understand the origin of the partial suppression of δ_{PMNS} with respect to δ_{CKM} let us recall the relevant numbers obtained in the quark sector:

$$J_{CKM} \propto 10^{-5} \quad \text{for} \quad (3.33)$$

$$\sin \phi_{12} = \lambda \sim 0.22, \quad \sin \phi_{13} \sim 0.04, \quad \sin \phi_{23} = \lambda^4 \sim 0.004 \quad \text{and} \quad \delta_{CKM} \sim \frac{\pi}{3}$$

Since the amount of CP violation in the \tilde{U}_ν^* matrix is under control, one can expect a moderate change of the value of J once \tilde{V}_{CKM} is multiplied by this factor in eq. (3.28) while a drastic change in the sines of the mixing angles that gave rise to large δ_{CKM} even the small values of $J_{CKM} \sim 10^{-5}$. Since there is no such enhancement in eq. (3.31) in case of the solar and atmospheric mixing, one can expect the magnitude of the δ_{PMNS} angle to change to roughly²⁶

$$\delta_{PMNS} \sim \delta_{CKM} \frac{J_{PMNS}}{J_{CKM}} \frac{s_{12}^q s_{13}^q s_{23}^q}{s_{12}^l s_{13}^l s_{23}^l} \times \text{cosine factors} \sim 1.4 \times 10^{-3} \delta_{CKM} \frac{J_{PMNS}}{J_{CKM}} \quad (3.34)$$

Finally, we must quantify the magnitude of J_{PMNS} , i.e. the change of J_{CKM} upon multiplying \tilde{V}_{CKM} by \tilde{U}_ν^* . Defining $X = \tilde{V}_{CKM} \tilde{U}_\nu^*$ the approximate value of $J_{PMNS} = \frac{1}{2} |\text{Im}(X_{11}^* X_{13} X_{31} X_{33}^*)|$ can be estimated by inspecting in detail the relevant matrix elements of X .

²⁶Here s_{ij}^q stands for the sines of the CKM mixing angles ϕ_{ij} while s_{ij}^l denotes the corresponding PMNS mixing parameters.

Neglecting the higher order terms, the matrix elements of our interest read

$$\begin{aligned}
X_{11} &= V_{11}U_{11} + V_{12}U_{21} + \dots \doteq U_{11} + \mathcal{O}(\lambda)U_{21} \\
X_{13} &= V_{11}U_{13} + V_{12}U_{23} + \dots \doteq U_{13} + \mathcal{O}(\lambda)U_{23} \\
X_{31} &= V_{32}U_{21} + V_{33}U_{31} + \dots \doteq U_{31} + V_{32}U_{21} \\
X_{33} &= V_{32}U_{32} + V_{33}U_{33} + \dots \doteq U_{33} + V_{32}U_{23}
\end{aligned} \tag{3.35}$$

To estimate the imaginary part of $X_{11}^*X_{13}X_{31}X_{33}^*$ let us compute the magnitudes and phases of these four factors separately:

- X_{11}^* : Since U_{11} is a real number of the order of 1 (being a cosine of the solar mixing angle) and $U_{21}^* = -c_{23}^l s_{12}^l - s_{23}^l s_{13}^l c_{12}^l e^{-i\delta_\nu} \doteq -\frac{1}{2} - \frac{1}{2}|U_{e3}|e^{-i\delta_\nu}$ we get $X_{11}^* \sim \mathcal{O}(1) \times e^{i\phi_{11}}$ where $|\tan \phi_{11}| \sim \mathcal{O}(\lambda)|U_{e3}| \sin \delta_\nu \lesssim 5 \times 10^{-3}$.
- X_{13} : Since U_{13} is practically U_{e3} and $U_{23} = c_{13}^l s_{23}^l \doteq 1/\sqrt{2}$ we get $X_{13} \sim \mathcal{O}(10^{-1}) \times e^{i\phi_{13}}$ where $|\tan \phi_{13}| \sim \sin \delta_\nu \lesssim 10^{-1}$.
- X_{31} : Since $U_{31} = s_{23}^l s_{12}^l - c_{23}^l s_{13}^l c_{12}^l e^{-i\delta_\nu} \doteq \frac{1}{2} - \frac{1}{2}|U_{e3}|e^{i\delta_\nu}$, $V_{32} = -s_{23}^q c_{12}^q - c_{23}^q s_{13}^q s_{12}^q e^{i\delta_{CKM}} \doteq -(4 + 0.07i) \times 10^{-2}$ and $U_{21} = -c_{23}^l s_{12}^l - s_{23}^l s_{13}^l c_{12}^l e^{i\delta_\nu} \doteq -\frac{1}{2} - \frac{1}{2}|U_{e3}|e^{i\delta_\nu}$ we get $X_{31} \sim \frac{1}{2} \times e^{i\phi_{31}}$ where $|\tan \phi_{31}| \sim |U_{e3}| \sin \delta_\nu \lesssim 2 \times 10^{-2}$.
- X_{33}^* : Since U_{33} is a real number of the order of $1/\sqrt{2}$, $V_{32}^* = -s_{23}^q c_{12}^q - c_{23}^q s_{13}^q s_{12}^q \times e^{-i\delta_{CKM}} \doteq -(4 - 0.07i) \times 10^{-2}$ and U_{23} is also a real number $\sim 1/\sqrt{2}$ we get $X_{33}^* \sim 1/\sqrt{2} \times e^{i\phi_{33}}$ where $|\tan \phi_{33}| \lesssim \times 10^{-3}$.

Notice that the would-be phases accompanying $V_{11} \propto e^{i\gamma_1}$ and $V_{33} \propto e^{i\gamma_3}$ indeed cancel among the $X_{11}^*X_{13}$ and X_{31} and X_{33}^* terms in J_{PMNS} and it was therefore legal to drop them at the beginning. The other phases in the higher order terms play only subleading role and do not affect the results substantially.

With this information at hand one can infer

$$X_{11}^*X_{13}X_{31}X_{33}^* \sim \frac{1}{3}\mathcal{O}(10^{-1})e^{i\phi} \quad \text{where} \quad |\tan \phi| \sim \sin \delta_\nu \lesssim 10^{-1} \tag{3.36}$$

From this it is already easy to obtain $J_{PMNS} \lesssim 2 \times 10^{-3}$ that yields

$$\delta_{PMNS} \lesssim 3 \times 10^{-1} \delta_{CKM} \sim 20^\circ \tag{3.37}$$

Therefore, the GUT-scale value of the Dirac CP-violating phase in the PMNS mixing matrix of the minimal SUSY SO(10) model is smaller than the CKM CP-phase of the quark sector. Notice that the numerical value on the right hand side of eq. (3.37) corresponds to the maximal value of the δ_ν parameter. In many cases (in particular for

$\beta_2 \sim \pi$ that is favoured by the charged lepton mass fit), the preferred value of δ_{PMNS} is even smaller.

The last remark concerns the possible effects of running of δ_{PMNS} from the GUT-scale down to the electroweak range. It is well known [86, 88, 104] that the leptonic Dirac CP-phase can be enhanced tremendously at M_Z even for $\delta_{PMNS}(GUT) = 0$ provided θ_{13} is very small ($\lesssim 1^\circ$) and the Majorana phases are not equal or opposite. However, as we shall see in section 3.7, the minimal SUSY $SO(10)$ predicts a stringent lower bound on θ_{13} of roughly $|U_{e3}| \gtrsim 6^\circ$ and the Majorana phases are strongly anticorrelated. Therefore, the upper bound (3.37) is radiatively stable.

3.7 Numerical analysis - CP violating Yukawa sector

Similarly to the real case discussed in section 3.5 a detailed scan over an independent set of parameters in relations (3.23) was performed. We use GUT the scale input data for quark and leptons as derived in ref. [92] with recent corrections indicated in Tables 3.3, 3.4 and 3.5. As before, $\tan\beta = 10$, 55 are considered as typical values for the MSSM gauge coupling unification underlying the one-step $SO(10)$ breaking scenario here considered [69].

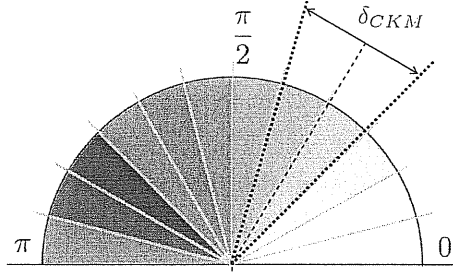
Let us again adopt 90% C.L. ranges for the heavy quark masses but allow for slightly larger ranges in the masses of the light quarks, see Tables 3.2 and 3.3 and discussion in section 3.4.1 (the values of m_u and m_d given in Table 3.2 used in previous studies [40, 44] correspond to 4.88 ± 0.57 MeV and 9.81 ± 0.65 MeV respectively at 1 GeV [90]). While m_u plays a subleading role in the mass sum rules, a light m_d favors the reproduction of the electron mass eigenvalue, as we discussed in subsection 3.6.1.

The present range for the \overline{MS} running mass of the down quark at 1 GeV is 5.4 to 10.8 MeV [93]. We will therefore allow for values of m_d at the GUT scale as low as 0.7 MeV. As for the strange quark mass an up to date range, which includes the lattice evaluations, is $m_s(2 \text{ GeV}) = 110 \pm 20$ MeV, corresponding at the GUT scale to 23 ± 6 MeV, c.f. Table 3.3.

The complex phases $\alpha_{2,3}$, $\beta_{1,2}$ are sampled in the whole range $[0, 2\pi)$. The phase ω shows then a correlation to the quark phases as a consequence of the tight relation between large atmospheric and $b - \tau$ Yukawa unification, which involves a partial cancellation among the terms in formula (3.27). Since the reduced up-quark mass \tilde{m}_u is by far the smallest parameter in the mass relations, α_1 does not seem to play any relevant role.

In Fig. 3.3 the density spectrum of the solutions of the charged lepton mass formula in eq. (3.24) is displayed as a function of δ_{CKM} in the interval $[0, \pi)$. As one can see the

Figure 3.3: The relative density spectrum of allowed solutions for the charged lepton masses is shown as a function of the CKM phase δ . Although there appear a preference for the quadrants with $\rho < 0$, there exists a significant number of solution with δ_{CKM} in the physical region. Quantitatively the ratio of the solution density in the preferred area (the darkest slice) to that in the $1\text{-}\sigma$ range is about 7 to 1.



relative density of solutions of the charged lepton sum rule is far from being negligible even when considering δ_{CKM} in the $1\text{-}\sigma$ range, contrary to the claims in refs. [41, 73]. To make this statement quantitative the ratio of the solution density in the most preferred area (the darkest slice in the second quadrant) to that in the $1\text{-}\sigma$ δ_{CKM} range is about 7 to 1.

As far as neutrino parameters are concerned, the solar mixing angle shows no longer the tight lower bound present in the CP-conserving case, namely $\sin^2 2\theta_{12}|_{CP=0} > 0.85$ (for $\tan \beta = 10$) [44]. On the other hand, the experimental improvement on the allowed values for the solar mixing sharpens a tension with the recent bounds on the strange quark mass²⁷.

Figures 3.9 and 3.11 demonstrate the compatibility of the predicted correlations with the recent neutrino experimental data. To achieve this, the strange quark mass is driven above 30 MeV at the GUT scale, that corresponds to $m_s(2 \text{ GeV}) > 140 \text{ MeV}$ (the solutions in the allowed region span a GUT scale strange quark mass in the 30 – 34 MeV range). Should the experimental value for the solar mixing angle settle above the present central value, it would represent a serious shortcoming of the type-II dominated

²⁷As a matter of fact, the strange quark mass plays a central role in generating the tension between the fit and the experimental data. On one hand, smaller values of \tilde{m}_s are preferred by the electron mass fit, c.f. formula (3.25), while large \tilde{m}_s is favoured by the shape of the type-II neutrino mass spectrum. With the recent update of the neutrino data [24], the anticorrelation among θ_{12} and $\Delta m_{\odot}^2/\Delta m_A^2$ (c.f. formula (3.20)) the simple scenario discussed here becomes strongly constrained, in particular for large $\tan \beta$ leading to further enhancement in the down-quark mass hierarchy.

minimal $SO(10)$ framework²⁸.

The lower bound for the $|U_{e3}|$ parameter is relaxed compared to the CP conserving case, although not as dramatically as for the solar angle. As Fig. 3.9 shows, for $\tan\beta = 10$ the constraint $|U_{e3}| \geq 0.15$ found in the CP conserving setting (see the discussion in ref. [44]) is lowered to about $|U_{e3}| \geq 0.1$.

In the case of $\tan\beta = 55$ we do not find any significant qualitatively different pattern. In particular the predicted range for the $|U_{e3}|$ parameter remains unaffected $|U_{e3}| \gtrsim 0.1$, c.f. Fig. 3.10. The persistence of such a non-vanishing bound is a clear signature of the tight correlation between lepton and quark Yukawa couplings in this framework, that makes $|U_{e3}| \simeq O(\lambda)$ [41]. The only difference with respect to the $\tan\beta = 10$ case stems from the fact to fulfill simultaneously all the recent experimental constraints [24] one must adopt the 95% C.L ranges for the neutrino data. The seed of this tension can be traced back to the fact that for $\tan\beta = 55$ the hierarchy in the down-quark as well as the charged lepton sectors is stronger and thus the $\Delta m_{\odot}^2/\Delta m_A^2$ parameter is naturally smaller. Pushing $\Delta m_{\odot}^2/\Delta m_A^2$ higher the anticorrelation with the solar mixing (3.20) reduces θ_{12} below the experimental limits, c.f. Fig. 3.11 and vice versa.

Explicit numerical examples:

To appreciate the relevance of the semianalytic results obtained in the previous sections let us give few explicit examples of the numerical output.

Example 1: Choosing the following set of input parameters

$$\begin{aligned}
m_u &\sim 0.57 \text{ MeV} & m_d &\sim 0.73 \text{ MeV} \\
m_c &\sim 235.7 \text{ MeV} & m_s &\sim 31.3 \text{ MeV} \\
m_t &\sim 90.0 \text{ GeV} & m_b &\sim 1.19 \text{ GeV} \\
\\
\sin\phi_{12} &\sim 0.2253 & \sin\phi_{23} &\sim 0.0331 \\
\sin\phi_{13} &\sim 0.0035 & \delta_{CKM} &\sim 75^{\circ} . \\
\\
\alpha_1 &\sim 144^{\circ} & \beta_1 &\sim 216.8^{\circ} \\
\alpha_2 &\sim 142^{\circ} & \beta_2 &\sim 224.6^{\circ} \\
\alpha_3 &\sim 1.2^{\circ} & \omega &\sim -0.2^{\circ} \\
|r| &\sim 0.748 & |k'| &\sim 0.256
\end{aligned}$$

²⁸Remarkably enough, even with the 2003 experimental inputs (Figures 3.8 and 3.10) this tension is not weakened as it comes namely from the lower bound on $\Delta m_{\odot}^2/\Delta m_A^2$ (see the previous footnote) that was not changed drastically in the recent parameter extractions [24].

the charged lepton mass matrix (normalized to the τ mass) reads:

$$100 k' \tilde{M}'_l \approx |k'| \times \begin{pmatrix} -0.146 + 0.004i & -0.134 + 0.016i & 0.35 + 2.862i \\ -0.134 + 0.016i & -6.985 - 0.197i & 5.321 - 11.506i \\ 0.35 + 2.862i & 5.321 - 11.506i & 97.846 + 8.567i \end{pmatrix}$$

The corresponding (GUT-scale) charged lepton masses are all within their 90% C.L. ranges: $m_e = 0.3585$ MeV, $m_\mu = 75.62$ MeV and $m_\tau = 1294.0$ MeV. The neutrino mass matrix is then given by

$$100 \tilde{M}'_\nu \propto \begin{pmatrix} -0.203 + 0.004i & -0.134 + 0.016i & 0.339 + 2.863i \\ -0.134 + 0.016i & -9.404 - 0.224i & 5.366 - 11.485i \\ 0.339 + 2.863i & 5.366 - 11.485i & 5.855 + 8.952i \end{pmatrix}$$

Keeping into account that the absolute mass scale is set by the VEV of the LH triplet in $\overline{126}_H$, one finds neutrino mass ratios and mixings ($\sin^2 2\theta_{12} = 0.82$, $\sin^2 2\theta_{23} = 0.93$, $|U_{e3}| = 0.11$, $\Delta m_{\odot}^2 / \Delta m_A^2 = 0.027$), all of them within the relevant present 90% C.L. experimental ranges, c.f. Table 3.1 ²⁹.

As far as the leptonic CP phases are concerned, the Dirac phase δ_{PMNS} turns out to be generally small ($< 15^\circ$), while the two neutrino Majorana phases $\varphi_{1,2}$ show an approximate 180° correlation. In the example reported one finds $\delta_{PMNS} = 4^\circ$, $\varphi_1 = 10^\circ$, $\varphi_2 = 191^\circ$. This feature is welcome as it ensures the radiative stability of the analytical bound for the Dirac-CP phase in the lepton sector, see section 3.6.3.

Example 2: The second example (with slightly higher m_s and reduced effective top-mass) follows from the input parameters

$$\begin{array}{ll} m_u \sim 0.69 \text{ MeV} & m_d \sim 1.0 \text{ MeV} \\ m_c \sim 273.9 \text{ MeV} & m_s \sim 32.8 \text{ MeV} \\ m_t \sim 64 \text{ GeV} & m_b \sim 1.16 \text{ GeV} \\ \\ \sin \phi_{12} \sim 0.2265 & \sin \phi_{23} \sim 0.0335 \\ \sin \phi_{13} \sim 0.0033 & \delta_{CKM} \sim 70^\circ . \end{array}$$

²⁹The comparison with the data in Table 3.1 must take into account the running of the parameters from the GUT scale to the weak scale. However, for normal hierarchy in the neutrino sector, the effects of running of the neutrino spectrum and leptonic mixings are very mild. For more details see section 3.4.2

$$\begin{aligned}
\alpha_1 &\sim 144^\circ & \beta_1 &\sim 221.7^\circ \\
\alpha_2 &\sim 137^\circ & \beta_2 &\sim 208.9^\circ \\
\alpha_3 &\sim 0^\circ & \omega &\sim 3.7^\circ \\
|r| &\sim 0.758 & |k'| &\sim 0.245
\end{aligned}$$

The charged lepton mass matrix (normalized to the τ mass) in this case reads:

$$100 k' \tilde{M}'_l \approx |k'| \times \begin{pmatrix} -0.194 + 0.002i & -0.286 + 0.069i & 0.212 + 2.927i \\ -0.286 + 0.069i & -7.475 - 0.624i & 3.604 - 12.981i \\ 0.212 + 2.927i & 3.604 - 12.981i & 97.968 + 0.001i \end{pmatrix}$$

The corresponding (GUT-scale) charged lepton masses are: $m_e = 0.3585$ MeV, $m_\mu = 75.72$ MeV and $m_\tau = 1290.8$ MeV. For the neutrino mass matrix we obtain

$$100 \tilde{M}'_\nu \propto \begin{pmatrix} -0.271 - 0.011i & -0.290 + 0.050i & 0.019 + 2.935i \\ -0.290 + 0.050i & -9.957 - 1.114i & 4.449 - 12.761i \\ 0.019 + 2.935i & 4.449 - 12.761i & 7.444 + 6.441i \end{pmatrix}$$

The neutrino mass ratios and mixings turn out to be ($\sin^2 2\theta_{12} = 0.80$, $\sin^2 2\theta_{23} = 0.93$, $|U_{e3}| = 0.13$, $\Delta m_\odot^2 / \Delta m_A^2 = 0.039$), all of them again within the relevant present 90% C.L. experimental ranges, c.f. Table 3.1.

The leptonic Dirac CP-phase δ_{PMNS} found in this case is $\delta_{PMNS} = 0.2^\circ$ while the Majorana ones are $\varphi_1 = 7.3^\circ$, $\varphi_2 = 186.4^\circ$. Again, one can see the strong anticorrelation in φ_1 and φ_2 .

With these data at hand one can easily check the quality of the simple analysis performed in sections (3.6.1) - (3.6.3). Recall that the proper fit of the electron mass formula and the physical placing of the CKM CP-phase required $\alpha_3 \sim 0$ and $\beta_1 \sim \pi$ and low values of m_d . The higher order terms could have brought additional improvement provided $\beta_2 \sim \pi$. Furthermore, the phase angle ω had to be very small to allow for automatically large atmospheric mixing as a consequence of the $b - \tau$ unification. We also identified a lower bound of order $\mathcal{O}(\lambda)$ on the U_{e3} entry of the PMNS mixing matrix. Finally, the Dirac CP-phase in the leptonic sector was expected to be small. Indeed, looking at the results above one can appreciate a very good agreement among all these theoretical arguments and the numerical fit.

It is worth commenting more on the dramatic effects brought by the recent improvements of the experimental data [24]. Comparing Figs. 3.9 with 3.8 one can see

Table 3.1: 90% C.L. ranges for neutrino mixing and mass parameters in 2003 [100, 101, 102] and 2005 [24]. The recent significant improvement on the Δm_{ij}^2 parameters is the major source of the tension on the CP-conserving Yukawa setups in the minimal renormalizable SUSY SO(10) model.

2003 data

	90% C.L. ranges		
θ_{12}	$0.71 \lesssim$	$\sin^2 2\theta_{12}$	$\lesssim 0.91$
θ_{23}	$0.90 \lesssim$	$\sin^2 2\theta_{23}$	
θ_{13}		$ \sin \theta_{13} $	$\lesssim 0.20$
Δm_{\odot}^2	$5 \times 10^{-5} \text{eV}^2 \lesssim$	Δm_{\odot}^2	$\lesssim 17 \times 10^{-5} \text{eV}^2$
Δm_A^2	$1.6 \times 10^{-3} \text{eV}^2 \lesssim$	$ \Delta m_A^2 $	$\lesssim 3.9 \times 10^{-3} \text{eV}^2$
$\Delta m_{\odot}^2 / \Delta m_A^2$	$1.9 \times 10^{-2} \lesssim$	$\Delta m_{\odot}^2 / \Delta m_A^2$	$\lesssim 6.9 \times 10^{-2}$

2005 data

	90% C.L. ranges		
θ_{12}	$0.79 \lesssim$	$\sin^2 2\theta_{12}$	$\lesssim 0.91$
θ_{23}	$0.93 \lesssim$	$\sin^2 2\theta_{23}$	
θ_{13}		$ \sin \theta_{13} $	$\lesssim 0.15$
Δm_{\odot}^2	$7.5 \times 10^{-5} \text{eV}^2 \lesssim$	Δm_{\odot}^2	$\lesssim 8.5 \times 10^{-5} \text{eV}^2$
Δm_A^2	$2.0 \times 10^{-3} \text{eV}^2 \lesssim$	$ \Delta m_A^2 $	$\lesssim 3.0 \times 10^{-3} \text{eV}^2$
$\Delta m_{\odot}^2 / \Delta m_A^2$	$2.7 \times 10^{-2} \lesssim$	$\Delta m_{\odot}^2 / \Delta m_A^2$	$\lesssim 4.0 \times 10^{-2}$

that the “volume” of the parametric space that remains compatible with experiments shrunk considerably with the recent update of experimental inputs [24]. The major effect comes from the improved experimental bounds on the neutrino mass squared differences and leptonic mixing angles. c.f. Table 3.1 that forbids ³⁰ a significant part of the previously (2003) allowed area in the parametre space. As a consequence, for large $\tan\beta$ we obtained a fit compatible with the data only when 95% C.L. ranges for the neutrino parameters were allowed.

We conclude that the minimal SUSY $SO(10)$ GUT, when complex Yukawa couplings are taken in their generality, is not ruled out by present data on the quark and leptons textures. On the other hand, a large solar mixing and a maximal atmospheric angle can hardly be accomodated. Nevertheless, the non-vanishing lower bound for $|U_{e3}|$ remains a very robust prediction of the model that falls within the reach of the planned long-baseline neutrino experiments.

³⁰namely because of the change in the recent $\Delta m_{\odot}^2/\Delta m_A^2$ experimental range

Table 3.2: Sample of values running quark masses (in $\overline{\text{MS}}$ scheme) given in analyses by Fusaoka and Koide (1998) [90] and Das and Parida (2000) [92]. The input data correspond to $\mu = 1$ GeV for the light quarks and $\mu = M_q^{pole}$ for the heavy quarks with M_{pole} above Λ_{QCD} . For sake of comparison with the latest experimental results, the light and heavy quark running masses at $\mu = 2$ GeV obtained by simple rescaling of the $\mu = 1$ GeV input values are also given. The supersymmetric threshold was taken at $M_S = 1$ TeV and $\tan\beta = 10$ and 55 is considered.

Effective GUT-scale quark masses
Fusaoka & Koide (1998) & Das & Parida (2000)

All values are given in units of MeV.

q	$m_q(1\text{GeV})$	$m_q(2\text{GeV})$	$m_q(M_Z)$	$m_q(M_G), t_\beta = 10$	$m_q(M_G), t_\beta = 55$
u	4.88 ± 0.57	$3.61^{+0.54}_{-0.58}$	$2.33^{+0.42}_{-0.45}$	$0.72^{+0.14}_{-0.15}$	$0.72^{+0.12}_{-0.16}$
d	9.81 ± 0.65	$7.27^{+0.72}_{-0.79}$	$4.69^{+0.60}_{-0.66}$	$1.50^{+0.42}_{-0.23}$	$1.50^{+0.42}_{-0.23}$
s	195.4 ± 12.5	$143.4^{+14.0}_{-15.5}$	$93.4^{+11.8}_{-13.0}$	$29.9^{+4.3}_{-4.5}$	$29.8^{+4.2}_{-4.5}$

All values are given in units of GeV

q	$m_q(M_q^{pole})$	$m_q(M_Z)$	$m_q(M_G), t_\beta = 10$	$m_q(M_G), t_\beta = 55$
c	$1.21^{+0.05}_{-0.06}$	$0.68^{+0.06}_{-0.06}$	$0.210^{+0.019}_{-0.021}$	$0.211^{+0.015}_{-0.021}$
b	$4.25^{+0.08}_{-0.09}$	$3.00^{+0.11}_{-0.11}$	$1.06^{+0.14}_{-0.09}$	$1.42^{+0.48}_{-0.19}$
t	170 ± 12	181 ± 13	82^{+30}_{-15}	95^{+69}_{-21}

Table 3.3: Recent changes in the quark sector input data [93, 97, 98] and the corresponding corrections to the relevant GUT-scale effective masses. The effect in the strange-quark mass plays a significant role in the numerical analysis, for more details see sections 3.4.1 and 3.7.

Effective GUT-scale quark masses - 2004 update

low scale masses		GUT scale values	
$m_{light}(2\text{GeV})$	$m_{heavy}(M^{pole})$	$m_q(M_G), t_\beta = 10$	$m_q(M_G), t_\beta = 55$
$m_u(2\text{GeV}) \sim$	$2.75 \pm 1.25 \text{ MeV}$	$0.45^{+0.25}_{-0.15} \text{ MeV}$	$0.45^{+0.20}_{-0.15} \text{ MeV}$
$m_d(2\text{GeV}) \sim$	$6.0 \pm 2.0 \text{ MeV}$	$1.3^{+0.7}_{-0.5} \text{ MeV}$	$1.3^{+0.7}_{-0.5} \text{ MeV}$
$m_s(2\text{GeV}) \sim$	$110 \pm 20 \text{ MeV}$	$23 \pm 6 \text{ MeV}$	$23 \pm 6 \text{ MeV}$
$m_c(M_c^{pole}) \sim$	$1.25 \pm 0.10 \text{ GeV}$	$216 \pm 35 \text{ MeV}$	$217 \pm 35 \text{ MeV}$
$m_b(M_b^{pole}) \sim$	$4.25 \pm 0.20 \text{ GeV}$	$1.06^{+0.35}_{-0.20} \text{ GeV}$	$1.4^{+0.8}_{-0.4} \text{ GeV}$
$m_t(M_t^{pole}) \sim$	$174.3 \pm 7.2 \text{ GeV}$	$82^{+12}_{-10} \text{ GeV}$	$97^{+50}_{-16} \text{ GeV}$

Table 3.4: The evolution of the CKM mixing angles and CP phase from M_Z [93] to the M_G scale for $\tan \beta = 10$ [90, 92]. The effects of running are significant (up to 15%) only for ϕ_{13} and ϕ_{23} . Varying $\tan \beta$ gives rise only to subleading corrections.

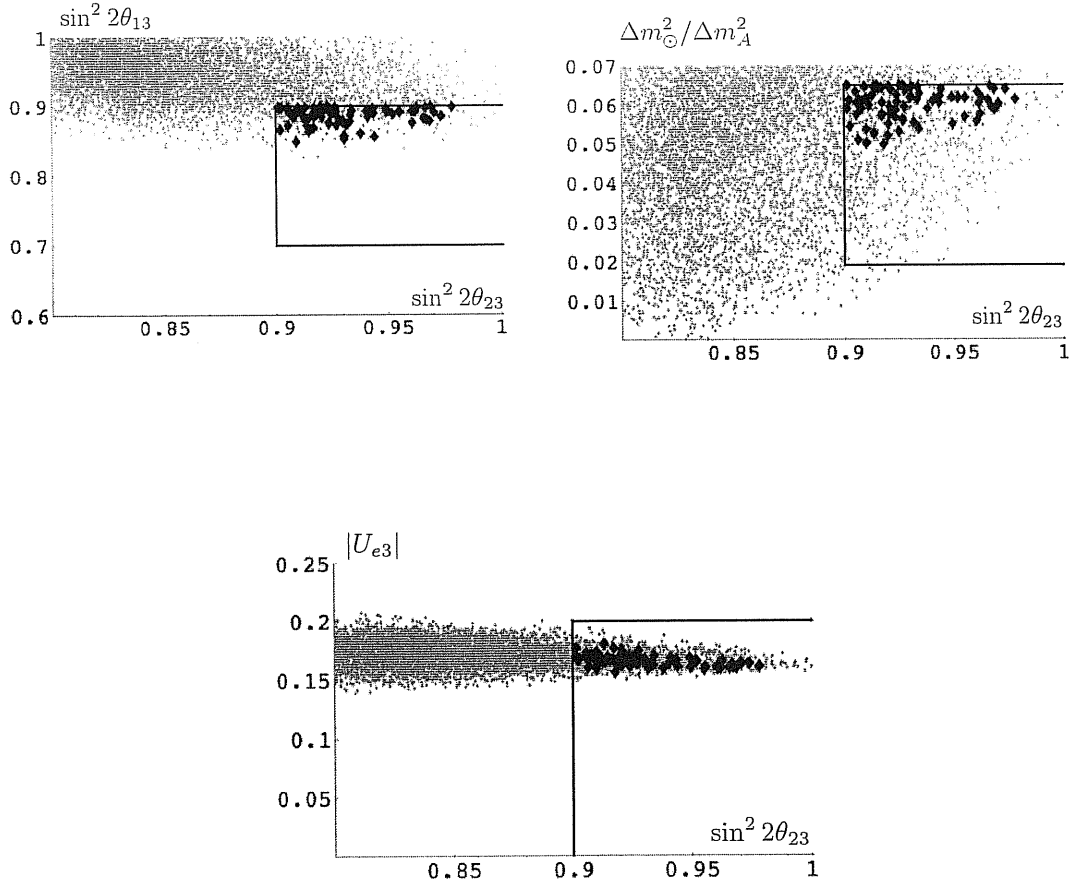
	$\mu = M_Z$	$\mu = 2 \times 10^{16} \text{ GeV}$
$\sin \phi_{12}$	0.2243 ± 0.0016	0.2243 ± 0.0016
$\sin \phi_{23}$	0.0413 ± 0.0015	0.0351 ± 0.0013
$\sin \phi_{13}$	0.0037 ± 0.0005	0.0032 ± 0.0004
δ_{CKM}	$60^\circ \pm 14^\circ$	$60^\circ \pm 14^\circ$

Table 3.5: The running effective charged lepton masses in the MSSM given in Das and Parida [92]. The errors come mainly from the uncertainties in the running VEVs and from the SUSY thresholds.

l	$m_l(M_Z)$	$m_l(M_G), t_\beta = 10$	$m_l(M_G), t_\beta = 55$
e	0.4868 MeV	0.3585 MeV	0.3565 MeV
μ	102.75 MeV	$75.67^{+0.05}_{-0.05}$ MeV	$75.29^{+0.05}_{-0.19}$ MeV
τ	1.746 GeV	$1.292^{+0.001}_{-0.001}$ GeV	$1.629^{+0.044}_{-0.029}$ GeV

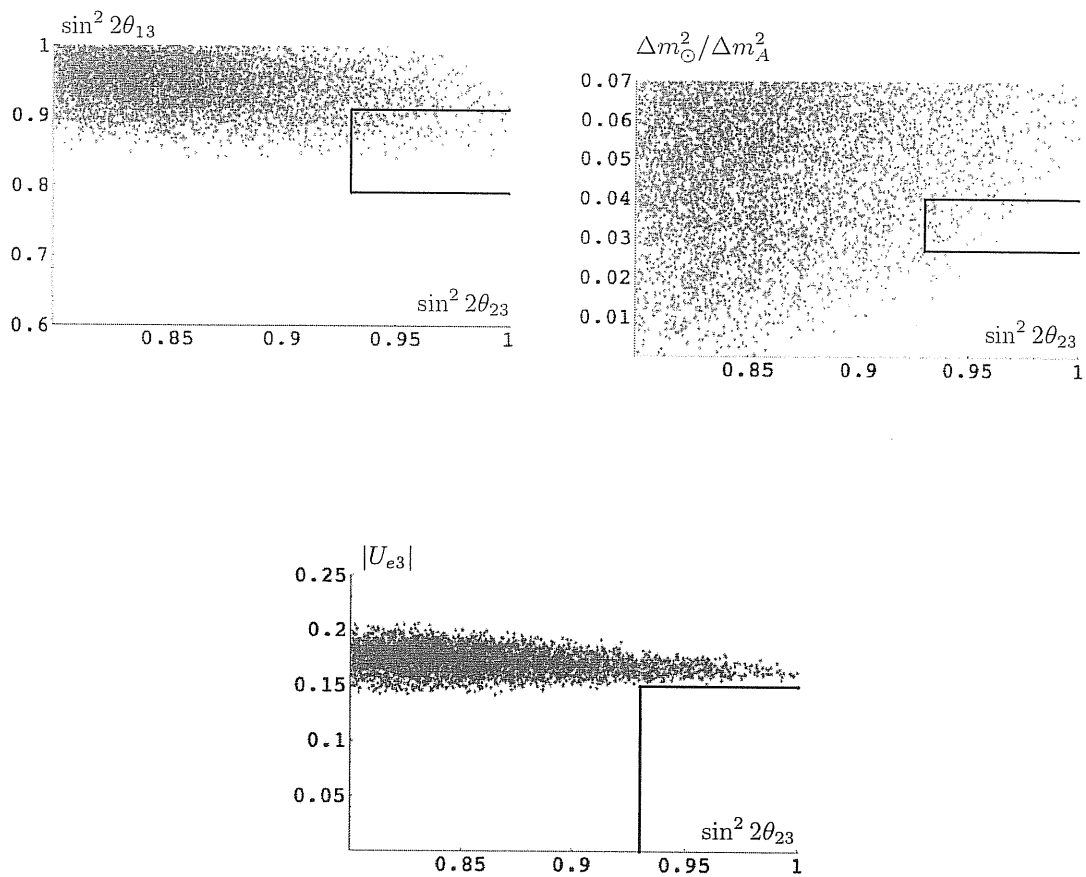
Minimal SUSY SO(10), CP-conserving Yukawa sector, $\tan\beta = 10$, 2003 data

Figure 3.4: Density plots of $\sin^2 2\theta_{12}$, $\Delta m_{\odot}^2/\Delta m_A^2$ and $|U_{e3}|$ are shown as functions of $\sin^2 2\theta_{23}$ in the minimal SUSY SO(10) model with CP conserving Yukawa sector discussed in section 3.5 and $\tan\beta = 10$. The experimental ranges for the leptonic mixing parameters are those considered in [40, 44]. The solid contours enclose the experimentally allowed regions at the 90% C.L. The dark areas correspond to the solutions that are consistent with all neutrino data. The effects of recent experimental data are depicted at Fig. 3.5.



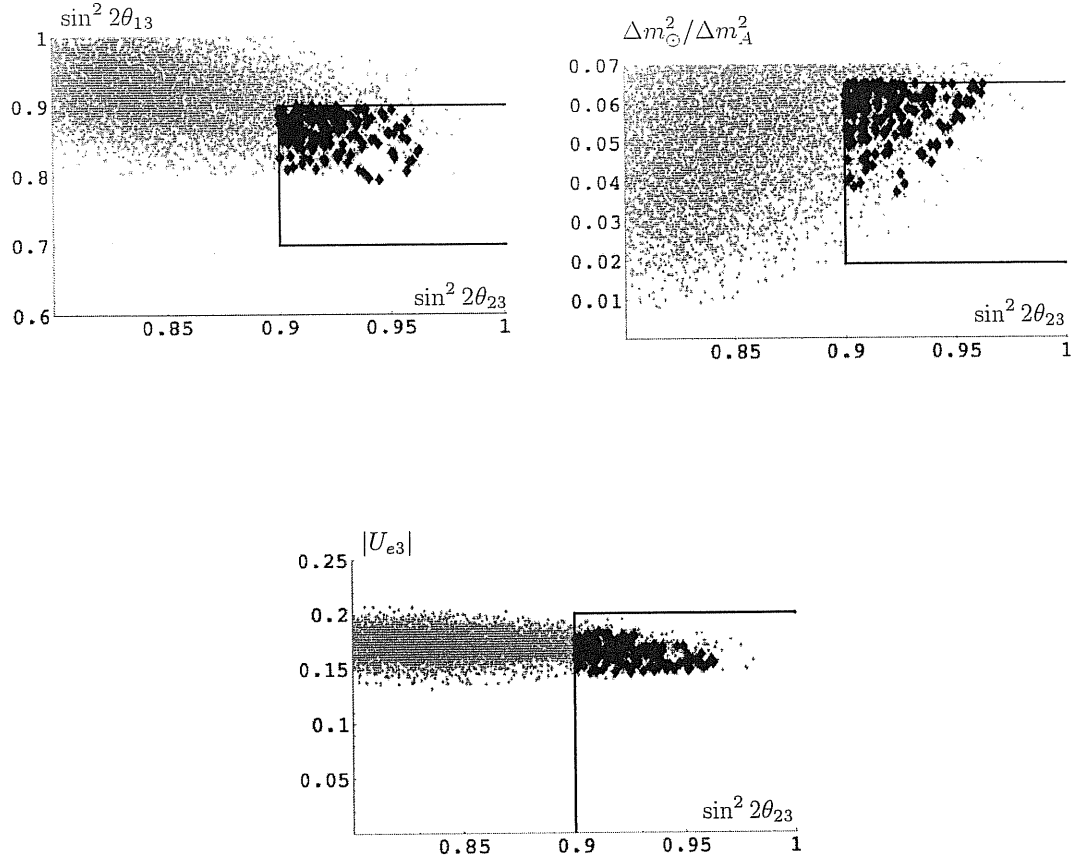
Minimal SUSY SO(10), CP-conserving Yukawa sector, $\tan\beta = 10$, 2005 data

Figure 3.5: Density plots of $\sin^2 2\theta_{12}$, $\Delta m_{\odot}^2/\Delta m_A^2$ and $|U_{e3}|$ are shown as functions of $\sin^2 2\theta_{23}$ in the minimal SUSY SO(10) model with CP conserving Yukawa sector discussed in section 3.5 and $\tan\beta = 10$. The experimental ranges for these parameters are those given in [24]. The solid contours enclose the experimentally allowed regions at the 90% C.L. There are no solutions simultaneously consistent with all neutrino data.



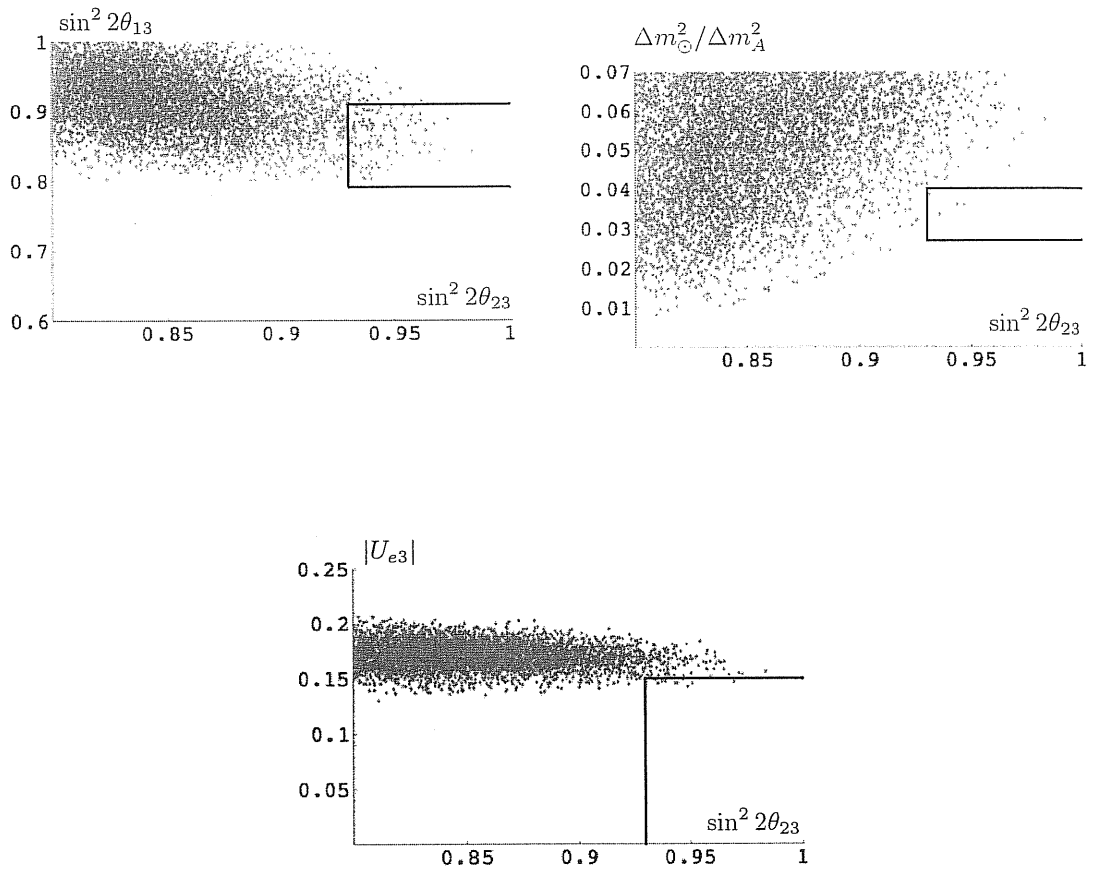
Minimal SUSY SO(10), CP-conserving Yukawa sector, $\tan\beta = 55$, 2003 data

Figure 3.6: Density plots of $\sin^2 2\theta_{12}$, $\Delta m_{\odot}^2/\Delta m_A^2$ and $|U_{e3}|$ are shown as functions of $\sin^2 2\theta_{23}$ in the minimal SUSY SO(10) model with CP conserving Yukawa sector discussed in section 3.5 and $\tan\beta = 55$. The experimental ranges for the leptonic mixing parameters are those considered in [40, 44]. The solid contours enclose the experimentally allowed regions at the 90% C.L. The dark areas correspond to the solutions that are consistent with all neutrino data. The effects of recent experimental data are depicted at Fig. 3.7.



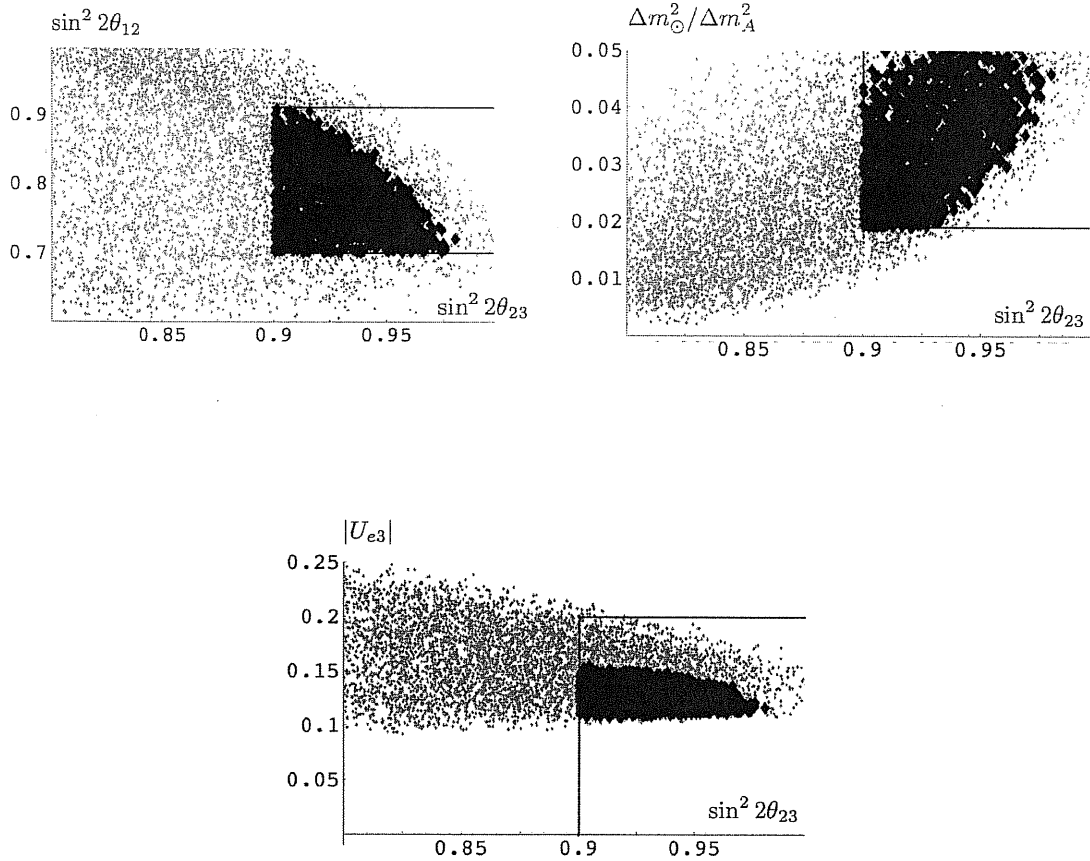
Minimal SUSY SO(10), CP-conserving Yukawa sector, $\tan \beta = 55$, 2005 data

Figure 3.7: Density plots of $\sin^2 2\theta_{12}$, $\Delta m_{\odot}^2/\Delta m_A^2$ and $|U_{e3}|$ are shown as functions of $\sin^2 2\theta_{23}$ in the minimal SUSY SO(10) model with CP conserving Yukawa sector discussed in section 3.5 and $\tan \beta = 55$. The experimental ranges for these parameters are those given in [24]. The solid contours enclose the experimentally allowed regions at the 90% C.L. There are no solutions simultaneously consistent with all neutrino data.



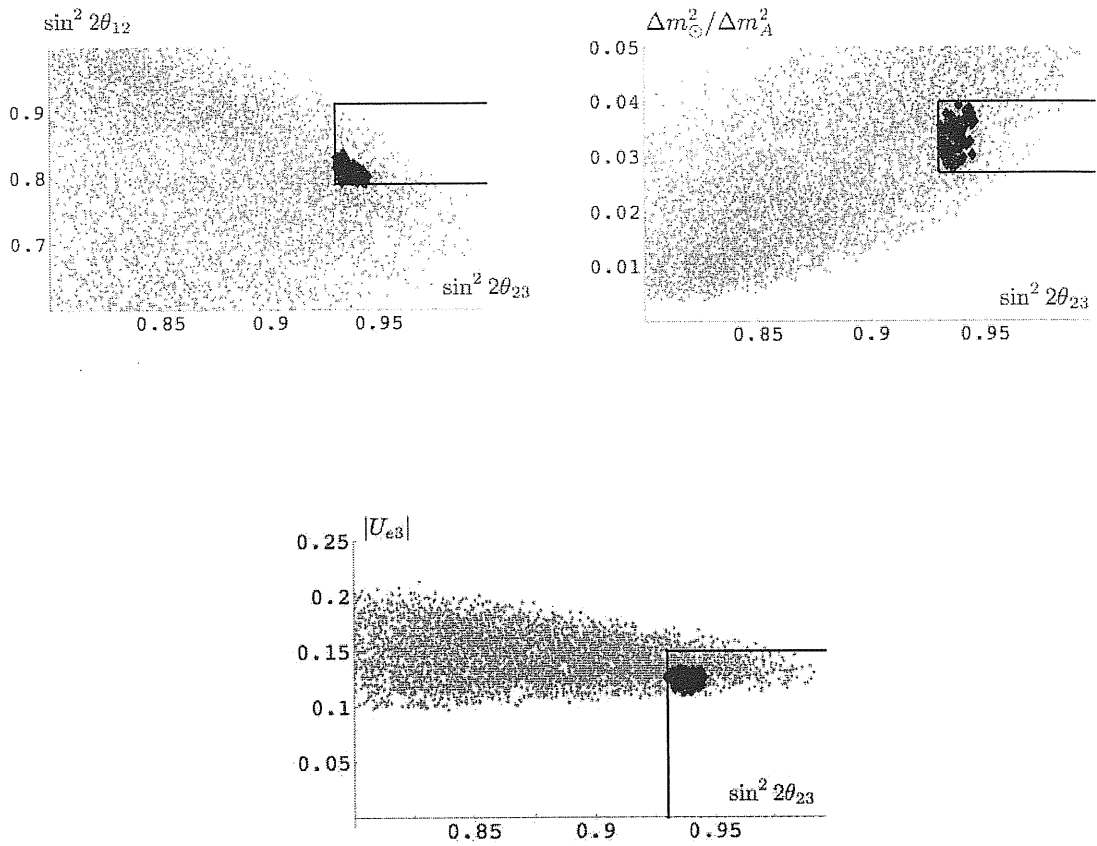
Minimal SUSY SO(10), CP-violating Yukawa sector, $\tan\beta = 10$, 2003 data

Figure 3.8: Density plots of $\sin^2 2\theta_{12}$, $\Delta m_{\odot}^2/\Delta m_A^2$ and $|U_{e3}|$ are shown as functions of $\sin^2 2\theta_{23}$ in the minimal SUSY SO(10) model with CP violating Yukawa sector discussed in section 3.7 for $\tan\beta = 10$. The experimental ranges for these parameters are those considered in [40, 44]. The solid contours enclose the experimentally allowed regions at the 90% C.L. The dark points correspond to solutions that are consistent with all neutrino data. The recent situation is depicted at Fig. 3.9



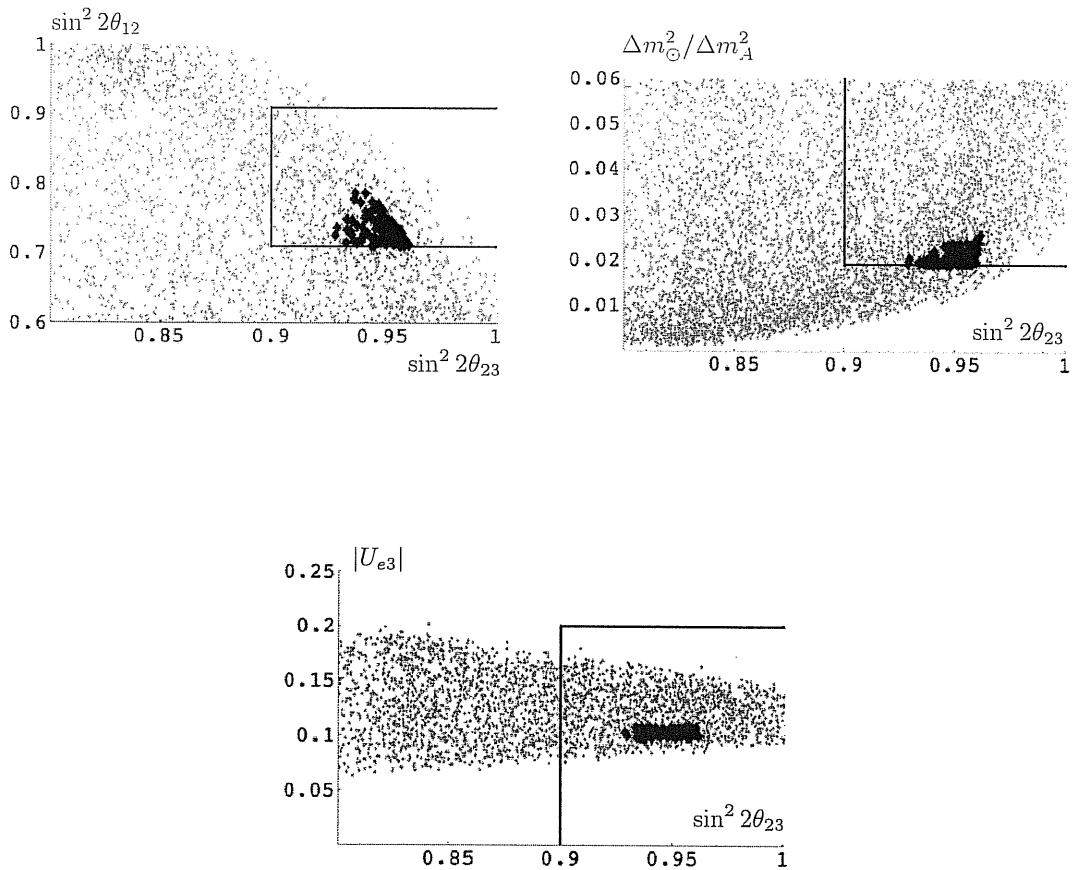
Minimal SUSY SO(10), CP-violating Yukawa sector, $\tan \beta = 10$, 2005 data

Figure 3.9: Density plots of $\sin^2 2\theta_{12}$, $\Delta m_{\odot}^2/\Delta m_A^2$ and $|U_{e3}|$ are shown as functions of $\sin^2 2\theta_{23}$ in the minimal SUSY SO(10) model with CP violating Yukawa sector discussed in section 3.7 for $\tan \beta = 10$. The experimental ranges for these parameters are those given in [24]. The solid contours enclose the experimentally allowed regions at the 90% C.L. The dark points correspond to solutions that are consistent with all neutrino data.



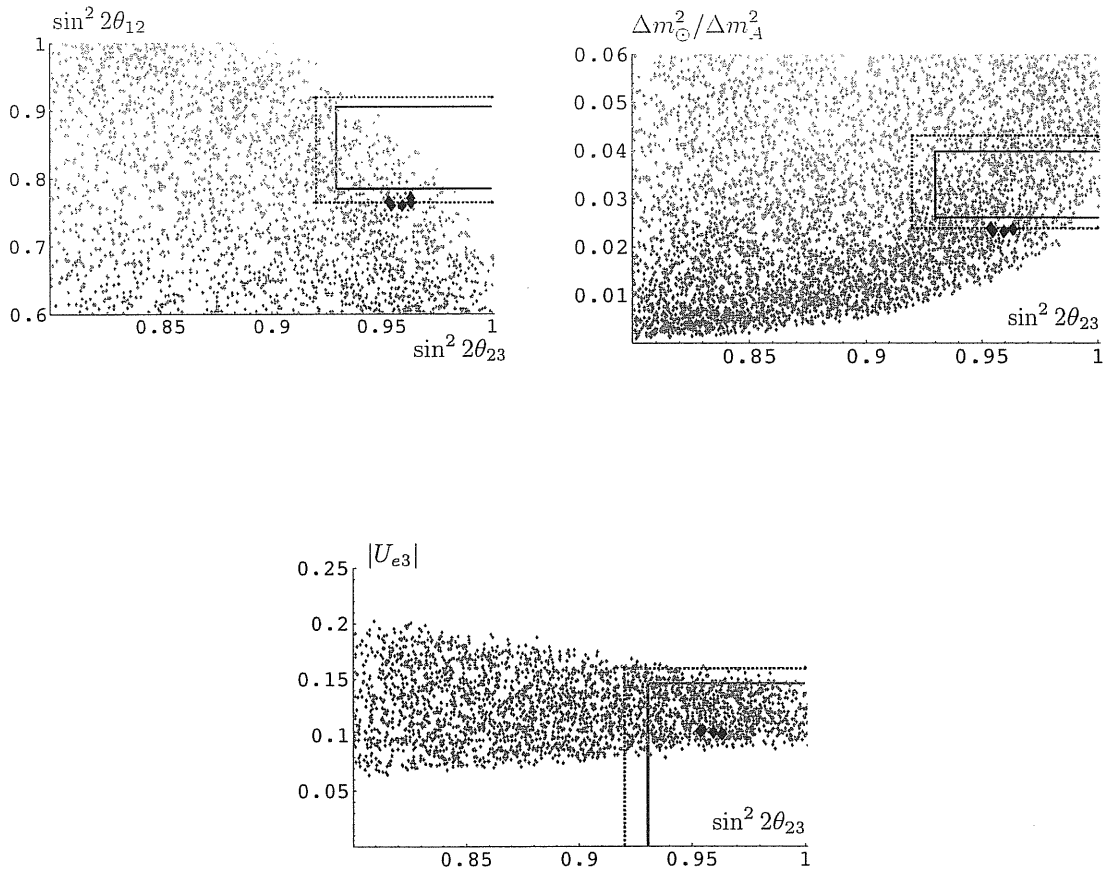
Minimal SUSY SO(10), CP-violating Yukawa sector, $\tan\beta = 55$, 2003 data

Figure 3.10: Density plots of $\sin^2 2\theta_{12}$, $\Delta m_{\odot}^2/\Delta m_A^2$ and $|U_{e3}|$ are shown as functions of $\sin^2 2\theta_{23}$ in the minimal SUSY SO(10) model with CP violating Yukawa sector discussed in section 3.7 for $\tan\beta = 55$. The experimental ranges for these parameters are those considered in [40, 44]. The solid contours enclose the experimentally allowed regions at the 90% C.L. The dark points correspond to solutions that are consistent with all neutrino data. The recent situation is depicted at Fig. 3.11



Minimal SUSY SO(10), CP-violating Yukawa sector, $\tan\beta = 55$, 2005 data

Figure 3.11: Density plots of $\sin^2 2\theta_{12}$, $\Delta m_{\odot}^2/\Delta m_A^2$ and $|U_{e3}|$ are shown as functions of $\sin^2 2\theta_{23}$ in the minimal SUSY SO(10) model with CP violating Yukawa sector discussed in section 3.7 for $\tan\beta = 55$. The experimental ranges for these parameters are those given in [24]. The solid and dashed contours enclose the experimentally allowed regions at 90% and 95% C.L. respectively. The dark points correspond to solutions that are consistent with all neutrino data 95% C.L. ranges. Due to the stronger hierarchy in the down quark and charged lepton sectors the values of the $\Delta m_{\odot}^2/\Delta m_A^2$ parameter are generally than in the $\tan\beta = 10$ case and can be lifted only for the price of reduced solar mixing. c.f. section 3.7.



Chapter 4

Quark and lepton masses and mixing in extensions of minimal renormalizable SUSY SO(10)

In the last chapter we investigated in detail the correlations among Yukawa couplings in the minimal renormalizable SUSY $SO(10)$ framework. We have seen that the minimal setup is very constrained, even so much that it fails to describe the observed pattern of the quark and lepton masses and mixing pattern until the input parameters are stretched within their 90% C.L. ranges ¹. The sharp *prediction* of $|U_{e3}| \gtrsim 0.09$ is a true smoking gun of the minimal scheme and the future long-baseline neutrino experiments² are capable to measure this PMNS matrix element up to values of almost an order of magnitude below this strict bound.

However, even within the minimal $SO(10)$ framework, at some level, the effects of nonrenormalizable effective operators coming from physics above the GUT scale must be taken into account. One should also keep in mind the fact that a class of alternative, but still viable scenarios arise once the 120-dimensional three-index antisymmetric tensor of the decomposition

$$16 \otimes 16 = 10 \oplus 126 \oplus 120, \quad (4.1)$$

is employed instead of (or even together with) the “standard” 10_H .

On the other hand, adding a third contribution to the minimal model Yukawa sum-rules 3.2 (be it a consequence of nonrenormalizable effects or the presence of an additional elementary Higgs fields at the GUT scale), the theory can easily loose all the

¹with a typical value of χ^2 in the 15-25 range

²like ICARUS, OPERA or CNGS, [105]

predictive power in the matter sector and become impossible to test. Therefore, such a class of extensions of the minimal renormalizable scenario, if supposed to address the issue of the quark and lepton masses and mixing in a nontrivial way, must be equipped by additional constraints coming either from dynamical reasons (as it is the case of effective operators) or put by hands like for instance additional GUT-scale symmetries. This singles out a class of “tractable” models of quark and lepton masses and mixing beyond the original minimal renormalizable framework discussed in the previous parts of this work.

A representative of this set, a minimally extended minimal SUSY $SO(10)$, is the subject of the rest of this chapter.

4.1 Minimal extension of minimal Yukawa sector

Clearly, to keep the big achievements of the minimal scheme (be it the interesting correlation among the $b - \tau$ Yukawa convergence and large atmospheric mixing angle in the type-II dominated case or the sharp lower bound on $|U_{e3}|$ obtained in the same scheme) intact, the effects of the new contributions in the Yukawa sector should not overwhelm the original structure.

Remarkably enough, the troubles of the renormalizable approach can be all traced back to “small entries” in the 1-2 sector of the relevant effective sum-rules. As a matter of fact, the smallness of the solar mixing that prevented us from obtaining better fits of the neutrino mass and mixing pattern in the minimal scheme, the robustness of the $|U_{e3}|$ lower bound and also the problems with getting a good electron mass fit for the physical region of the CKM CP phase come from the mismatch of subleading, typically per-mille order terms therein. Therefore, one can expect all these issues to be potentially addressed by even strongly suppressed additional contributions in eq. (3.2) without spoiling the neat features of scheme.

Naturally, regardless of their true origin, such terms can be viewed as effects of non-renormalizable operators generated at scales higher than M_{GUT} , perhaps at M_{Planck} . Since there are only three factors in the decomposition 4.1, there are also only three classes of contributions entering the effective Yukawa sum-rules eq. (3.2) that can be uniquely identified by their $SO(10)$ symmetry properties.

4.1.1 Effects of an additional antisymmetric Yukawa contribution

As we shall see, from these three options the case of 120 is of particular interest, because

- The antisymmetric nature of the Yukawa structure coming from an additional contribution transforming as 120 of $SO(10)$ brings the minimal number of new

parameters: the three complex entries of a $3 \otimes 3$ antisymmetric matrix and two independent ratios of these contributions to the effective sum-rules (3.2).

- As shown in Appendix C.1. the antisymmetry of Y_{120} implies that the eigenvalues of the symmetric mass matrices are unmodified up to $\mathcal{O}(\varepsilon_x^2)$ corrections where ε_x measures the “smallness” of the additional term. This suggests that the 120_H induced mass corrections may affect at the leading order the determination of the mixing angle in such a way not to destabilize the good fit of the mass eigenvalues obtained in the minimal model. This feature is relevant for qualitative understanding of the numerical discussion presented in the next section (see also Appendix B).

Both these properties are highly welcome from the point of view of a numerical analysis that, as we shall see, remains to large extent tractable even in such case. In what follows this option is worked out in detail.

Let us therefore consider an extension of the minimal renormalizable framework in which a pure (strongly suppressed) antisymmetric correction to the quark and lepton effective Yukawa sum-rules (3.2) arises from effects of an additional quasidecoupled 120_H representation in the Higgs sector of the model [44]. Recall that effects of an additional 120_H were already studied in the literature long time ago, but never in this setup and always biased by additional requirements making the general setting with three Yukawa couplings tractable, see e.g. [74] and references therein.

4.2 Adding a small Y_{120} to the minimal Yukawa sum-rules

An important feature of the 120-dimensional representation of $SO(10)$ is its $SU(2)_L$ doublet contents : unlike 10_H or $\overline{120}_H$, 120_H contains 2 copies of the $SU(2)_L \otimes SU(2)_R$ bidoublets residing in the components with Pati-Salam quantum numbers $(1, 2, 2)_{120}$ and $(15, 2, 2)_{120}$. Therefore, the effective minimal model $SU(2)_L$ doublet mass matrices are enlarged by 2 rows and columns and in general the MSSM doublet VEVs would have nonzero projection in the direction of these components as well. In other words, there shall be four new effective VEVs playing a role in the effective Yukawa sum-rules in this framework, see section 4.3.

4.2.1 Group-theory properties of 120_H

From the group-theory point of view, the 120-dimensional representation of $SO(10)$ is spanned over the space of three-index antisymmetric tensors. As a consequence, the

couplings of the 120_H Higgs doublets to the fermionic bilinears must be antisymmetric in the generation indices, see e.g. [106].

Another important feature of 120_H stems from the fact that (up to the VEVs of the MSSM doublet components) it can not participate on the spontaneous breakdown of the $SO(10)$ symmetry³ and thus the need of the 210 - (or a $45 \oplus 54$ if one does not require renormalizability, see section 2.1.2) and 126-dimensional multiplets is justified even in the presence of 120_H . In general, one can think about avoiding 10_H if 120_H is present, but usually the fundamental representation is taken as the most natural source of the Standard model doublets in the Higgs sector and it for sure can not be done if 120_H is almost decoupled.

4.2.2 The model

Using a simplified and self-explanatory notation the Yukawa part of the superpotential of the model under consideration reads

$$W_Y = 16_F (Y_{10} 10_H + Y_{126} \overline{126}_H + Y_{120} 120_H) 16_F \quad (4.2)$$

while the Higgs part is given by

$$\begin{aligned} W_H = & M_{10} 10_H^2 + M_{126} \overline{126}_H 126_H + M_{210} 210_H^2 + M_{120} 120_H^2 + \\ & + \lambda 210_H^3 + \eta 210_H \overline{126}_H 126_H + 10_H 210_H (\alpha 126_H + \beta \overline{126}_H) + \\ & + \eta' 210_H 120_H 120_H + \gamma 10_H 210_H 120_H + 120_H 210_H (\alpha' 126_H + \beta' \overline{126}_H) \end{aligned} \quad (4.3)$$

where, as we have seen, the 3×3 matrices (in general complex) Y_{10} and Y_{126} are symmetric while Y_{120} is antisymmetric.

For the discussion that follows it is convenient to write down the explicit decomposition of the $SO(10)$ Higgs representations under the $SU(4)_{PS} \otimes SU(2)_L \otimes SU(2)_R$:

$$\begin{aligned} 10 &= (1, 2, 2) \oplus (6, 1, 1) \\ \overline{126} &= (15, 2, 2) \oplus (\overline{10}, 3, 1) \oplus (10, 1, 3) \oplus (6, 1, 1) \\ 126 &= (15, 2, 2) \oplus (10, 3, 1) \oplus (\overline{10}, 1, 3) \oplus (6, 1, 1) \\ 120 &= (1, 2, 2) \oplus (15, 2, 2) \oplus (\overline{10}, 1, 1) \oplus (10, 1, 1) \oplus (6, 3, 1) \oplus (6, 1, 3) \\ 210 &= (15, 1, 3) \oplus (15, 3, 1) \oplus (\overline{10}, 2, 2) \oplus (10, 2, 2) \oplus (6, 2, 2) \oplus (15, 1, 1) \oplus (1, 1, 1) \end{aligned} \quad (4.4)$$

It is also helpful to recall the $SU(3)_c \otimes U(1)_{B-L}$ decomposition of the relevant $SU(4)_{PS}$ multiplets (with standard model $B - L$ normalization):

$$6 = (3, -2/3) \oplus (\overline{3}, +2/3)$$

³c.f. Appendix B.3

$$\begin{aligned}
10 &= (6, +2/3) \oplus (3, -2/3) \oplus (1, -2) \\
15 &= (8, 0) \oplus (3, +4/3) \oplus (\bar{3}, -4/3) \oplus (1, 0)
\end{aligned}
\tag{4.5}$$

Since 120_H does not contribute to $SO(10)$ breaking, one may assume that the same (direct) breaking pattern like in the minimal SUSY $SO(10)$ is achieved [34, 69]. Recall that in such a case, the non vanishing VEV of the $(1, 1, 1)_{210}$ (and optionally $(15, 1, 1)_{210}$) component of 210_H triggers the breaking of $SO(10)$ down to $SU(4)_{PS} \otimes SU(2)_L \otimes SU(2)_R$ (or $SU(3)_c \otimes SU(2)_L \otimes SU(2)_R \otimes U(1)_{B-L}$). The subsequent left-right symmetry breaking step to $SU(3)_c \otimes SU(2)_L \otimes U(1)_Y$ of Standard Model is achieved at the scale $M_R \leq M_G$ by VEVs of $(15, 1, 3)_{210}$, $(\bar{10}, 1, 3)_{126}$ and $(10, 1, 3)_{\bar{126}}$. Since the $B-L$ charge of the color singlets contained in 10 (and 15) of $SU(4)_{PS}$ is even, R-parity is preserved. The final electroweak breaking step is obtained by the traditional VEVs induced by weak scale SUSY soft-breaking terms on the light LH doublets obtained from the colorless components of the bidoublets present in eq. (4.5). Since 210_H mixes 126_H , $\bar{126}_H$, as well as 120_H , with 10_H one expects that all the color singlet LH doublets mix to give (via minimal fine tuning) the two light Higgs doublets of MSSM, leaving the other states heavy.

In this respect the bidoublet components in the 120_H representation may exhibit a specific feature that is crucial for the consistency of the simple model (leading to a strongly suppressed purely antisymmetric correction to the relevant Yukawa rules) we are trying to construct. Since none of the 120_H components participates at the spontaneous breaking of $SO(10)$ down to the MSSM group, the mass parameter M_{120} in eq. (4.4) is not constrained by the VEV conditions and one can make it large, perhaps as large as the Planck scale [107, 108], without requiring any fine tuning among the mass and the couplings in the potential. By this assumption, one gets a rationale for the required decoupling effect of 120_H of the order of roughly $M_G/M_{Pl} \sim 10^{-3}$. In such a case, the 120_H colorless $SU(2)_L$ doublet components acquire an induced VEV suppressed by the above factor with respect to the doublets contained in the other representations⁴.

Relations among the VEVs of the relevant components can be obtained, neglecting explicit soft SUSY breaking, from the F-term (and D-term) flatness of the supersymmetric vacuum, i.e. by requiring $\langle F_X \rangle = \langle \partial W / \partial X \rangle = 0$ for any superfield X in the superpotential, replaced by its scalar component.

Considering the $SO(10)$ superpotential in eq. (4.4) and its decomposition in terms of $SU(4)_{PS} \otimes SU(2)_L \otimes SU(2)_R$, of which some relevant terms are

$$126_H \otimes \bar{126}_H \otimes 210_H = (\bar{10}, 1, 3)_{126} (10, 1, 3)_{\bar{126}} (15, 1, 1)_{210} \oplus \dots$$

⁴Remarkably enough, the same game can be played also with 10 if alternative schemes are considered.

$$\begin{aligned}
10_H \otimes 120_H \otimes 210_H &= (15, 2, 2)_{120}(1, 2, 2)_{10}(15, 1, 1)_{210} \oplus \\
&\quad \oplus (1, 2, 2)_{120}(1, 2, 2)_{10}(1, 1, 1)_{210} \oplus \dots \\
10_H \otimes 126_H \otimes 210_H &= (15, 2, 2)_{126}(1, 2, 2)_{10}(15, 1, 1)_{210} \oplus \\
&\quad \oplus (10, 3, 1)_{126}(1, 2, 2)_{10}(\overline{10}, 2, 2)_{210} \oplus \dots \\
10_H \otimes \overline{126}_H \otimes 210_H &= (10, 1, 3)_{\overline{126}}(1, 2, 2)_{10}(\overline{10}, 2, 2)_{210} \oplus \dots ,
\end{aligned}$$

the vacuum F-flatness in the 120_H bidoublet directions yields

$$\begin{aligned}
\langle (15, 2, 2)_{120} \rangle &\sim \frac{M_R^2}{M_{120}M_{210}} \langle (1, 2, 2)_{10} \rangle \\
\langle (1, 2, 2)_{120} \rangle &\sim \frac{M_G}{M_{120}} \langle (1, 2, 2)_{10} \rangle ,
\end{aligned} \tag{4.6}$$

where $O(1)$ couplings are assumed and $\langle (\overline{10}, 1, 3)_{126} \rangle = \langle (10, 1, 3)_{\overline{126}} \rangle \sim M_R$ (as required by D-flatness at M_R). The induced VEVs of the relevant colorless $\overline{126}_H$ left-doublet components are not affected by 120_H and as in the minimal scenario

$$\langle (15, 2, 2)_{\overline{126}} \rangle \sim \frac{M_R^2}{M_{126}M_{210}} \langle (1, 2, 2)_{10} \rangle \quad \langle (\overline{10}, 3, 1)_{\overline{126}} \rangle \sim \frac{M_R}{M_{210}} \frac{\langle (1, 2, 2)_{10} \rangle^2}{M_{126}} \tag{4.7}$$

The small $SU(2)_L$ triplet VEV subsequently leads to the type-II Majorana mass for neutrinos.

In the single-step breaking scenario⁵, the assumption $M_{120} \sim M_{Pl}$ and relations (4.6)-(4.7) yield the desired $O(M_G/M_{Pl})$ suppression of the 120_H $SU(2)_L$ doublet VEVs with respect to those in 10_H and $\overline{126}_H$. Since this result is controlled by the decoupling of the 120_H representation, such a suppression is not spoiled by the soft SUSY breaking potential triggering the weak scale the $SU(2)_L \times U(1)_Y$ breaking.

4.3 Effective Yukawa sum-rules

The most general structure of the fermion mass matrices in the renormalizable $SO(10)$ model with all possible types of Higgs fields coupled to fermions is given by [109, 110]

$$\begin{aligned}
M_u &= Y_{10}v_u^{10} + Y_{126}v_u^{126} + Y_{120}v_u^{120} , \\
M_d &= Y_{10}v_d^{10} + Y_{126}v_d^{126} + Y_{120}v_d^{120} , \\
M_\nu^d &= Y_{10}v_u^{10} - 3Y_{126}v_u^{126} + Y_{120}v_\nu^{120} , \\
M_l &= Y_{10}v_d^{10} - 3Y_{126}v_d^{126} + Y_{120}v_l^{120} , \\
M_\nu^s &= v^S Y_{126} \\
M_\nu^t &= v^T Y_{126}
\end{aligned} \tag{4.8}$$

⁵corresponding to a rough coincidence of M_R with M_G

Here v_x^{120} are linear combinations of the four 120_H isodoublet VEVs residing in the $(1, 2, 2)_{120}$ and $(15, 2, 2)_{120}$ of $SU(4)_{PS} \otimes SU(2)_L \otimes SU(2)_R$

$$\begin{aligned} v_u^{120} &\equiv \langle (15, 2, 2)_u \rangle, & v_d^{120} &\equiv \langle (1, 2, 2)_d \rangle + \langle (15, 2, 2)_d \rangle \\ v_\nu^{120} &\equiv \langle (1, 2, 2)_u \rangle, & v_l^{120} &\equiv \langle (1, 2, 2)_d \rangle - 3\langle (15, 2, 2)_d \rangle \end{aligned}$$

The -3 factor in v_l^{120} originates from the same mechanism like the -3 term in (4.8), c.f. Appendix B.5. Notice that since there are no $SU(2)_R$ singlets neither triplets in 120_H there is no contribution to the Majorana mass matrices coming from Y_{120} . This could be easily seen also from the antisymmetry of Y_{120} : it can not contribute to M_ν^s and M_ν^t that (as any Majorana mass matrix) must be symmetric in generation indices. To achieve the desired tractable structure of the sum-rules (4.8) from now on we take $v_x^{120}/v_x^{10,126} \sim M_G/M_{Pl}$ and the 120_H contributions to the mass matrices shall be treated as perturbations.

4.3.1 Phasecounting

Apart of the 8 minimal model phases (7 in the pure triplet seesaw case) one gets in general 6 (5) more phases coming from the 7 (6) new complex parameters v_u^{120} , v_d^{120} , v_l^{120} and v_ν^{120} (the last being obviously absent in the triplet dominated case). This comes from the fact that as before for the Y_{10} and Y_{126} one of the phases of the effective VEVs can be reabsorbed in the redefinition of Y_{120} . In total, we end up with 15 independent phases in the most general case while there are 13 phase parameters if the seesaw formula for the light neutrino masses is dominated by the triplet contribution.

4.3.2 Counting all real parameters

On top of these 15 (13)⁶ phases one must add the 13 “magnitudes” of the quark and lepton mass and mixing parameters considered in the minimal setup (c.f. section 3.1.3) and 5 more in the extended case. As before, not all the phases in the general neutrino mass formula are independent and in general, one can get rid of two of them - only the relative phase among the Dirac neutrino mass matrix and the Majorana piece in the denominator of the type-I term matters and also the overall phase of the neutrino mass matrix is irrelevant. In total, the number of parameters to deal with becomes enormous: 33 in the most general case and 31 in the triplet dominated scheme.

Therefore, even in the very minimalistic case considered here, it is hard to analyze the extended model in full generality. Rather than that, let us focus on few illustrations

⁶Number in paranthesis corresponds to the type-II dominated seesaw case.

of the possible effects that a quasidecoupled 120-dimensional Higgs representation can bring paying particular attention on the influence of the additional terms in eq. (4.8) on the correlations among the leptonic mixing angles and the shape of the neutrino spectrum.

4.4 Quark and lepton mass and mixing correlations

As in the case of the minimal model one can further narrow the area of the parametric space potentially leading to a realistic output by a detailed inspection of analytic formulae that could bring several hints about the relevance of some of the input parameters. As before, let us stick on the case of a triplet dominating the seesaw formula taking the advantage of an almost automatic large atmospheric mixing angle and a slightly reduced the number of free parameters, c.f. section 3.2.

4.4.1 Effective sum-rules - real setup

Let us start with inspecting the general form of the effective in the considered setting. The minimal model formulae (3.14) and (3.15) change to

$$\begin{aligned} k\tilde{M}_l &= \tilde{M}_u + r\tilde{M}_d + Y_{120}(k\varepsilon_l - \varepsilon_u - r\varepsilon_d) , \\ M_\nu &\propto [M_l - M_d + Y_{120}(m_b\varepsilon_d - m_\tau\varepsilon_l)] , \end{aligned} \quad (4.9)$$

As before, the tilded matrices are normalized so that the absolute value of their maximal generalized eigenvalue⁷ is one. The smallness of the VEVs of doublets descending from 120_H is expressed by the short-hand notation

$$\varepsilon_u \equiv \frac{v_u^{120}}{m_t} , \quad \varepsilon_d \equiv \frac{v_d^{120}}{m_b} , \quad \varepsilon_l \equiv \frac{v_l^{120}}{m_\tau} . \quad (4.10)$$

so that $\varepsilon_x \lesssim \mathcal{O}(10^{-3})$. The main difference with respect to the minimal model formulae (3.14) and (3.15) stems from the fact that the mass matrices of charged fermions are no longer symmetric and can be diagonalized only by means of a *biorthogonal* transformation

$$M_x = V_x^R D_x V_x^{LT} , \quad x = u, d, l$$

so that

$$kV_d^{RT} \tilde{M}_l V_d^L = W^T \tilde{D}_u V_{CKM} + r\tilde{D}_d + Y'_{120}(k\varepsilon_l - \varepsilon_u - r\varepsilon_d) \quad (4.11)$$

provided

$$W \equiv V_u^{RT} V_d^R , \quad V_{CKM} \equiv V_u^{LT} V_d^L , \quad Y'_{120} \equiv V_d^{RT} Y_{120} V_d^L .$$

⁷By “generalized eigenvalues” we mean the magnitudes of entries of diagonal part of a general bi-unitary decomposition.

The neutrino mass matrix reads now

$$V_d^{LT} M_\nu V_d^L = m_0 V_d^{LT} V_d^R \left[V_d^{RT} \tilde{M}_l V_d^L - \frac{m_b}{m_\tau} \tilde{D}_d + Y'_{120} \left(\frac{m_b}{m_\tau} \varepsilon_d - \varepsilon_l \right) \right], \quad (4.12)$$

where m_0 is an overall neutrino mass scale. Note that although there is an explicit asymmetry $\sim Y'_{120}$ in the formula (4.12), $V_d^{LT} M_\nu V_d^L$, being a Majorana mass matrix, remains symmetric in any *basis* due to an interplay among the V_d^L , V_d^R and Y'_{120} factors above. Once the matrices on the left-hand side of eq. (4.11) and eq. (4.16) are reconstructed, the lepton mixing matrix U_{PMNS} is given by

$$U_{PMNS} \equiv U_l^T U_\nu, \quad (4.13)$$

where

$$V_d^{LT} M_l^T M_l V_d^L \equiv U_l D_l^2 U_l^T, \quad V_d^{LT} M_\nu V_d^L \equiv U_\nu D_\nu U_\nu^T.$$

Notice that eq. (4.13) does not depend on V_d^L .

4.4.2 Right-handed quark mixing matrix

The missing ingredient needed to perform the fitting procedure of charged lepton masses⁸ is the right-handed quark mixing matrix W . Since for $\varepsilon_x = 0$ one has $W = V_{CKM}$, it is convenient to expand W around V_{CKM} in powers of ε_x . Using the results of the analysis given in Appendix C.1 one obtains

$$W = V_{CKM} + 2(-\varepsilon_u Z'_u V_{CKM} + \varepsilon_d V_{CKM} Z'_d) + \mathcal{O}(\varepsilon_x^2), \quad (4.14)$$

where the antisymmetric matrices $Z'_{u,d}$ are given by

$$(Z'_x)_{ij} = \frac{(Y'_x)_{ij}}{(\tilde{D}_x)_{ii} + (\tilde{D}_x)_{jj}} \quad (4.15)$$

and $Y'_u \equiv V_{CKM} Y'_{120} V_{CKM}^T$, $Y'_d \equiv Y'_{120}$.

Formulae (4.12) and (4.14) indicate that Y'_{120} and not Y_{120} should be used as an input of the numerical analysis. Notice that though Y'_{120} is not in general antisymmetric, the departure from the exact antisymmetry is of the order of the small parameters. Therefore, this provides an $\mathcal{O}(\varepsilon^2)$ contribution to the relevant formulae that can be neglected at the desired level of accuracy.

There is an important observation coming from formula (4.15) that allows one to understand the mechanism through which as small as one per mille perturbation of

⁸in analogy to the minimal model case discussed in detail in sections 3.5 and 3.7

the minimal setup can lead to much larger effects in the correlations predicted by the model. The denominator of eq. (4.15) is $\mathcal{O}(1)$ for i or $j = 3$ but much smaller for $i = 1, j = 2$ (for $i = j$ the numerator vanishes due to the antisymmetry property of Y' matrices). Therefore, the 12-element of the relevant Z' matrices are of the order of m_3/m_2 (where $m_{2,3}$ are the masses of the second and third generation quarks (m_b/m_s for down-type quarks while m_t/m_c for up-quarks) that compensates the smallness of the $\varepsilon_{u,d}$ parameters defined in eq. (4.10) and enhances the “effective strength” of the 120_H perturbations from the “apparent magnitude” of roughly $\varepsilon_{d,u}$ to approximately $\varepsilon_{d,u}m_{b,t}/m_{s,c}$.

This in general affects the consistency of the approximate prescription for the right-handed quark mixing matrix W (4.14) and leads to several constraints on the magnitude of the $\varepsilon_{u,d}$ parameters to keep the perturbative approach under control. In particular, the effects coming from the large hierarchy in the up-quark sector can be so large that it is better to impose $\varepsilon_u \lesssim 10^{-4}$ and make $\varepsilon_{d,l}$ the dominant sources of the desired effects.

It is interesting that even having $\varepsilon_u = 0$ identically, outputs of the numerical analysis of eqs. (4.11)–(4.14) are practically unaffected. This originates from the “democratic structure” of the ε_x parameters in eq. (4.11) and eq. (4.14). The effects of $\varepsilon_u \sim 10^{-4}$ in these formulæ can be easily mimiced by a proper choice of the ε_d parameter in (4.14) and by an interplay among ε_d and ε_l in eq. (4.11). Moreover, the neutrino mass relation (4.12) is ⁹ ε_u -independent. Thus, in the numerical analysis we take $\varepsilon_u = 0$. Moreover, let us simplify the situation putting also $\varepsilon_l = 0$. Though this leads to a slight loss of generality, it is not a problem here as long as we do not intent to perform a full-featured numerical fit but give just few examples of the possible effects of adding a 120_H to the minimal SUSY SO(10) model.

Effects of a quasidecoupled 120_H on the neutrino spectrum

Let us now inspect in more detail the formula for the neutrino mass matrix (4.12). From the approximate expressions (see Appendix C.1)

$$V_d^{LT} V_d^R \approx 1 + 2\varepsilon_d Z'_d$$

and

$$V_d^{LT} V_u^R = V_{CKM}^T (1 + 2\varepsilon_u Z'_u)$$

together with eq. (4.15), one obtains

$$V_d^{LT} M_\nu V_d^L = M'_\nu + \Delta M'_\nu, \quad (4.16)$$

⁹up to the $V_d^{RT} \tilde{M}_l V_d^L$ part discussed before

where M'_ν is the “minimal model” form of the neutrino mass formula (3.15) and

$$\Delta M'_\nu = \frac{m_0}{k} \left[\varepsilon_u V_{CKM}^T \left(2Z'_u \tilde{D}_u - Y'_u \right) V_{CKM} + \varepsilon_d \left(r - \frac{m_b}{m_\tau} k \right) \left(2Z'_d \tilde{D}_d - Y'_d \right) \right]. \quad (4.17)$$

Using eq. (4.15) and taking into account the hierarchy among quark masses, one obtains, up to order ε_x corrections ($x = u, d$),

$$\left(2Z'_x \tilde{D}_x - Y'_x \right)_{ij} \approx (Y'_x)_{ij} \text{Sign}(j - i) \equiv (Y_x^s)_{ij}. \quad (4.18)$$

Neglecting for simplicity $\mathcal{O}(\lambda)$ terms one can express the net effects on in the neutrino sector by means of a symmetric matrix $V_{CKM}^T Y_u^s V_{CKM} \sim Y_d^s \equiv Y_{120}^s$ which finally leads to

$$\Delta M'_\nu \approx \frac{m_0}{k} \left[\varepsilon_u + \varepsilon_d \left(r - \frac{m_b}{m_\tau} k \right) \right] Y_{120}^s. \quad (4.19)$$

The form of $\Delta M'_\nu$ allows for a direct and simple assessment of the effects of the Y'_{120} -matrix entries on the minimal model neutrino mass spectrum and lepton mixings¹⁰.

In Appendix D formula eq. (4.19) is used to give several semianalytic hints for better understanding of the subsequent numerical analysis.

4.4.3 Effective sum-rules - complex case

The discussion in the CP violating setup with all relevant phase parameters taken into account is slightly more complicated. As in the minimal model case, one can first rescale eq. (4.9) by a global phase such that r becomes real ($r = -|r|e^{i\phi_r}$) and define $k' = k e^{-i\phi_r}$ and diagonalize all the quark mass matrices by means of *biunitary* transformations

$$\tilde{M}_x = V_x^R \tilde{D}_x V_x^{LT} \quad (4.20)$$

The general sum-rules (4.9) are then recast as follows:

$$k' V_d^{R\dagger} \tilde{M}_l V_d^{L*} = V_d^{R\dagger} V_u^R \tilde{D}_u V_{CKM}^0 - |r| \tilde{D}_d + Y'_{120} (k' \varepsilon_l - e^{-i\phi_r} \varepsilon_u + |r| \varepsilon_d) \quad (4.21)$$

$$k' V_d^{R\dagger} M_\nu V_d^{L*} \propto k' V_d^{R\dagger} \tilde{M}_l V_d^{L*} - Y'_{120} k' \varepsilon_l - |k'| e^{i\omega} \left| \frac{m_b}{m_\tau} \right| \left(\tilde{D}_d - Y'_{120} \varepsilon_d \right)$$

where

$$k' \equiv k e^{-i\phi_r}, \quad Y'_{120} \equiv V_d^{R\dagger} Y_{120} V_d^{L*}$$

and

$$V_u^{LT} V_d^{L*} \equiv V_{CKM}^0 = P_u V_{CKM} P_d$$

¹⁰It is interesting that eq. (4.19) does not depend on ε_l and the relevant corrections therefore originate entirely from the quark sector parameters.

Since the antisymmetric components in eq. (4.8) are small, the right-handed quark mixing matrix $W \equiv V_u^{RT} V_d^{R*}$ can be again estimated perturbatively, see Appendix C.2. In the complex case, the relevant equation reads ($x = u, d$):

$$W = V_{CKM}^0 + 2(-|\varepsilon_u| Z'_u{}^* V_{CKM}^0 + |\varepsilon_d| V_{CKM}^0 Z'_d{}^*)$$

The antihermitean ($M^T = -M^*$) matrices Z'_x obey

$$\begin{aligned} Z'_u \tilde{D}_u + \tilde{D}_u Z'_u{}^* &= e^{i\phi_u} V_{CKM}^{0*} Y'_{120} V_{CKM}^{0\dagger} \equiv A_u \\ Z'_d \tilde{D}_d + \tilde{D}_d Z'_d{}^* &= e^{i\phi_d} Y'_{120} \equiv A_d \end{aligned} \quad (4.22)$$

where $\varepsilon_{u,d} = e^{i\phi_{u,d}} |\varepsilon_{u,d}|$. Eqs. (4.22) are then solved by (c.f. Appendix C.2)

$$\operatorname{Re}(Z'_x)_{ij} = \frac{\operatorname{Re}(A_x)_{ij}}{(\tilde{D}_x)_{ii} + (\tilde{D}_x)_{jj}} \quad \operatorname{Im}(Z'_x)_{ij} = \frac{-\operatorname{Im}(A_x)_{ij}}{(\tilde{D}_x)_{ii} - (\tilde{D}_x)_{jj}} \quad (4.23)$$

It is easy to see that putting all relevant phases to 0 or π the formulae of section 4.4.1 are reproduced.

4.4.4 Screening effects of CKM CP violating phase in the electron mass formula

Using the hierarchy of the right-hand side of eq. (4.21), one can again¹¹ expand the magnitude of the normalized electron mass in powers of λ :

$$|k' \tilde{m}_e| e^{i\phi} = T_{MM} + \Delta T_{120} \quad (4.24)$$

The symbol T_{MM} stands for the minimal model contribution (the right-hand side of eq. (3.24)). The correction coming from the additional terms in eq. (4.21) can be written as

$$\Delta T_{120} = -\frac{|r|}{F_s} e^{i\beta_1} F_{\varepsilon_d}^2 [(Y'_{120})_{12}]^2 \lambda^5 + \mathcal{O}(\lambda^6). \quad (4.25)$$

where $F_s \equiv \frac{m_s}{m_b} / \lambda^3$ and $F_{\varepsilon_d} \equiv \varepsilon_d / \lambda^4$ are $\mathcal{O}(1)$ form factors [44]. Notice that the $\mathcal{O}(\lambda^5)$ term of ΔT_{120} is in general larger than the Λ^2 term on the RHS of eq. (3.24) and thus the partial cancellation of the leading $\mathcal{O}(\lambda^4)$ in eq. (4.24) can be easily achieved. As a consequence, one may expect the CKM phase not to be biased toward unphysical values, as it happens in the minimal setup.

Inspecting in detail of the $\mathcal{O}(\lambda^5)$ term in ΔT_{120} and the leading $\mathcal{O}(\lambda^4)$ term in (3.24), a possible way to make these two terms interfere destructively is by taking

¹¹c.f. formula (3.24) in section 3.6.1

purely imaginary entries of the Yukawa matrix Y'_{120} , while assuming no spontaneous CP violation. This particular form of the Yukawa coupling is considered in ref. [74] in a model equipped by an additional global flavor symmetry.

4.4.5 GUT scale input parameters

Since the additional 120-dimensional Higgs representation does not enter the symmetry breaking pattern (up to the electroweak VEVs induced on the bidoublet components) there is no need for an additional fine-tuning that could potentially bring some new Higgs states below the GUT-scale [69]. Therefore, the Yukawa running in the extended model is identical to the minimal case over the whole ‘‘GUT desert’’ and the effective mass parameters entering the numerical analysis can be inherited from that case, see section 3.4.1.

4.5 Numerical analysis - CP conserving Yukawa sector

As in the minimal setting, for simplicity reasons the numerical analysis is performed for real parameters only at the first stage. As was already announced, even a per mille perturbation of the minimal framework sum-rules (3.2) can be capable to change the lower bound on $|U_{e3}|$ and also the solar mixing can be reduced considerably.

Together with the GUT-scale quark mass ranges and mixings given in section 3.4.1 we need to input the additional parameters¹² - Y'_{120} , ε_u , ε_d and ε_l . With this information in hand an extensive scan within the allowed quark mass and mixing ranges is performed. For each point within the scanned region, W is given by eq. (4.14). Notice that as in the minimal model case for each r there remains a freedom to shift m_b (and/or m_t) together with m_d, m_s, v_d^{120} (m_u, m_c, v_u^{120}) within the allowed ranges, while keeping $\tilde{D}_{u,d}$ and $\varepsilon_{u,d}$ constant. For different values of m_b , one set of parameters fitting eq. (4.11) is mapped into another fitting set with different solutions of the neutrino mass matrices in eq. (4.12). This procedure generates as a numerical artifact the ‘chains’ of solutions that are visible at Figures 4.2.

For illustration purposes let us present the results for the following form of the antisymmetric matrix Y'_{120} :

$$Y'_{120} = a \begin{pmatrix} 0 & 1 & 1 \\ \cdot & 0 & -1 \\ \cdot & \cdot & 0 \end{pmatrix}. \quad (4.26)$$

¹²Fixing overall scales of $\varepsilon_x Y'_{120}$, only 5 parameters remain independent.

As shown in Appendix D, thanks to the reduced values of $\Delta m_{\odot}^2/\Delta m_A^2$ that are obtained, the texture in eq. (4.26) allows for a substantial suppression of the solar mixing angle with respect to the corresponding minimal model solutions as well as for reduced values of $|U_{e3}|$. The parameters $v_{u,d}^{120}$ are taken as

$$v_{u,d}^{120} \sim \frac{M_G}{M_{Pl}} v_{u,d}^{10} \approx 10^{-1} (\sin \beta, \cos \beta) \text{ GeV}.$$

Since $(Z'_{u,d})_{12} \approx (Y'_{120})_{12} m_{t,b}/m_{c,s}$ (see eq. (4.15)), the leading order expansion (4.14) for W is a good approximation for $a \lesssim 0.1$. The typical sizes of the $\varepsilon_{u,d} Y'_{120}{}^{s}$ terms in eqs. (4.11) and (4.19) evaluated at the GUT scale and for $\tan \beta = 10$ are then given by

$$\begin{aligned} \varepsilon_u (Y'_{120})_{ij} &\approx a \frac{10^{-1} \text{ GeV}}{m_t} \approx \mathcal{O}(10^{-4}), \\ \varepsilon_d (Y'_{120})_{ij} &\approx a \frac{10^{-2} \text{ GeV}}{m_b} \approx \mathcal{O}(10^{-3}). \end{aligned} \quad (4.27)$$

To compare in an efficient way the deviations obtained in the extended $SO(10)$ scenario with respect to the minimal model results¹³, let us present the relevant density plots for $\tan \beta = 10$ and $1\text{-}\sigma$ ranges of the quark masses, while taking the central values of the quark mixing angles. Considering the 90% C.L. range $0.019 \leq \Delta m_{\odot}^2/\Delta m_A^2 \leq 0.069$ (corresponding to the 2003 neutrino oscillation data [21, 23]) the allowed area for the U_{e3} parameter as a function of $\sin^2 2\theta_{23} > 0.8$ is shown at the third plot of Fig. 4.2. The minimal model lower bound $|U_{e3}| \gtrsim 0.16$ is relaxed by the 120_H corrections to $0.11 < |U_{e3}| < 0.14$ (in this setting). Even within such constrained setup the atmospheric mixing is allowed to be well within the 90% C.L. experimental region and even close to maximal.

The first plot of Fig. 4.2 displays the change of the predicted values of $\sin^2 2\theta_{12}$ as a function of $\sin^2 2\theta_{23}$. In the extended setup one obtains $\sin^2 2\theta_{12} \gtrsim 0.71$, thus covering the whole 90% C.L. allowed range, while in the minimal model $\sin^2 2\theta_{12} \gtrsim 0.88$. For $\Delta m_{\odot}^2/\Delta m_A^2 \lesssim 0.05$ one obtains $\sin^2 2\theta_{12} \gtrsim 0.92$ and 0.77 for the minimal and extended models respectively. The presence of the 120_H -corrections allows, by reducing the values of $\Delta m_{\odot}^2/\Delta m_A^2$,¹⁴ for lower values of the solar and larger values of the atmospheric mixing angles.

¹³c.f. section 3.5 and Figures 3.4 and 3.6

¹⁴c.f. Appendix D

4.6 Numerical analysis - CP violating Yukawa sector

In case of complex form of the effective Yukawa sum-rules (4.21), the results obtained in section 4.4.4 motivate the following choice of the relevant input parameters:

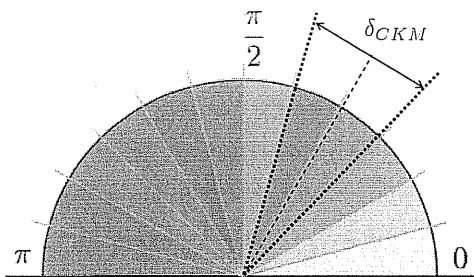
$$Y'_{120} = i \begin{pmatrix} 0 & 1 & -1 \\ \cdot & 0 & 1 \\ \cdot & \cdot & 0 \end{pmatrix},$$

and

$$|\varepsilon_d| = 10^{-3}, |\varepsilon_u| = 10^{-4}, \phi_{u,d} = 0,$$

while as before we put $\varepsilon_l = 0$ for simplicity reasons¹⁵. In Fig. 4.1 the relative density of the charged lepton mass solutions is displayed as a function of the CKM phase. As

Figure 4.1: The relative densities of the charged lepton mass solutions are shown as a function of the CKM phase δ in the model with a quasidecoupled antisymmetric Yukawa coupling in the game for the setup described in the text and 90% C.L. input data from Table 3.2.



expected on analytical grounds in section 4.4.4, the tension driving the CKM phase to the second or third quadrant is almost completely screened by the small 120_H induced terms, making the physical δ_{CKM} a natural outcome of the numerical scan. Correspondingly, it turns out that the presently allowed ranges for the solar and atmospheric mixing can be fully covered by tuning the additional contributions. For an illustration see Fig. 4.3.

It is however worth emphasizing that in spite of the additional freedom in the parameter space a non-vanishing lower bound for $|U_{e3}|$ persists, as in the minimal scheme, c.f. section 3.7. This is shown at Fig. 4.3, obtained for 90% C.L. input data

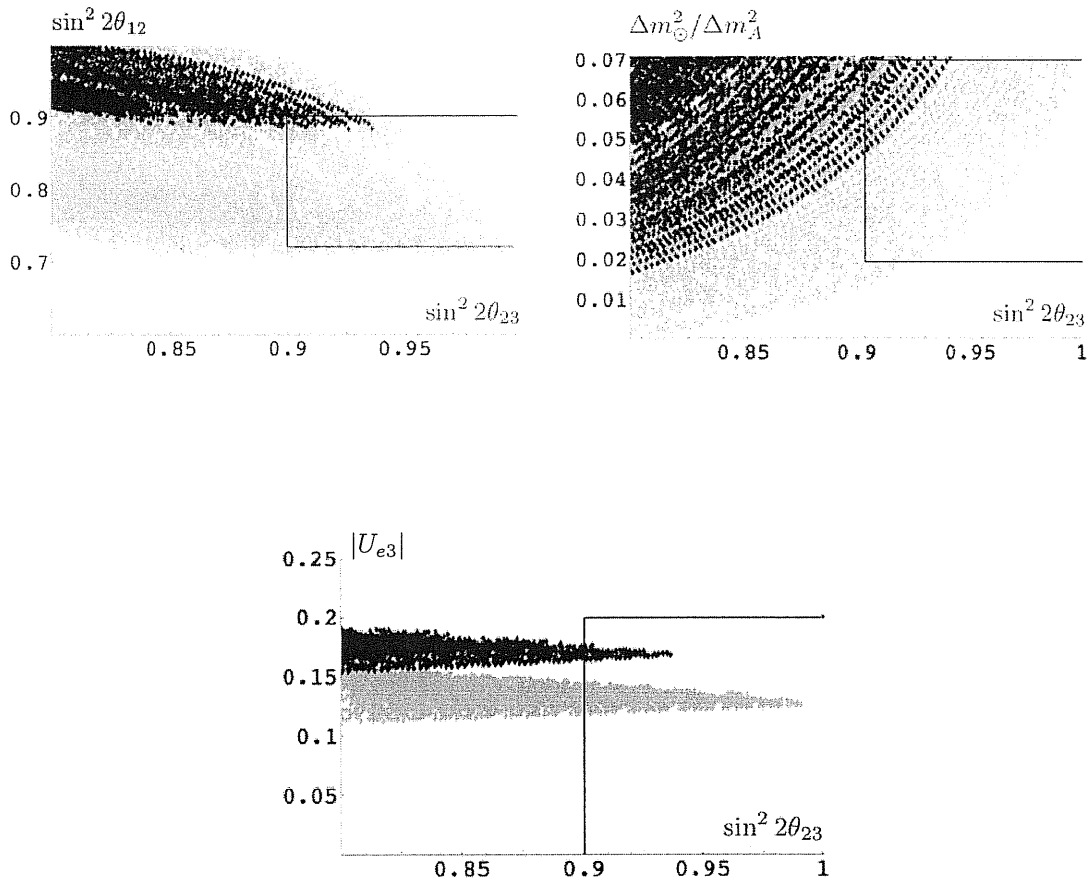
¹⁵The magnitudes of $|\varepsilon_u|$ and $|\varepsilon_d|$ ensure the relevance of the perturbative approach.

in the setup discussed above. As expected, the effect on the solar mixing angle is dramatic and the minimal model correlations are strongly relaxed leading to almost uniform “distribution” of the solutions in plots 4.3.

To conclude, we have seen that the effects of subleading corrections to the minimal SUSY $SO(10)$ effective Yukawa sum-rules (3.2) can be substantial even if their overall magnitude does not exceed a per-mille level of the leading contributions. As we demonstrated on the particular case of a small antisymmetric correction descending from a quasidecoupled 120_H added to the minimal SUSY $SO(10)$ Higgs sector, relatively large effects on the θ_{13} and $|U_{e3}|$ lepton mixing parameters can be generated. Remarkably enough, the lower bound on $|U_{e3}|$ persists and falls into the range of the future experimental surveys.

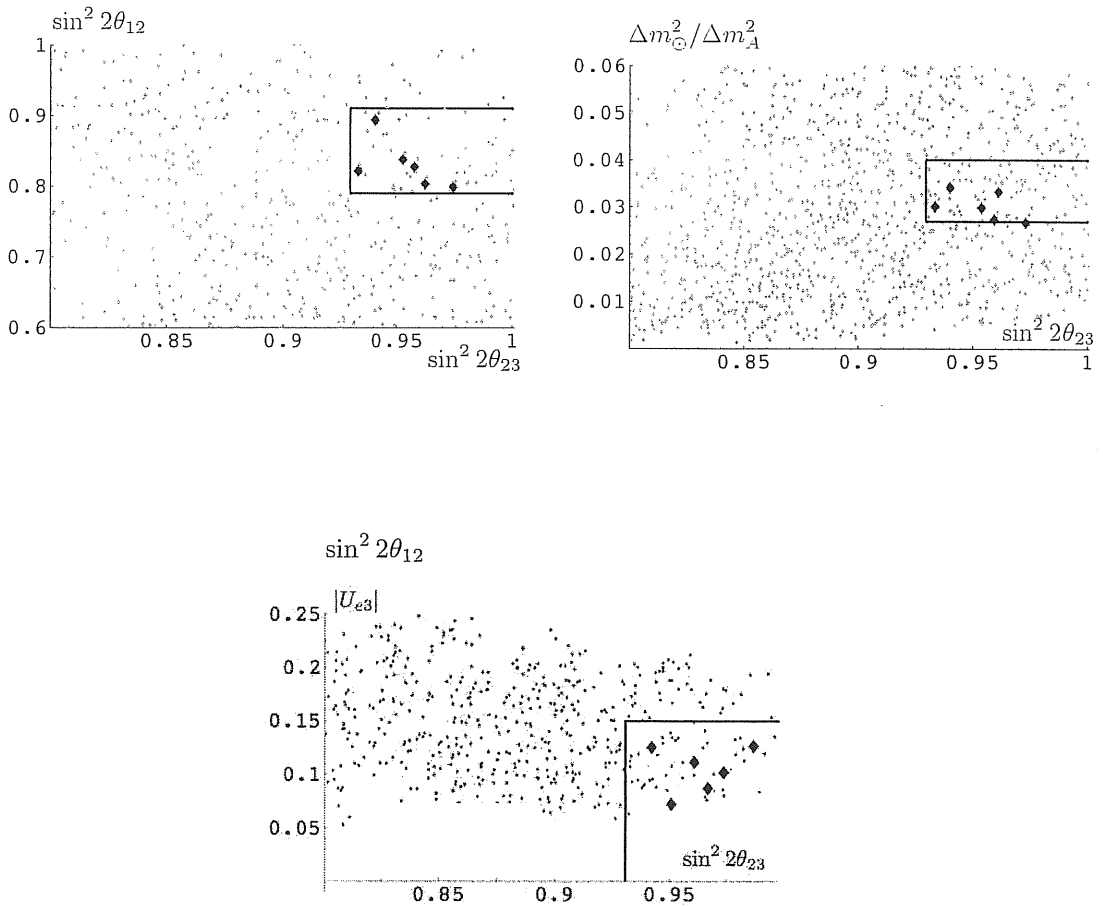
Extended versus minimal SUSY SO(10) for CP conserving Yukawa sector

Figure 4.2: Sample of density plots for $\sin^2 2\theta_{12}$, $|U_{e3}|$ and $|\Delta m_{\odot}^2/\Delta m_A^2|$ as functions of $\sin^2 2\theta_{23}$ in the minimal renormalizable SUSY SO(10) (in black) and in the minimal extension with a quasidecoupled 120_H contribution (in gray), in both cases for CP conserving Yukawa sector and $\tan\beta = 10$. The solid contours enclose the experimentally allowed regions at the 90% C.L. as it was in 2003.



Extended SUSY SO(10) model, CP violating Yukawa sector

Figure 4.3: A sample of typical density plots for $\sin^2 2\theta_{12}$, $\Delta m_{\odot}^2/\Delta m_A^2$ and $|U_{e3}|$ as functions of $\sin^2 2\theta_{23}$ in the renormalizable SUSY SO(10) model with complex Yukawa couplings and an additional subleading 120_H Yukawa term. The solid contours correspond to the current regions 90% C.L. for the current neutrino oscillation data given in [24].



Chapter 5

$SO(10)$ models with $16_H \oplus \overline{16}_H$

So far we were working within a class of SUSY $SO(10)$ unifications in which the GUT-scale gauge symmetry was broken down to the $SU(3)_c \otimes SU(2)_L \otimes U(1)_Y$ of SM by a system of Higgs multiplets containing a pair of 126-dimensional components of the 5-index antisymmetric tensor of $SO(10)$. However, looking at Table 1.1, this is obviously not the only way to break the intermediate left-right symmetry¹. Clearly, the desired breaking can be achieved by the VEVs of a spinorial $16_H \oplus \overline{16}_H$ Higgs multiplet. Moreover, it seems very difficult to get $126_H \oplus \overline{126}_H$ from the string theory compactifications [111]. Last, but not least, large dimensionality of the Higgs representations faced in previous chapters rises the issue of an enormous number of the elementary Higgs states populating the GUT-scale neighborhoods. These are just few reasons to spend some time on SUSY $SO(10)$ GUTs in which the high rank spinors are traded for simpler representations, in particular on models with $16_H \oplus \overline{16}_H$ instead of $126_H \oplus \overline{126}_H$ in the Higgs sector.

As we shall see, there are many qualitative differences among these two approaches. First of all, using $16_H \oplus \overline{16}_H$ instead of $126_H \oplus \overline{126}_H$, one loses one of the important ingredients in the effective Yukawa sum-rules at the renormalizable level, because there is obviously no $SO(10)$ singlet within the product of $16_F 16_F$ with neither 16_H nor $\overline{16}_H$. To correct for this, higher dimensional operators are usually invoked.

Another issue arises once the 16_H in the Higgs sector couples to the matter spinors 16_F by means of additional matter fermions residing in the $SO(10)$ vector or singlet irreps (as it is often the case if $SO(10)$ is considered as a subgroup of E_6). As we shall see, in such cases the “standard” seesaw mechanism for the light neutrino masses changes considerably.

¹As before, to avoid the problems with proton decay we do not consider the breaking chains containing $SU(5)$.

In what follows let us inspect in brief some of these questions and comment on salient points that can make this type of the $SO(10)$ GUT schemes particularly interesting not only from the theoretical point of view but also for its possible phenomenological consequences.

5.1 Net effects of $16_H \oplus \overline{16}_H$

Let us start with general remarks on the possible effects of the spinorial multiplets in the Higgs sector of an $SO(10)$ model. First, recall the $SU(3)_c \otimes SU(2)_L \otimes SU(2)_R \otimes U(1)_{B-L}$ decompositions of 16_H and $\overline{16}_H$:

$$\begin{aligned} 16_H &= (3, 2, 1, +1/3) \oplus (1, 2, 1, -1) \oplus (\overline{3}, 1, 2, -1/3) \oplus (1, 1, 2, +1) \\ \overline{16}_H &= (\overline{3}, 2, 1, -1/3) \oplus (1, 2, 1, +1) \oplus (3, 1, 2, +1/3) \oplus (1, 1, 2, -1) \end{aligned}$$

Clearly, without $\overline{126}_H$ there are no $SU(2)_L \otimes SU(2)_R$ triplets that could give rise to the Majorana neutrino masses at the renormalizable level. As a consequence, the smallness of the light neutrino masses usually follows from an appropriate set of effective operators or arises in more intricate pattern, like for instances the cascade seesaw mechanism in models with matter singlets, see section 5.3. Recently, the idea of split-supersymmetry revealed an option to make use of the so-called Witten's mechanism [42, 43] in the limiting case $m_{SUSY} \rightarrow M_G$ to construct an "effective" $\overline{126}_H$ radiatively; for a brief overview see section 5.2.1.

5.1.1 $d = 4$ proton decay

Unless additional symmetries are imposed, this class of GUTs suffers from extremely rapid proton decay, see e.g. [112] and references therein. To understand this, notice that at the level of effective operators there is nothing that forbids the following $SO(10)$ gauge invariant term in the superpotential:

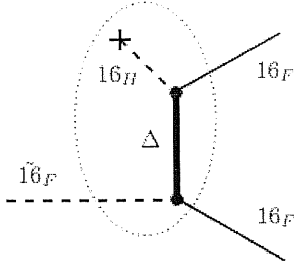
$$\mathcal{W} \ni \frac{\lambda^{ijk}}{M} 16_F^i 16_F^j 16_F^k 16_H + \dots \quad (5.1)$$

Clearly, once $B-L$ symmetry is broken by the VEVs of $16_H \oplus \overline{16}_H$, a pair of dangerous effective $d = 4$ operators is induced

$$\mathcal{W} \ni Q_L L_L D_L^c \frac{\langle \tilde{N}_L^c \rangle}{M} + U_L^c D_L^c D_L^c \frac{\langle \tilde{N}_L^c \rangle}{M} + \dots \quad (5.2)$$

that, put together, gives a proton lifetime of roughly 10^{-5} yr, roughly 38 orders of magnitude shorter than the experimental limits.

Figure 5.1: The basic structure of the dangerous $d = 4$ operators driving the rapid proton decay in SUSY $SO(10)$ models with spinorial representations in the Higgs sector. The particle propagator suppression is clearly insufficient to account for the measured proton decay width of roughly $\Gamma_p \sim (10^{33} \text{yr})^{-1}$.



5.1.2 R-parity

Another important issue of the models with a spinorial Higgs representation used to break the left-right symmetry is the R -parity breakdown that occurs once the $SU(3)_c \otimes SU(2)_L \otimes U(1)_Y$ neutral components of $16_H \oplus \overline{16}_H$ receive $B - L$ breaking VEVs. Unlike the case of $126_H \oplus \overline{126}_H$, where the $B - L$ charges of the relevant VEVs were even (± 2), driving the R -symmetry to be broken by 2 units while leaving the R -parity $(-1)^{3(B-L)+2S}$ intact, the components of $16_H \oplus \overline{16}_H$ receiving the $B - L$ VEVs are $B - L$ odd and R -parity is in general violated raising the issues of the LSP stability etc. However, this problem can be avoided for the price of imposing additional symmetries forbidding explicitly the dangerous terms in the superpotential.

5.1.3 Quark and lepton masses and mixing

Another qualitative difference with respect to the models with the $\overline{126}_H \oplus 126_H$ pair in the Higgs sector originates from the fact that the leading contributions to the effective quark and lepton masses (i.e. those generated by renormalizable terms) come from the representations that are blind to the choice of the GUT-scale symmetry breaking pattern², usually 10_H or 120_H , see e.g. [43]. Therefore, the Majorana masses of neutrinos do not come directly from the appropriate Yukawa couplings³ and in order to obtain such terms, alternative scenarios must be proposed. For illustration purposes, let us discuss two basic mechanisms that attracted attention quite recently.

²unless there is a mixing with other doublets coming from “large” representations like for instance 210_H . In the “conservative” setups one usually attempts to avoid such large Higgs representations; the “standard” choice of the GUT-breaking multiplets is 45_H and/or 54_H .

³unlike in scenarios with $\overline{126}_H$ where Y_{126} , playing a key role in the quark and lepton Yukawa sum-rules, governed also the Majorana masses, c.f. eq. (3.2)

5.2 Witten’s mechanism in $SO(10)$ GUTs

If the loop-induced effective operators are not killed a-priori like in the standard low-energy SUSY scenarios⁴, the desired effective Majorana entries in $SO(10)$ models without $\overline{126}_H$ can be generated at two-loop level by means of a simple radiative mechanism found by Witten [42].

The idea is to contract a pair of spinors in the Higgs sector in such a way to provide for an effective $\overline{126}_H$ arising from their product and transmit its VEV to the matter bilinear using a particular two-loop diagram. More details can be found in [42] or in more recent studies [43, 113] and references therein. The nice feature of this approach is the calculability of the loop contributions⁵. Apparently, the “standard” requirement of low-energy supersymmetry discards this mechanism due to the cancellation of the fermionic and bosonic contributions in the loops. However, with the advent of split-supersymmetry [114, 115] this scheme was revived with nontrivial consequences for the effective quark and lepton masses and mixing patterns.

5.2.1 Witten’s mechanism in split-SUSY $SO(10)$

More technically, the problem of implementing the Witten’s mechanism in the “standard” $SO(10)$ scenarios stems from the fact that the kinematic functions parametrizing the contributions of the relevant two-loop diagrams must vanish in the $m_S/M_G \rightarrow 0$ regime, where m_S is the SUSY breaking scale, typically of the TeV order. Recall that the low-energy SUSY is needed namely to achieve the proper gauge-coupling unification and to protect the hierarchies. However, relaxing the latter requirement, the split-SUSY framework provide a natural option for the Witten mechanism in potentially realistic GUT models.

The main point [114, 115] consists in splitting the sparticle spectrum in such a way to keep at the TeV scale only the fermionic superpartners of the MSSM gauge and Higgs bosons (gauginos and higgsinos) while pushing the scalar ones (squarks and sleptons) to a higher scale μ_S , well above the TeV range. Notice that this does not affect the gauge coupling unification (at one loop) as the squarks and sleptons enter in full $SU(5)$ multiplets (only the value of α_G is slightly reduced) while provides for solutions of many of the “naturalness” problems of the MSSM, be it the SUSY CP-problem or the issues of flavour changing neutral currents or electric dipole moments, all tracing back to the relatively low scale of sfermion masses in the standard approach.

⁴for instance if there is no SUSY or it is “split” enough, see section 5.2.1

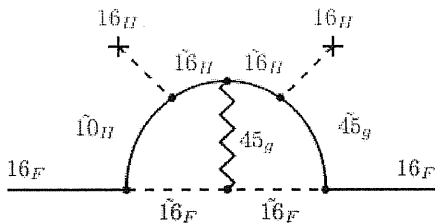
⁵i.e. they can be expressed in terms of masses and couplings that are already in the model without a new information that would inevitably enter at the level of effective operators

Pushing μ_S up to the M_G , at which the Witten's mechanism operates, the “no-renormalization” argument is compromised and only the loop factors make the effective $\overline{126}$ slightly suppressed with respect to the tree-level operators. Indeed, as it was shown in [43], the typical shape of the radiatively generated Majorana neutrino mass term reads

$$M_\nu \sim \left(\frac{\alpha_G}{\pi}\right)^2 Y_x \frac{v_R^2}{M_G} \times \mathcal{O}(1) \quad (5.3)$$

where Y_x is the Yukawa coupling of the 10_H or 120_H (that must be there to break the chiral symmetry), $\frac{v_R^2}{M_G}$ is a typical scale factor originating from the GUT-scale VEVs of the pair of Higgs spinors⁶, c.f. [42] and $\mathcal{O}(1)$ stands for the loop function that is no longer SUSY-suppressed. Since at one-loop level the gauge-coupling unification works

Figure 5.2: The topology of the two-loop diagrams that generate the effective Majorana masses for neutrino and additional contributions to the Dirac masses of the charged matter fermions in the SUSY version of the so-called Witten's mechanism in $SO(10)$ [42, 69].



the same way like in the minimal SUSY $SO(10)$ model⁷, the v_R scale should be quite close to M_G , c.f. section 2.2.1 and [69].

Notice that the suppression of such effective Majorana masses with respect to those generated at tree-level in “standard” $SO(10)$ GUTs⁸ leads to the corresponding enhancement of the light neutrino masses coming from the singlet (type-I) seesaw while the triplet (type-II) contributions are suppressed by the same amount and thus usually negligible.

Another interesting aspect of such schemes concerns the Dirac masses of the charged leptons and quarks. Naturally, there must always be at least one Yukawa vertex providing for the desired chirality flip as a seed of the Witten's mechanism. On top of

⁶To be more specific, v_R being the scale at which the spinorial Higgses receive the $SU(2)_R \otimes U(1)_{B-L}$ -breaking VEVs.

⁷up to the shift of the GUT-scale gauge coupling

⁸by effects of the $SU(2)_L \otimes SU(2)_R$ triplets of $\overline{126}_H$

that, the graphs of the type (Fig. 5.2) give rise also to an additional radiatively induced contribution to the masses of the charged fermions⁹. It is then natural to ask if such effects can provide for the departure from the degeneracy of the effective quark and lepton Yukawa matrices in the simplest models with only a pair of 10_H Higgs multiplets coupled to the matter bilinear at the renormalizable level.

5.2.2 Problems of the split-SUSY $SO(10)$ model with pair of 10_H only - a call for 120_H

Clearly, a single Yukawa matrix is not enough for a potentially realistic description of the quark and lepton mixing phenomena. Indeed, since also the radiative effects are proportional to this matrix, c.f. eq. (5.3), the radiative mechanism can not bring anything new but modify the overall scale of the Yukawa couplings only. Thus there is no way to generate the desired CKM mixing pattern. Therefore, one should add at least one more 10_H or 120_H [69] to account for a potentially realistic situation in the quark sector.

The rest of this section is devoted to a semianalytic argument that even having a pair of 10-dimensional Higgs multiplets one can not disentangle the unwanted strong correlation among the down-type quarks and charged leptons in such a way to accommodate properly the different mass hierarchies in these two sectors.

With a pair of 10_H there are two Pati-Salam bidoublets that can receive (at the $SU(3)_c \otimes SU(2)_L \otimes U(1)_Y$ level) electroweak VEVs. This leads to the following tree-level relations for the quark and charged lepton effective masses matrices

$$\begin{aligned} Y_u v_u &= Y_1 v_1^u + Y_2 v_2^u &\equiv M_u \\ Y_d v_d &= Y_1 v_1^d + Y_2 v_2^d &\equiv M_d \\ Y_l v_d &= Y_1 v_1^d + Y_2 v_2^d &\equiv M_l \end{aligned} \tag{5.4}$$

Clearly, the spectra of charged leptons and down-quarks are degenerate. The two-loop Witten's correction to these relations can be written in the form¹⁰ [43, 113]:

$$\Delta M_x = \left(\frac{\alpha}{\pi}\right)^2 (c_x^1 Y_1 + c_x^2 Y_2) \frac{v_x M_R}{M_G} \times \mathcal{O}(1) \tag{5.5}$$

They are proportional to a linear combination¹¹ of the two Yukawa couplings with coefficients given by the entries of the appropriate light Higgs doublet mixing matrix, c.f.

⁹with the only obvious difference in the internal structure of the relevant graphs

¹⁰Here v_x are the VEVs of the $(1, 2, \pm 1)$ components of $16_H \oplus \overline{16}_H$ entering the two-loop diagrams at Fig. 5.2.

¹¹Notice that there is only one Yukawa vertex in the graph 5.2.

section 2.2.4. Omitting the $\mathcal{O}(1)$ loop factor one can define a parameter $\varepsilon \equiv \left(\frac{\alpha}{\pi}\right)^2 \frac{M_R}{M_G}$ as a measure of the relative size of the radiative correction. Normalizing

$$\tilde{v}^{u,d} \equiv \sqrt{\left(v_1^{u,d}\right)^2 + \left(v_2^{u,d}\right)^2}$$

to m_t and m_b respectively, one can write

$$\begin{pmatrix} \tilde{M}_u \\ \tilde{M}_d \end{pmatrix} = \begin{pmatrix} d_1^u & d_2^u \\ d_1^d & d_2^d \end{pmatrix} \begin{pmatrix} Y_1 \\ Y_2 \end{pmatrix} \quad (5.6)$$

$$\frac{m_\tau}{m_b} \tilde{M}_l = Y_1 d_1^l + Y_2 d_2^l$$

provided

$$\begin{aligned} d_1^u &\equiv \cos \alpha_u + \varepsilon c_u^1 & d_2^u &\equiv \sin \alpha_u + \varepsilon c_u^2 \\ d_1^d &\equiv \cos \alpha_d + \varepsilon c_d^1 & d_2^d &\equiv \sin \alpha_d + \varepsilon c_d^2 \\ d_1^l &\equiv \cos \alpha_d + \varepsilon c_l^1 & d_2^l &\equiv \sin \alpha_d + \varepsilon c_l^2 \end{aligned}$$

where $\alpha_{u,d}$ parametrize the projections of $v_{1,2}^{u,d}$ to $\tilde{v}^{u,d}$. All d_x^i are in general $\mathcal{O}(1)$ -parameters unless $\alpha_{u,d}$ are close to 0 or π . Inverting relation (5.6) and plugging Y_1 and Y_2 one can bring the lepton mass sum-rule into the familiar form studied in great detail in section 3

$$k \tilde{M}_l = \tilde{M}_u + r \tilde{M}_d \quad (5.7)$$

and obtain relations for the parameters k and r in the form

$$k = \frac{m_\tau}{m_b} \frac{\Delta}{\varepsilon(d_2^d \Delta c_1 - d_1^d \Delta c_2)} \quad \text{and} \quad r = \frac{\Delta - \varepsilon(d_2^u \Delta c_1 - d_1^u \Delta c_2)}{\varepsilon(d_2^d \Delta c_1 - d_1^d \Delta c_2)} \quad (5.8)$$

Here Δ stands for the determinant of the 2×2 matrix in eq. (5.6) and $\Delta c_i \equiv c_i^i - c_d^i$. Using the results of section 3¹² one can claim that for a successful fit of the charged lepton masses in this scheme $|k| \lesssim 1$ and $|r| \sim 1$ is needed. This requirement puts a strong constraint on the value of Δ , in particular

$$\det \begin{pmatrix} d_1^u & d_2^u \\ d_1^d & d_2^d \end{pmatrix} \lesssim \mathcal{O}(\varepsilon) \quad (5.9)$$

¹²Strictly speaking, the GUT-scale effective quark and lepton masses used as an input of the analysis of section 3.4.1 differ from the data relevant in the split-SUSY case. However, the ratios of the quark and lepton masses that are the only relevant parameters in formula 5.7 are not changed drastically and one can expect results very similar to those obtained in part 3.7.

that leads to $\alpha_u - \alpha_d \lesssim \mathcal{O}(\varepsilon)$, in obvious clash with the difference in hierarchies in the up- and down-quark sector unless ε is as large as 10^{-2} and an intricate conspiracy among other parameters occurs.

Therefore, it is almost impossible to save the unwanted down-quark and charged-lepton degeneracy in the split-SUSY $SO(10)$ model with a pair of 10-dimensional Higgs representatinos by means of the two-loop radiative corrections originating from the Witten's mechanism. The model clearly calls for a more complicated structure of the flavor-active Higgs multiplets like for instance $10_H \oplus 120_H$.

5.3 Cascade seesaw in models with matter singlets

Another interesting implementation of the seesaw idea can be achieved by extending the matter sector of a model with $16_H \oplus \overline{16}_H$ by matter singlets. This can be motivated for example by the possibility of embedding the $SO(10)$ group into an exceptional group E_6 where the matter fermions are hosted in 27_F ¹³. Having at hand an additional matter singlet (denoted from now on S_L) one can form a new Yukawa term of the form¹⁴

$$\mathcal{W}_Y = F^{ij} 16_F^i 1_F^j \overline{16}_H + \dots \quad (5.10)$$

Since the quantum numbers of S_L are the same like those of ν_L^c , these states can mix below the $SO(10)$ scale and such an effect should be taken into account in the construction of the neutrino mass matrix. Indeed, adding also the mass term for the singlet and the Yukawa interaction of the matter 16_F with the “standard” 10_H

$$\mathcal{W}_Y = F^{ij} 16_F^i 1_F^j \overline{16}_H + Y^{ij} 16_F^i 16_F^j 10_H + M^{ij} 1_F^i 1_F^j + \dots \quad (5.11)$$

one obtains a 3×3 (in family blocks) neutrino mass matrix [116, 117] (in the $\{\nu_L, \nu_L^c, S_L\}$ basis)

$$M_\nu = \begin{pmatrix} 0 & Yv & 0 \\ Y^T v & 0 & Fv_R \\ 0 & F^T v_R & M \end{pmatrix} \quad (5.12)$$

arising upon $B - L$ symmetry breaking driven by nonzero VEVs of $(1, 1, 2, -1)_{\overline{16}} \oplus (1, 1, 2, +1)_{16}$ ¹⁵ and a subsequent $SU(2)_L \otimes U(1)_Y$ breakdown by the VEVs of the bidoublet $(1, 2, 2, 0)_{10}$

$$\langle (1, 2, +1)_{10} \rangle \equiv v \quad \langle (1, 1, 0)_{\overline{16}} \rangle \equiv v_R \quad (5.13)$$

¹³Note that 27_F decays into $16_F \oplus 1_F \oplus 10_F$ at the $SO(10)$ level

¹⁴For simplicity only one pair of $16_H \oplus \overline{16}_H$ is assumed for the time being.

¹⁵As before, unless specified otherwise, the Pati-Salam $SU(4)_{PS} \otimes SU(2)_L \otimes SU(2)_R$ notation is used.

where $SU(3)_c \otimes SU(2)_L \otimes U(1)_Y$ notation is used for clarity. This leads to the following “effective” seesaw formula for the light neutrino mass matrix:

$$m_\nu \doteq -\frac{v^2}{v_R^2} Y (F M^{-1} F^T)^{-1} Y^T \quad (5.14)$$

Assuming three generations of the matter singlets (in such a case F becomes a 3×3 matrix) this gets simplified into¹⁶

$$m_\nu \doteq -\frac{v^2}{v_R^2} (Y F^{T-1}) M (Y F^{T-1})^T \quad (5.15)$$

Phenomenologically, this scheme is more rich than the standard 2×2 seesaw formula [118] because of the second scale M that can be used to enhance the neutrino masses, often oversuppressed in scenarios with v_{B-L} too close to the GUT scale. Alternatively, one can try to bring the $B - L$ breaking scale down to an experimentally accessible range if M is small enough to keep M/v_R^2 untouched. For such a case, it has been shown [119, 120] that lepton flavour and CP can be violated at appreciable levels even in absence of supersymmetry, provided the v_R scale is sufficiently low. Note that the smallness of M could be natural in t’Hooft’s sense [121], as the symmetry enhances when M goes to zero. Indeed, in such a case the global lepton-number symmetry is exactly conserved and all three light neutrinos are strictly massless.

5.4 The inverse seesaw mechanism

This is the key observation made first by Mohapatra and Valle [116] in 1986 (originally in the $SU(3)_c \otimes SU(2)_L \otimes U(1)_Y$ context) that gave rise to the so called “inverse” seesaw mechanism for theories which lack representations required to implement the canonical seesaw. However, in general case, the problem of understanding the smallness of neutrino masses is traded for the problem of understanding the smallness of M . As we shall see in this section, this can be partially avoided if one concerns the embedding of the inverse seesaw structure into a SUSY $SO(10)$ framework [122].

In the left-right symmetric schemes (like for example $SO(10)$ broken to $SU(4)_{PS} \otimes SU(2)_L \otimes SU(2)_R$ or $SU(3)_c \otimes SU(2)_L \otimes SU(2)_R \otimes U(1)_{B-L}$), the formula 5.12 receives naturally an additional contribution. Indeed, the left-right symmetry gives rise to an induced VEV also for the $(1, 2, 1, +1)_{\overline{16}} \oplus (1, 2, 1, -1)_{16}$ components of $\overline{16}_H \otimes 16_H$ ¹⁷

¹⁶Invertibility of F is assumed.

¹⁷The “mirror” components of 16_H is used in SUSY context prevent the D-terms arising from these components to break supersymmetry at the $B - L$ scale.

that, consequently, generates a nonzero 13 entry in eq. (5.12) through the term¹⁸

$$F^{ij}(1, 2, -1)_{16_F}(1, 1, 0)_{1_F}\langle(1, 2, +1)_{\overline{16}_H}\rangle \rightarrow F^{ij}L_L^{iT}C^{-1}S_L^jv_L + h.c. \quad (5.16)$$

where $v_L \equiv \langle(1, 2, 1, +1)_{\overline{16}}\rangle$. Therefore, the neutrino mass matrix changes to

$$M_\nu = \begin{pmatrix} 0 & Yv & Fv_L \\ Y^Tv & 0 & Fv_R \\ F^Tv_L & F^Tv_R & M \end{pmatrix} \quad (5.17)$$

which leads to an additional term in the seesaw formula [118]:

$$m_\nu \doteq -\frac{v^2}{v_R^2}(YF^{T-1})M(YF^{T-1})^T + \frac{vLv}{v_R}(Y + Y^T) \quad (5.18)$$

If, in general, there is more than one copy of $\overline{16}_H$ receiving a $B - L$ breaking VEV, the 13 component ceases to be proportional to the 23 one and one should write instead¹⁹

$$M_\nu = \begin{pmatrix} 0 & Yv & \tilde{F}v_L \\ Y^Tv & 0 & Fv_R \\ \tilde{F}^Tv_L & F^Tv_R & M \end{pmatrix} \quad (5.19)$$

provided $\tilde{F}^{ij}v_L = \sum_k F^{ijk}v_L^k$, while $F^{ij}v_R = \sum_k F^{ijk}v_R^k$ and

$$m_\nu \doteq -\frac{v^2}{v_R^2}(YF^{T-1})M(YF^{T-1})^T + \frac{vLv}{v_R} \left[Y(\tilde{F}F^{-1})^T + (\tilde{F}F^{-1})Y^T \right] \quad (5.20)$$

In the most general case, one obtains two very different contributions to the light neutrino masses. The first term in eq. (5.20) is the standard 3×3 contribution proportional to M/v_R^2 discussed in brief in the previous paragraph. However, putting M to zero (that could be motivated in the same manner like before²⁰) the neutrinos remain massive because of the second term in eq. (5.20) that is completely M -independent.

In such a case the neutrino mass scale is governed by the ratio $v_L v / v_R$. In SUSY $SO(10)$, the magnitude of this quantity can be estimated inspecting a typical superpotential like

$$W \ni M_{16}16_H\overline{16}_H + \rho 16_H 16_H 10_H + \text{H. c.}$$

¹⁸For clarity the $SU(3)_c \otimes SU(2)_L \otimes U(1)_Y$ quantum numbers are used in this formula.

¹⁹For this to occur also the left-right parity should be broken at this stage.

²⁰as long as v_L much smaller than the other nonzero entries in (5.19); notice that this is always the case.

The mechanism the VEV of $\chi_L = (1, 2, +1)_{SM} \in (1, 2, 1, +1)_{\overline{16}}$ is generated at the level of the $B - L$ breakdown²¹ can be seen from the structure of the F-terms. For example, $F_{(1,2,1,\pm 1)}^\dagger$ is proportional to

$$F_{(1,2,1,\pm 1)}^\dagger \propto M_{16}(1, 2, 1, \mp 1)_{16} + \rho(1, 1, 2, \mp 1)_{16}(1, 2, 2, 0)_{10} + \dots$$

After giving a nonzero VEV to the $(1, 1, 2, \mp 1)$ components (to break $B - L$) and to the traditional doublet pair in 10_H (to break $SU(3)_c \otimes SU(2)_L \otimes U(1)_Y$) the requirement to stay in a supersymmetric vacuum leads to

$$v_L = \langle \chi_L \rangle \simeq \langle (1, 2, 1, \mp 1)_{16} \rangle \simeq \rho \frac{v_R v}{M_{16}} \quad (5.21)$$

Thus, in this scenario, the overall scale of the light neutrino masses is no longer governed by the $B - L$ scale (because v_R cancels) and one obtains

$$m_\nu \simeq \frac{v^2}{M_{16}} \rho \left[Y(F\tilde{F}^{-1})^T + (F\tilde{F}^{-1})Y^T \right] \quad (5.22)$$

where M_{16} must be close to the GUT scale to prevent fast $d = 5$ proton decay. Thus, in this scheme, the $B - L$ scale is decoupled from the seesaw formula!

Note that in order to accommodate the neutrino data [123], there could be a need to enhance the numerator of eq. (5.22) compensating for (roughly) a GUT scale mass in the denominator. However, this can happen for example if $F \neq \tilde{F}$ that could naturally be the case if the v_R VEV is “distributed” into at least two copies of $16_H \oplus \overline{16}_H$ present at the $SO(10)$ level.

5.5 Inverse seesaw scheme in SUSY GUTs

The option to decouple the $B - L$ scale from the seesaw mechanism is very attractive. However, in a consistent supersymmetric GUT, the embedding of the inverse seesaw mechanism rises several issues:

- The $\nu_L^c S_L$ entry v_R generated by VEVs of Higgs multiplets $\chi_R = (1, 1, 2, -1)_{\overline{16}}$ and $\bar{\chi}_R = (1, 1, 2, +1)_{\overline{16}}$ breaks the $B - L$ symmetry, now gauged. The corresponding scale $\langle \chi_R \rangle$ must be compatible with gauge coupling unification. Together with the requirement of low-energy supersymmetry (to stabilize the hierarchies), this puts rather strong constraints on placing of the various multiplets into the “desert” below M_G .
- To keep the model testable (at least in principle), the “population of the desert” should follow the minimal survival hypothesis, c.f. [124] and references therein.

²¹driven by $(1, 1, 2, -1)_{\overline{16}} \oplus (1, 1, 2, +1)_{16}$

- The singlet $MS_L S_L$ mass should be small.

Let us now discuss these points and show that there indeed exists a supersymmetric $SO(10)$ model that can address all these questions in a satisfactory way and provides for an alternative understanding of the smallness of neutrino masses within the grand unified framework.

First recall that there are several mechanisms that could be used to get rid of the $S_L S_L$ -term in Eq. (5.19). For example, one can invoke an embedding of $SO(10)$ into the E_6 group where the fermionic singlet is a member of a 27-dimensional irreducible representation with the familiar $SO(10) \otimes U(1)_X$ decomposition

$$27_F = 1_F^4 \oplus 16_F^1 \oplus 10_F^{-2} \quad (5.23)$$

If there is no $351'$ Higgs representation at the E_6 -scale, the enormous $U(1)$ -charge of the $1_F 1_F$ matter bilinear is hardly saturated. Thus, as long as the corresponding $U(1)$ is unbroken one gets $M = 0$. Even if one breaks the $U(1)$ symmetry at some lower scale, it could be rather complicated to generate an effective SS -entry, which brings further suppression even at the level of effective operators. Following the inverse seesaw concept [116], from now the 33 term in (5.19) is neglected.

Prior approaching the details of the gauge-coupling unification pattern, let us give a few more comments on the structure of the seesaw formula in this case.

5.5.1 The seesaw structure

Putting the 33 entry of eq. (5.19) to zero, the generalized “inverse seesaw” neutrino mass matrix reads

$$M_\nu = \begin{pmatrix} 0 & Yv & Fv_L \\ Y^T v & 0 & \tilde{F}v_R \\ F^T v_L & \tilde{F}^T v_R & 0 \end{pmatrix} \quad (5.24)$$

The diagrammatic structure of the seesaw formula (5.22) arising from this structure is depicted at Fig. 5.3. In contrast to both the canonical seesaw in Eq. (3) and the inverse seesaw, Eq. (5.15), this new seesaw is linear in the Dirac Yukawa structure Y . Notice also that the current mechanism, apart from being unified, is also quite distinct from other left-right symmetric attempts like for instance [125, 126].

Concerning the stability of the texture zeros at $\nu_L^c \nu_L^c$ and $S_L S_L$ positions in formula (5.24), it can be protected as long as the $U(1)_R$ and the $U(1)_X$ (of $E_6 \supset SO(10) \otimes U(1)_X$ in E_6 inspired setups) are exact. Indeed, $U(1)_X$ must be broken at the ν_R scale ($16_H \oplus \overline{16}_H$ are $U(1)_X$ -charged). However, the charge of χ_R 's is such that the relevant operators arise only at higher orders and may be neglected.

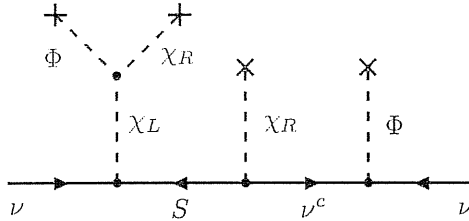


Figure 5.3: The Feynman graph giving rise to the considered SUSY $SO(10)$ inverse seesaw mechanism (up to transposition). The neutrino masses do not impose any constraints on the magnitude of the $B - L$ breaking scale that (if compatible with gauge running) can be quite low.

5.6 Minimally finetuned SUSY $SO(10)$ inverse seesaw model

Before examining in detail the options to achieve the gauge coupling unification with low $B - L$ scale, the structure of the model should be specified. As we shall see in what follows, the constraints coming from this requirement are rather strict and point to a specific class of models with the $SO(10)$ D-parity broken at the GUT scale.

5.6.1 The symmetry breaking pattern

As it was pointed out by Deshpande et al. [127], the scale at which the $SU(2)_R \otimes U(1)_{B-L}$ symmetry is broken to $U(1)_Y$ can be arbitrarily low if the “desert” from M_Z to M_G is populated properly. In their case this was achieved by putting *three* copies of $(1, 1, 2, +1) \oplus (1, 1, 2, -1)$ coming from $16_H \oplus \overline{16}_H$ right at the v_R scale. The (one-loop) MSSM running of α_Y^{-1} can be “effectively” extended above the v_R scale ($\alpha_Y^{-1} = \frac{3}{5}\alpha_R^{-1} + \frac{2}{5}\alpha_{B-L}^{-1}$) by a conspiracy between the running of α_{B-L}^{-1} and α_R^{-1} while α_3 and α_L are untouched. However, such a scheme is rather *ad hoc* as one needs to push three identical copies of a Higgs multiplet below the GUT scale, at odds with the “minimal fine-tuning” [128, 124].

Instead, let us show that there is a more compelling SUSY $SO(10)$ scheme in which low $B - L$ can be achieved without such a redundancy. Recalling the well known fact that within the class of minimally finetuned SUSY GUTs it is very hard (if not impossible) to push the $SU(2)_R$ breaking scale well below M_G [69], one should look for a scenario where the $SU(2)_R$ breaking scale V_R is separated from the $U(1)_{B-L} \otimes U(1)_R$ breaking taking place at the v_R scale, $V_R \gg v_R$, that implies the SSB chain

$$SU(2)_R \otimes U(1)_{B-L} \rightarrow U(1)_R \otimes U(1)_{B-L} \rightarrow U(1)_Y. \quad (5.25)$$

To stay “minimally fine-tuned”, at each step one should assume just those multiplets

that are needed to break the relevant symmetry. The $SO(10)$ breaking should be achieved in such a way to break the D-parity, otherwise the g_L and g_R couplings coincide up to $SU(2)_R$ breaking scale and also the desert population must be left-right symmetric. However, such a minimal particle content below V_R can not account for proper gauge-coupling unification, see section 5.6.3. Subsequently, a light admixture of $(1, 1, 3, 0)$ multiplets²² residing for example in 45 or 210 of $SO(10)$ drives the breaking (5.25)²³. The final step,

$$SU(3)_c \otimes SU(2)_L \otimes U(1)_R \otimes U(1)_{B-L} \rightarrow SU(3)_c \otimes SU(2)_L \otimes U(1)_Y \quad (5.26)$$

is achieved by giving VEVs to a light admixture of $(1, 1, -\frac{1}{2}, +1)_{\overline{16}} \oplus (1, 1, +\frac{1}{2}, -1)_{16}$ scalars (in $SU(3)_c \otimes SU(2)_L \otimes U(1)_R \otimes U(1)_{B-L}$ notation) of $16_H \oplus \overline{16}_H$ ²⁴. With this information at hand one can fully specify the ingredients of a minimal SUSY $SO(10)$ setup that can accommodate the mechanism described above.

5.6.2 Structure of the Higgs sector

As usual we use three copies of 16_F^i to accommodate the SM fermions and for each of them we add a singlet fermion 1_F^i to play the role of S_L . A realistic matter spectrum requires more than one copy of 10_H Higgs multiplet, or for instance $10_H \oplus 120_H$. As it was argued before, at least two copies of $16_H \oplus \overline{16}_H$ should be used to implement the inverse seesaw mechanism with potentially realistic neutrino spectrum. To prevent fast proton decay via dimension 4 operators (c.f. section 5.1.1) let us assign the matter fermions in 16_F and 1_F with a discrete matter parity that forbids the mixing of 16_F and 16_H ²⁵. Finally, let us add 45_H and 210_H to trigger the proper symmetry breaking pattern with no D-parity below the GUT scale [129, 130, 131]. The $SO(10)$ invariant Yukawa superpotential then reads

$$W_Y = Y_{aij} 16_F^i 16_F^j 10_H^a + F_{ijk} 16_F^i 1_F^j \overline{16}_H^k \quad (5.27)$$

The Higgs superpotential is

$$W_H = M_{16}^{kl} 16_H^k \overline{16}_H^l + M_{10}^{ab} 10_H^a 10_H^b + M_{45} 45_H 45_H + M_{210} 210_H 210_H + \quad (5.28)$$

²²Since the Pati-Salam symmetry is broken at the large scale from now on we use the quantum numbers of the $SU(3)_c \otimes SU(2)_L \otimes SU(2)_R \otimes U(1)_{B-L}$ and $SU(3)_c \otimes SU(2)_L \otimes U(1)_R \otimes U(1)_{B-L}$ subgroups.

²³Recall that a VEV of an adjoint representation does not reduce the rank of a gauge group.

²⁴If $SU(2)_R$ is broken to $U(1)_R$, the minimal survival hypothesis forbids the multiplets with opposite charge assignment, i.e. $(1, 1, +\frac{1}{2}, +1) \oplus (1, 1, -\frac{1}{2}, -1)$ of $16_H \oplus \overline{16}_H$ that remain at the $SU(2)_R$ scale.

²⁵Other discrete symmetries might be also needed to reduce the number of parameters and help with the doublet-triplet splitting problem.

$$\begin{aligned}
& + \rho_{klm} 16_H^k 16_H^l 10_H^m + \bar{\rho}_{klm} \bar{16}_H^k \bar{16}_H^l 10_H^m + \sigma_{kl} 16_H^k \bar{16}_H^l 45_H + \omega_{kl} 16_H^k \bar{16}_H^l 210_H + \\
& + \lambda 45_H^3 + \kappa 45_H^2 210_H + \xi 45_H 210_H^2 + \zeta 210_H^3
\end{aligned}$$

The symmetry breaking pattern briefly described in section 5.6.1 is then achieved as follows. The components of 210_H and 45_H that receive GUT-scale VEVs and trigger the breaking of $SO(10)$ to $SU(3)_c \otimes SU(2)_L \otimes SU(2)_R \otimes U(1)_{B-L}$ are (in Pati-Salam language) $210_H \ni (15, 1, 1) \oplus (1, 1, 1)$ and $45_H \ni (15, 1, 1)$. As shown in [129, 130, 131], this pattern can accommodate just the desired D-parity breaking allowing for an intermediate left-right symmetric group with an asymmetric particle content, leading to distinct g_L and g_R below M_G . The subsequent $SU(2)_R \rightarrow U(1)_R$ breaking at V_R is induced by the VEV of a light superposition of $(1, 1, 3, 0)_{210}$ and $(1, 1, 3, 0)_{45}$ that can mix below the GUT scale. Next, the $U(1)_R \otimes U(1)_{B-L}$ is broken down at v_R by the VEVs of the light component of type $(1, 1, +\frac{1}{2}, -1) \oplus (1, 1, -\frac{1}{2}, +1)$ coming from $(1, 1, 2, -1) \oplus (1, 1, 2, 1)$ of $16_H \oplus \bar{16}_H$. The final SM breaking step is as usual provided by the VEVs of the $(1, 2, 2, 0)$ bidoublet components. Note that unlike the example given in [127], there is no artificial redundancy in the number of light states living at intermediate scales.

5.6.3 One-loop gauge coupling unification

Let us finally show that the setup specified above obeys the condition of gauge coupling unification. Using the normalization convention $2\pi t(\mu) = \ln(\mu/M_Z)$ we have (for $M_A < M_B$)

$$\alpha_i^{-1}(M_A) = \alpha_i^{-1}(M_B) + b_i(t_B - t_A)$$

in the ranges $[M_Z, M_S]$, $[M_S, v_R]$ and $[v_R, M_{GUT}]$. M_S is the SUSY breaking scale taken at ~ 1 TeV. Between v_R and V_R the two $U(1)$ factors mix and the running of α_R^{-1} and α_{B-L}^{-1} requires separate treatment [132]. The Cartan operators obey the traditional formula (with "physically" normalized $B-L$ and Y_W) $Y_W = 2T_3^R + (B-L)$. Recall that the $SO(10)$ normalization of b_{B-L} is $b'_{B-L} = \frac{3}{8}b_{B-L}$.

Once the D -parity is broken below M_G we have $g_L \neq g_R$. The Higgs sector in the stage down to V_R is as follows:

$$1 \times (1, 1, 3, 0), \quad 1 \times (1, 1, 2, +1) \oplus (1, 1, 2, -1) \text{ and } 1 \times (1, 2, 2, 0).$$

This gives rise to the b -coefficients

$$\begin{pmatrix} b_3 \\ b_L \\ b_R \\ b_{B-L} \end{pmatrix} = \begin{pmatrix} -3 \\ 1 \\ 4 \\ 20 \end{pmatrix} \tag{5.29}$$

At the subsequent stage from V_R to v_R we keep only the weak scale bidoublet $(1, 2, 2, 0)$ (that below V_R splits into a pair of L-doublets with quantum numbers $(1, 2, +\frac{1}{2}, 0) \oplus (1, 2, -\frac{1}{2}, 0)$ under the $SU(3)_c \otimes SU(2)_L \otimes U(1)_R \otimes U(1)_{B-L}$ group) and a part of $(1, 1, 2, +1) \oplus (1, 1, 2, -1)$ that is needed to break $U(1)_R \otimes U(1)_{B-L}$ to $U(1)_Y$ - a pair of χ_R and $\bar{\chi}_R$ fields $(1, 1, +\frac{1}{2}, -1) \oplus (1, 1, -\frac{1}{2}, +1)$. Since these components are neutral with respect to all SM charges, the position of the v_R scale does not affect the running of the “effective α_1^{-1} ” (given by the appropriate matching condition) and the only effects arise from the absence of the righthanded W -bosons at this stage. Using the $SU(2)_R$ normalization of the $U(1)_R$ charge the matching condition at V_R becomes trivial. The relevant b-coefficients of $SU(3)_c \otimes SU(2)_L$ and the matrix of anomalous dimensions of the mixed $U(1)_R \otimes U(1)_{B-L}$ couplings are $b_3 = -3$, $b_L = 1$ and

$$\begin{pmatrix} \gamma_{11} & \gamma_{12} \\ \gamma_{21} & \gamma_{22} \end{pmatrix} = \begin{pmatrix} \frac{15}{2} & -1 \\ -1 & 18 \end{pmatrix}. \quad (5.30)$$

Below the v_R scale the model is the ordinary MSSM with the b-coefficients

$$\begin{pmatrix} b_3 \\ b_L \\ b_Y \end{pmatrix} = \begin{pmatrix} -3 \\ -1 \\ \frac{33}{5} \end{pmatrix} \quad (5.31)$$

and finally, the b-coefficients for the SM stage below the M_S scale are

$$\begin{pmatrix} b_3 \\ b_L \\ b_Y \end{pmatrix} = \begin{pmatrix} -7 \\ -3 \\ \frac{21}{5} \end{pmatrix} \quad (5.32)$$

The v_R -scale matching condition reads

$$\alpha_Y^{-1}(v_R) = \frac{3}{5}\alpha_R^{-1}(v_R) + \frac{2}{5}\alpha_{(B-L)'}^{-1}(v_R).$$

Recalling that

$$\alpha_1^{-1}(M_Z) = \frac{3}{5} [1 - \sin^2\theta_W(M_Z)] \alpha^{-1}(M_Z) \quad (5.33)$$

and

$$\alpha_2^{-1}(M_Z) = \sin^2\theta_W(M_Z)\alpha^{-1}(M_Z)$$

the initial condition (for central values of the input parameters) is $\alpha_1^{-1}(M_Z) \doteq 59.38$, $\alpha_2^{-1}(M_Z) \doteq 29.93$ and $\alpha_3^{-1}(M_Z) \doteq 8.47$ [93].

Inspecting the results of the numerical analysis (Figs.5.4 and 5.5) one confirms that the v_R scale does not affect the predicted value of $\alpha_1^{-1}(M_Z)$ and remains essentially

free at one-loop level. Thus, the unification pattern is fixed entirely by the interplay of M_S and V_R . The lower bound $V_R \gtrsim 10^{14}$ GeV is consistent with the “standard” minimally fine-tuned SUSY $SO(10)$ behaviour, see for instance [69].

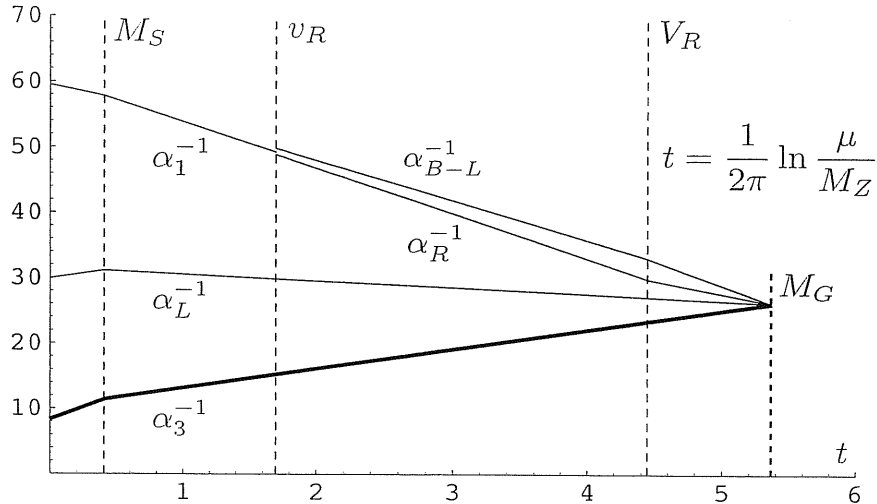


Figure 5.4: The one-loop gauge coupling unification in the model described in the text. The D-parity is broken at M_G and the intermediate scales V_R and v_R correspond to the $SU(2)_R \rightarrow U(1)_R$ and $U(1)_R \otimes U(1)_{B-L} \rightarrow U(1)_Y$ breaking respectively.

5.6.4 Other physical implications

Accommodating the option to push the $B - L$ very close to the weak scale this scheme incorporates several sources of “new physics”, in principle within the reach of the future experimental facilities, see e.g. [133] and references therein. For instance, the additional Z' boson associated with the $U(1)_{B-L}$ breaking can be light enough to affect the physics at the TeV scale and the lepton flavor violating processes like $\mu \rightarrow e\gamma$ can be enhanced substantially due to the change in running of the off-diagonal entries of the slepton SUSY-breaking terms [134]. Also the leptogenesis scenario gets changed if the right-handed neutrinos are light, see e.g. [135] and references therein. Although partially discussed in the literature [136, 137] (and references therein) these issues call for further developments.

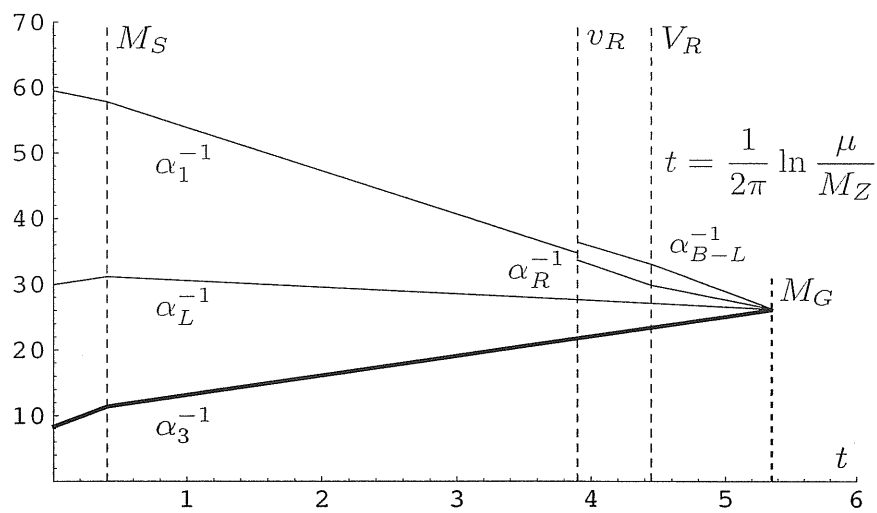


Figure 5.5: Same as in Fig. 5.4 for the case of higher v_R . As expected, the prediction for $\alpha_1^{-1}(M_Z)$ does not depend on the position of the v_R scale.

Conclusions and outlook

Looking out from the first true window to the physics beyond the Standard Model opened by the recent neutrino oscillation experiments, the idea of grand unification is recovered as a viable framework for studies of the neutrino masses and their mixing. Although the almost bimaximal mixing pattern in the leptonic sector differs drastically from what one would naively expect on the basis of quark-lepton symmetries, it emerges naturally in GUT models based on the $SO(10)$ gauge group.

The major part of this work was devoted to the analysis of quark and lepton masses and mixing in the particular case of the minimal SUSY $SO(10)$ grand unified theory in the case the $SU(2)_L$ -triplet contribution dominates the seesaw formula. At variance with existing expectations, it was shown that this framework can accommodate the physical CKM-CP phase and simultaneously account for a 90% C.L. fit of the quark and lepton mass and mixing parameters albeit showing a tension between light quark masses and the latest neutrino data. Moreover, it was argued that in such cases the Dirac CP-phase in the neutrino sector is considerably smaller than the CKM CP-phase with an upper bound of about 20° and it is not destabilized by radiative corrections. The lower bound on the 1-3 entry of the PMNS lepton mixing matrix $|U_{e3}| > 0.16$ was reexamined in detail and shown to relax to roughly $|U_{e3}| > 0.10$, that makes it still compatible with the recent data neutrino parameter extractions albeit within the experimental reach in near future. Several semianalytic relations were derived to provide for a better understanding of the results of the extensive numerical analysis. The central role of the strange quark mass was pointed out in view of the potential clash among the recently improved bounds on the solar mixing angle and the mass-squared difference ratio in the neutrino sector.

It was argued that some of the neutrino sector parameters, in particular $|U_{e3}|$ and the solar mixing angle, are also very sensitive to the subleading corrections. The perturbative effects of antisymmetric Yukawa terms, introduced by a quasidecoupled 120-dimensional Higgs representation proposed to address the tension of the minimal framework, were examined in detail. It was demonstrated that even a per-mile suppression of

such operators can not screen their effects, that in some cases can be as large as tens of percent of the unperturbed values. It was shown that also the CKM CP-phase issue finds a natural resolution in such an extended framework. On the other hand, the θ_{13} bound, though relaxed, remains incompatible with zero. This keeps the model testable in ongoing and future experimental surveys.

In the second part of the manuscript a class of $SO(10)$ models utilizing a spinorial Higgs representation was considered. It was argued that to implement the Witten's "radiative seesaw" mechanism in the class of minimal split-SUSY $SO(10)$ models while preserving a potentially realistic Yukawa structure, a 120-dimensional Higgs representation coupled to matter fermions should be considered. Finally, a SUSY $SO(10)$ realization of the so called "inverse" seesaw mechanism was studied in detail. In particular, it was shown that there exists a minimally finetuned setup in which the $B - L$ scale can be very low while keeping the gauge-coupling unification intact.

In spite of the longevity of GUTs, still much more has to be done. Concerning the minimal SUSY $SO(10)$ fits of the quark and lepton data, there is a variety of reasonably consistent numerical results obtained by different groups using different numerical methods. Therefore, a global χ^2 -fit (though rather demanding) would be highly welcome, both in the triplet and singlet dominated seesaw case as well as in general, if tractable. Meanwhile, it would be nice to understand conditions under which the triplet contribution dominates the seesaw formula. Though there are some preliminary studies [138], a decisive analysis is still missing. Last, but not least, since in some classes of models there remain only small regions in the parameter space that are still consistent with the recent neutrino mixing data, the proton lifetime can be strongly constrained in such schemes. It is also of interest to study in detail the lepton-flavor violation processes within the class of SUSY $SO(10)$ models with low $B - L$ scale as it can lead to enhancements of the off-diagonal entries in the evolution of the mSUGRA soft-SUSY breaking terms.

Acknowledgements

I wish to thank my supervisor, Stefano Bertolini from SISSA for the patience and encouragement throughout preparing this work. I am grateful to Goran Sejnanović from the International Centre for Theoretical Physics in Trieste and Borut Bajc from Josef Stefan Institute in Ljubljana for many helpful discussions and comments. I am indebted to Prof. Jose F. Valle from IFIC for hospitality during my visits to Valencia. Last, but not least, I wish to thank my family for the enormous patience and support during the hectic period of writing these thesis.

Appendix A

PMNS lepton mixing matrix

A general 3×3 unitary matrix can be written in the so-called “standard notation” as

$$U = P_L V P_R$$

where

$$V \equiv \begin{pmatrix} c_{12}c_{13} & s_{12}c_{13} & s_{13}e^{-i\delta} \\ -c_{23}s_{12} - s_{23}s_{13}c_{12}e^{i\delta} & c_{23}c_{12} - s_{23}s_{13}s_{12}e^{i\delta} & s_{23}c_{13} \\ s_{23}s_{12} - c_{23}s_{13}c_{12}e^{i\delta} & -s_{23}c_{12} - c_{23}s_{13}s_{12}e^{i\delta} & c_{23}c_{13} \end{pmatrix} \equiv U_{PMNS} \quad (\text{A.1})$$

and

$$P_L \equiv \begin{pmatrix} e^{i\delta_1} & & \\ & e^{i\delta_2} & \\ & & e^{i\delta_3} \end{pmatrix} \quad \text{and} \quad P_R \equiv \begin{pmatrix} e^{i\frac{\phi_1}{2}} & & \\ & e^{i\frac{\phi_2}{2}} & \\ & & 1 \end{pmatrix} \quad (\text{A.2})$$

are the CKM-like mixing matrix and a pair of phase matrices respectively. Applied on the Pontecorvo-Maki-Nakagawa-Sakata mixing matrix [20] parametrizing the misalignment of the charged lepton and light neutrino mass bases, the angles in U_{PMNS} become the three mixing parameters measured in the neutrino oscillation experiments.

The phases in P_L can be absorbed in the redefinition of the charged lepton fields. The δ parameter is the so-called Dirac PMNS phase parametrizing the amount of CP-violation in neutrino oscillations, in analogy with the CKM CP-phase of the quark sector. If neutrinos are Majorana particles, the phases ϕ_1 and ϕ_2 can not be rotated away and become physical quantities. Unfortunately, the neutrino oscillation data are sensitive only to the absolute values of the neutrino masses and can not be used to determine these parameters. However, ϕ_1 and ϕ_2 can be measured in the double- β decay experiments [25].

The measurements give usually only the information on the matrix elements of U . The PNMS parameters - the mixing angles and the Dirac CP-phases - can be then reconstructed as:

$$\theta_{12} = \text{Atan} \frac{|U_{11}|}{|U_{11}|}, \quad \theta_{23} = \text{Atan} \frac{|U_{23}|}{|U_{33}|}, \quad \theta_{13} = \text{Asin} |U_{13}| \quad (\text{A.3})$$

The amount of the CP violation due to the Dirac CP phase δ can be determined from the so-called Jarlskog invariant [103]

$$J \equiv \frac{1}{2} |\text{Im}(U_{11}^* U_{12} U_{21} U_{22}^*)| = \frac{1}{2} |\text{Im}(U_{11}^* U_{13} U_{31} U_{33}^*)| = \frac{1}{2} |\text{Im}(U_{22}^* U_{23} U_{32} U_{33}^*)| \quad (\text{A.4})$$

by means of the formula

$$|\sin \delta| = 2J(c_{12}c_{13}^2c_{23}s_{12}s_{13}s_{23})^{-1} \quad (\text{A.5})$$

If one is interested also in the sign of δ the relevant expression reads

$$\delta = -\text{Arg} \left(\frac{U_{ii}^* U_{ij} U_{ji} U_{jj}^*}{c_{12}c_{13}^2c_{23}s_{12}s_{13}s_{23}} + \frac{c_{12}c_{13}s_{13}}{s_{12}s_{23}} \right) \quad (\text{A.6})$$

regardless of the choice of $i \neq j$. The Majorana phases can be finally obtained from

$$\phi_1 = 2\text{Arg} e^{i\delta} U_{13} U_{11}^* \quad \text{and} \quad \phi_2 = 2\text{Arg} e^{i\delta} U_{13} U_{12}^* \quad (\text{A.7})$$

Appendix B

$SO(10)$ group theory

This appendix comments in brief on some of the salient features of $SO(10)$ and its representations that are discussed in the text. A more detailed information can be found in reviews [61, 30, 139] or on more formal grounds in any group-theory textbook.

B.1 The $SO(10)$ group

$SO(10)$ is a proper orthogonal group of rotations in a 10-dimensional vector space. Each element of $SO(10)$ must obey the following conditions

$$G^T G = 1, \quad \det G = +1 \quad (\text{B.1})$$

Concerning the generators denoted by Σ , these relations lead to

$$\Sigma^T = -\Sigma, \quad \text{Tr} \Sigma = 0 \quad (\text{B.2})$$

$$[\Sigma^{\mu\nu}, \Sigma^{\rho\sigma}] = \delta^{\nu\sigma} \Sigma^{\mu\rho} - \delta^{\nu\rho} \Sigma^{\mu\sigma} + \delta^{\mu\rho} \Sigma^{\nu\sigma} - \delta^{\mu\sigma} \Sigma^{\nu\rho} \quad (\text{B.3})$$

From here it is easy to see that $SO(10)$ is 45-dimensional. As a compact Lie group it posses finite-dimensional representations studied in the subsequent section.

B.2 The $SO(10)$ spinors

The construction of the spinorial representations of $SO(10)$ goes along the same line like for the other orthogonal groups. Recall first that for an $SO(2n)$ group with $n > 1$ there is a pair of inequivalent spinorial representations, each of dimensionality 2^{n-1} ; in case of $SO(10)$ one thus gets $16 \oplus \overline{16}$. The explicit construction utilizes five pairs of ladder operators a_i and a_i^\dagger obeying

$$\{a_i, a_j^\dagger\} = \delta_{ij}, \quad \{a_i, a_j\} = 0 \quad \text{and} \quad \{a_i^\dagger, a_j^\dagger\} = 0 \quad (\text{B.4})$$

It is easy to verify that $A_{ij} \equiv a_i^\dagger a_j$ yields $[A_{ij}, A_{kl}] = \delta_{jk} A_{il} - \delta_{il} A_{kj}$, that is nothing but the Lie algebra of $SU(5)$ [140]. Let us denote $(i, j, k, l, m \in \{1, 2, 3, 4, 5\})$:

$$\begin{aligned}
|e^{(1)}\rangle &\equiv |0\rangle \\
|e_i^{(5)}\rangle &\equiv a_i^\dagger |0\rangle \\
|e_{ij}^{(10)}\rangle &\equiv \frac{1}{2!} a_{[i}^\dagger a_{j]}^\dagger |0\rangle \\
|e^{(\overline{10})lm}\rangle &\equiv \frac{1}{3!} \varepsilon^{ijklm} a_i^\dagger a_j^\dagger a_k^\dagger |0\rangle \\
|e^{(\overline{5})m}\rangle &\equiv \frac{1}{4!} \varepsilon^{ijklm} a_i^\dagger a_j^\dagger a_k^\dagger a_l^\dagger |0\rangle \\
|e^{(\overline{1})}\rangle &\equiv \frac{1}{5!} \varepsilon^{ijklm} a_i^\dagger a_j^\dagger a_k^\dagger a_l^\dagger a_m^\dagger |0\rangle
\end{aligned} \tag{B.5}$$

Clearly, the operators A_{ij} span irreducible representations of $SU(5)$ over these 6 subspaces. Their dimensionalities are given by the corresponding superscript.

Defining $\Gamma_{2i-1} \equiv i(a_i^\dagger - a_i)$ and $\Gamma_{2i} \equiv (a_i^\dagger + a_i)$ one obtains a rank-5 Clifford algebra with positive-definite diagonal

$$\{\Gamma_\mu, \Gamma_\nu\} = \delta_{\mu\nu} 1 \tag{B.6}$$

In analogy with the Lorenz spinors the generators obeying the $SO(10)$ commutation relations (B.3) are obtained as

$$\Sigma_{\mu\nu} \equiv \frac{1}{2i} [\Gamma_\mu, \Gamma_\nu] \tag{B.7}$$

These operators act on the Hilbert space \mathcal{H} given by the direct sum of all the $SU(5)$ components (B.5). However, as a representation of $SO(10)$ this set is not irreducible. For a general $SO(2n)$ group there exists a ‘‘parity’’ transformation defined as $\Gamma_0 = i\Gamma_1\Gamma_2\dots\Gamma_{2n}$ that assigns +1 to the states with even number of a^\dagger in eq. (B.5) and -1 to those with odd number of a^\dagger . Since Γ_0 commutes with all $\Sigma_{\mu\nu}$ it defines 2 distinct invariant subspaces

$$|16\rangle \equiv |e^{(1)}\rangle \oplus |e_{ij}^{(10)}\rangle \oplus |e^{(\overline{5})m}\rangle \quad \text{and} \quad |\overline{16}\rangle \equiv |e_i^{(5)}\rangle \oplus |e^{(\overline{10})lm}\rangle \oplus |e^{(\overline{1})}\rangle \tag{B.8}$$

In a more common notation, these relations are often written as

$$16 = 1 \oplus 10 \oplus \overline{5} \quad \text{and} \quad \overline{16} = 1 \oplus \overline{10} \oplus 5 \tag{B.9}$$

that is nothing but the famous decomposition of the $SO(10)$ spinors into the $SU(5)$ scalar, vector and antisymmetric tensor hosting the SM matter multiplets.

The last object we shall need is the analogue of the charge conjugation operator of the Lorenz group. This is necessary since matter resides in an $SO(10)$ spinor with only

one chirality and thus all the bilinears must be constructed in a ‘‘Majorana fashion’’. It is easy to verify that the role of the Lorenz C matrix¹ is in case of $SO(10)$ played by

$$B \propto \Gamma_1 \Gamma_3 \Gamma_5 \Gamma_7 \Gamma_9 \quad (\text{B.10})$$

B.3 The $SO(10)$ tensors

The list of basic $SO(10)$ tensors that appear in this work is given Table B.1. However, only the vector and two antisymmetric tensors can be coupled to the matter bilinears, because there are only three objects that can be constructed within the tensor product of $16 \otimes 16$. In notation of the previous section they are

$$\langle 16 | B \Gamma_\mu | 16 \rangle, \quad \langle 16 | B \Gamma_{[\mu} \Gamma_\nu \Gamma_{\sigma]} | 16 \rangle \quad \text{and} \quad \langle 16 | B \Gamma_{[\mu} \Gamma_\nu \Gamma_\sigma \Gamma_\kappa \Gamma_{\rho]} | 16 \rangle \quad (\text{B.11})$$

They correspond to the vectorial 10, 3-index antisymmetric tensor of dimension $10!/7!3! = 120$ and a co-called self-dual part of a 5-index antisymmetric tensor² of dimension $\frac{1}{2}10!/5!^2 = 126$. Note that the 10-index fully antisymmetric tensor defines a duality map given by

$$T_{i_1 i_2 \dots i_n} \rightarrow \tilde{T}_{j_1 j_2 \dots j_k} = \frac{i^n}{n!} \varepsilon_{j_1 j_2 \dots j_k i_1 i_2 \dots i_n} T_{i_1 i_2 \dots i_n}, \quad k = 10 - n, \quad n = 1, \dots, 10 \quad (\text{B.12})$$

This map slices the 252-dimensional 5-index antisymmetric tensor into a pair of irreducible representations with opposite parities with respect to this transformation. The selfdual part usually denoted by 126 obeys $\tilde{126}_{j_1 j_2 \dots j_k} = 126_{j_1 j_2 \dots j_k}$ while the antiselfdual component called $\overline{126}$ is identified by the opposite sign, $\overline{126}_{j_1 j_2 \dots j_k} = -\overline{126}_{j_1 j_2 \dots j_k}$. The other tensors can be constructed in a standard way starting from the 10-dimensional vector.

B.3.1 $SO(10)$ tensor products

To construct the $SO(10)$ invariants one should look at the $SO(10)$ decompositions of tensor products of the irreps used as the building blocks of a model. For our purposes, the most important are [78, 61]:

$$\begin{aligned} 16 \otimes 16 &= 10 \oplus 120 \oplus 126 \\ 10 \otimes 10 &= 1 \oplus 45 \oplus 54 \\ 120 \otimes 10 &= 45 \oplus 210 \oplus \dots \end{aligned}$$

¹Recall the standard definition $C \propto \gamma_1 \gamma_3$ in the Dirac realization of the Clifford algebra generated by $SO(3, 1)$.

²The anti-selfdual tensor arises instead in case of $\overline{16} \otimes \overline{16}$.

Table B.1: The basic properties of $SO(10)$ irreducible tensors up to dimension 210.

dimension	indices	symmetries	properties
10	1	-	vector
45	2	antisymmetric	adjoint
54	2	symmetric	
120	3	antisymmetric	
126	5	antisymmetric	5-index selfdual
$\overline{126}$	5	antisymmetric	5-index antiselfdual
210	4	antisymmetric	

$$\begin{aligned}
126 \otimes 10 &= 210 \oplus \dots \\
210 \otimes 10 &= 120 \oplus 126 \oplus \overline{126} \oplus \dots \\
120 \otimes 120 &= 1 \oplus 45 \oplus 54 \oplus 210 \oplus \dots \\
126 \otimes 120 &= 45 \oplus 210 \oplus \dots \\
\overline{126} \otimes 126 &= 1 \oplus 54 \oplus \dots \\
210 \otimes 210 &= 1 \oplus 45 \oplus 54 \oplus 210 \oplus \dots
\end{aligned} \tag{B.13}$$

One can see that the pattern of contractions is such that the matter can be naturally light as there is no singlet in $16 \otimes 16$, while the Higgs multiplets, accommodated typically in 10, 45, 54, 120, $\overline{126}$ and/or 210 live naturally around the GUT-scale.

B.4 The $SO(10)$ subgroups

There are 2 physically interesting maximal subgroups of $SO(10)$. Apart of the $SU(5) \otimes U(1)$ we encountered in Appendix B.2, there is the so-called Pati-Salam subgroup $SU(4)_{PS} \otimes SU(2)_L \otimes SU(2)_R$ that can be identified in the decomposition $SO(10) \supset SO(6) \otimes SO(4)$ as $SO(6) \sim SU(4)$ and $SO(4) \sim SU(2) \otimes SU(2)$. Gauging the $SU(4)_{PS}$ subgroup, the lepton number can be interpreted as a “fourth color” [77, 19]. Apart of the $SU(3)_c$ of QCD, it contains an $U(1)$ factor that can be interpreted as $B - L$ where B and L are the baryon and lepton numbers respectively. The left-right symmetric nature and the straightforward identification of the Standard Model $SU(3)_c \otimes SU(2)_L \otimes U(1)_Y$ group in $SU(4)_{PS} \otimes SU(2)_L \otimes SU(2)_R$ makes the Pati-Salam subgroup of $SO(10)$ particularly suitable as a bookkeeping tool for the decompositions of various $SO(10)$ multiplets

B.4.1 Pati-Salam decomposition of basic $SO(10)$ irreps

The Pati-Salam decompositions of the basic $SO(10)$ multiplets are [61]³:

$$\begin{aligned}
10 &= (1, 2, 2) \oplus (6, 1, 1) \\
16 &= (4, 2, 1) \oplus (\bar{4}, 1, 2) \\
45 &= (1, 3, 1) \oplus (1, 1, 3) \oplus (15, 1, 1) \oplus (6, 2, 2) \\
54 &= (1, 1, 1) \oplus (1, 3, 3) \oplus (20', 1, 1) \oplus (6, 2, 2) \\
120 &= (1, 2, 2) \oplus (10, 1, 1) \oplus (\bar{10}, 1, 1) \oplus (6, 3, 1) \oplus (6, 1, 3) \oplus (15, 2, 2) \\
\bar{126} &= (6, 1, 1) \oplus (10, 3, 1) \oplus (\bar{10}, 1, 3) \oplus (15, 2, 2) \\
210 &= (1, 1, 1) \oplus (15, 1, 1) \oplus (6, 2, 2) \oplus (15, 3, 1) \oplus (15, 1, 3) \oplus (10, 2, 2) \oplus (\bar{10}, 2, 2)
\end{aligned} \tag{B.14}$$

From these formulae one can see for instance that the 10 in the Higgs sector can not break $SO(10)$ without simultaneous breakdown of $SU(3)_c \otimes SU(2)_L \otimes U(1)_Y$ of the Standard Model. On the other hand, this can be easily done by imposing a VEV on components of the other multiplets, for instance $(1, 1, 1)_{54}$ or $(1, 1, 1)_{210}$ leading to $SU(4)_{PS} \otimes SU(2)_L \otimes SU(2)_R$ as an intermediate symmetry, or $(15, 1, 1)_{210}$ giving rise to⁴ $SU(3)_c \otimes SU(2)_L \otimes SU(2)_R \otimes U(1)_{B-L}$. The role of the other $SU(4)$ multiplets becomes clear giving the decompositions under the $SU(3)_c \otimes SU(2)_L \otimes U(1)_Y$ of SM.

B.4.2 $SU(3)_c \otimes U(1)_{B-L}$ decompositions of basic $SU(4)$ irreps

The relevant decompositions can be easily reconstructed once the embedding of the $SU(3)_c$ triplet and singlet is identified. Indeed, since⁵ $4 = (3, +1/3) \oplus (1, -1)$ under $SU(3)_c \otimes U(1)_{B-L}$, one obtains

$$\begin{aligned}
\bar{4} &= (\bar{3}, -1/3) \oplus (1, +1) \\
6 &= (\bar{3}, +2/3) \oplus (\bar{3}, -2/3) \\
10 &= (1, +2) \oplus (3, +2/3) \oplus (6, -2/3) \\
15 &= (1, 0) \oplus (8, 0) \oplus (\bar{3}, +4/3) \oplus (\bar{3}, -4/3)
\end{aligned} \tag{B.15}$$

These relations together with (B.14) and the analog of the Gell-Mann-Nishijima relation in the left-right symmetric models

$$Q = T_L^3 + T_R^3 + \frac{1}{2}(B - L) \quad \Leftrightarrow \quad Q = T_L^3 + \frac{Y_W}{2} \quad \text{provided} \quad Y_W = 2T_R^2 + (B - L)$$

³The equivalence of the fundamental and antifundamental of $SU(2)$ is often used.

⁴Recall that 15 is the adjoint of $SU(4)$ and as such does not reduce the rank. The same holds for the triplets of the $SU(2)$ subgroups that can provide the breakdown to $U(1)$ factors.

⁵The normalization of the $U(1)_{B-L}$ generator is such that $B - L$ of a quark state is $+1/3$.

are already sufficient to identify all the $SU(3)_c \otimes SU(2)_L \otimes U(1)_Y$ quantum numbers of the states residing in the spinorial 16

$$16 = (3, 2, +1/3) \oplus (1, 2, -1) \oplus (\bar{3}, 1, -4/3) \oplus (\bar{3}, 1, +2/3) \oplus (1, 1, 0) \oplus (1, 1, +2)$$

Indeed, these are exactly the quantum numbers of $Q_L, L_L, U_L^c, D_L^c, N_L^c$ and E_L^c . Next, looking at the adjoint 15 of $SU(4)_{PS}$, one can identify the SM gluons $(8, 1, 0)_{45}$ residing in the adjoint 45 of $SO(10)$. It also becomes clear why 120 of $SO(10)$ can not be used to break the GUT-scale symmetries in a physically viable way: the only components that could at least in principle do the job are those with the $SU(3)_c \otimes SU(2)_L \otimes SU(2)_R \otimes U(1)_{B-L}$ decomposition $(1, 1, 1, \pm 2)_{120}$ residing in $(10, 1, 1)_{120} \oplus (\bar{10}, 1, 1)_{120}$ in relations (B.14). However, none of them is Y_W -neutral and thus breaks $SU(3)_c \otimes SU(2)_L \otimes U(1)_Y$ as well.

On the other hand, there are 2 different multiplets in 120 of $SO(10)$ that can receive an electroweak VEV - they are $(1, 2, 2)_{120}$ and $(15, 2, 2)_{120}$ of $SU(4)_{PS} \otimes SU(2)_L \otimes SU(2)_R$. This type of multiplets residing also in 10 and $\bar{126} \oplus 126$ of $SO(10)$ gives rise to a pair of MSSM Higgs doublets with the $SU(3)_c \otimes SU(2)_L \otimes U(1)_Y$ quantum numbers $(1, 2, \pm 1)$ that can be used to give Dirac masses to the matter fermions. It is perhaps worth pointing out that such components arise also from the $(10, 2, 2)_{210}$ and $(\bar{10}, 2, 2)_{210}$ though not in such a symmetric way as in the case of the $SU(2)_L \otimes SU(2)_R$ “bidoublets” before. Indeed, at the SM level, $(1, 2, +1)$ is contained in $(10, 2, 2)_{210}$ while $(1, 2, -1)$ resides in $(\bar{10}, 2, 2)_{210}$.

The last remark concerns the Higgs components that can generate the Majorana masses of neutrinos (at the renormalizable level). Since the lepton number of the Majorana mass terms is ± 2 , the only options are the multiplets containing 10 of the Pati-Salam $SU(4)$. As we have seen, $(10, 1, 1)_{120} \oplus (\bar{10}, 1, 1)_{120}$ can not receive large VEVs and the same holds for $(10, 2, 2)_{210} \oplus (\bar{10}, 2, 2)_{210}$ that breaks $SU(3)_c \otimes SU(2)_L \otimes U(1)_Y$ and does not couple to matter. Thus, the only option is $(10, 3, 1)_{\bar{126}} \oplus (\bar{10}, 1, 3)_{\bar{126}}$ that can couple to the matter bilinear and contains both the $SU(2)_L$ singlet and triplet representations, $(1, 1, 0)_{\bar{126}}$ and $(1, 3, 0)_{\bar{126}}$ of $SU(3)_c \otimes SU(2)_L \otimes U(1)_Y$ coming from the $(1, 3, 1, +2)_{\bar{126}}$ and $(1, 1, 3, -2)_{\bar{126}}$ components of $\bar{126}$ ⁶.

At the nonrenormalizable level, the situation changes drastically as there are many tensor products containing 10, 120 and $\bar{126}$ in the $SO(10)$ decompositions (B.13). On the other hand, if a tree-contribution is present, the higher-scale suppressed effective operators in most cases provide only for subleading corrections. Nevertheless, such effects could be important if the tree-level terms are for some reason small, c.f. section 4.

⁶with respect to $SU(3)_c \otimes SU(2)_L \otimes SU(2)_R \otimes U(1)_{B-L}$

B.5 Origin of the -3 factors of $\overline{126}_H$ doublets

There are several ways to see the emergence of the welcome “ -3 ” factor in the effective Yukawa sum-rules in SUSY $SO(10)$ with the light MSSM doublets spanned over the appropriate directions in $\overline{126}_H$. Let us present two elementary methods, the first based on the direct inspection of the relevant invariants while the other one using the transformation properties of the electroweak VEVs of $\overline{126}_H$.

B.5.1 Direct decomposition of the relevant $SO(10)$ invariants

Using the notation defined in the previous section one can attempt to fully decompose the relevant $SO(10)$ invariants, in particular the one corresponding to $16_F \overline{126}_H 16_F$. This consists in evaluating the matrix elements of all operators of the form $B \Gamma_{1,3,5} \Gamma_{2,4,6} \Gamma_7 \Gamma_8 \Gamma_{9,10}$ in the subspaces of the spinorial 16 of $SO(10)$ spanning the $\bar{5}$, 10 and 1 irreps of $SU(5) \subset SO(10)$. Recall that in the standard notation 1,..,6 are the indices of a triplet and an antitriplet of $SU(3)_c$ while 7,8,9 and 10 are those of the weak isospin doublets. The Dirac mass bilinears of the SM fermions arise from the following $SU(5)$ contractions, c.f. section 1.1.

$$\begin{aligned}
(u^c)_L^T C^{-1} u_L + h.c. &\in 10, 10 \\
(d^c)_L^T C^{-1} d_L + h.c. &\in 10, \bar{5} \\
(\nu^c)_L^T C^{-1} \nu_L + h.c. &\in 1, \bar{5} \\
(l^c)_L^T C^{-1} l_L + h.c. &\in 10, \bar{5}
\end{aligned} \tag{B.16}$$

The Clebsch-Gordon decomposition of these structures is then inferred using the ladder operator formalism given in Appendix B.2. The Hilbert space of the matter spinor 16_F is spanned by the vectors of the type

$$|\psi\rangle = |0\rangle\psi(1) + \frac{1}{2!} a_i^\dagger a_j^\dagger |0\rangle\psi(10)^{ij} + \frac{1}{4!} \varepsilon^{ijklm} a_i^\dagger a_j^\dagger a_k^\dagger a_l^\dagger |0\rangle\psi(\bar{5})_m \tag{B.17}$$

To form an $SO(10)$ covariant object using two spinors of the same “ $SO(10)$ -chirality” there is a need employ an analog of the charge-conjugation matrix (C in the Lorentz group case) and form a Majorana structure of the form $16_F^T C^{-1} B X 16_F$, where X is the tensor under consideration. In the spinorial basis the B matrix is given by eq. (B.10) and the tensors X are built from the corresponding “vector” of the Γ_μ matrices. With this information at hand one obtains

$$\begin{aligned}
16_F^T C^{-1} B X 16_F = & \tag{B.18} \\
(\psi^T(1), \psi^T(10)^{ij}, \psi^T(\bar{5})_m) C^{-1} & \begin{pmatrix} C^{(1,1)} & C_{kl}^{(1,10)} & C^{(1,\bar{5})n} \\ C_{ij}^{(10,1)} & C_{ij,kl}^{(10,10)} & C_{ij}^{(10,\bar{5})n} \\ C^{(\bar{5},1)m} & C_{kl}^{(\bar{5},10)m} & C^{(\bar{5},\bar{5})mn} \end{pmatrix} \begin{pmatrix} \psi(1) \\ \psi(10)^{kl} \\ \psi(\bar{5})_n \end{pmatrix}
\end{aligned}$$

The coefficients $C^{(X,Y)}$ are given by the scalar products (suppressing the indices of the tensor X)

$$\begin{aligned}
C^{(1,1)} &\equiv \langle e^{(1)} | BX | e^{(1)} \rangle \\
C_{kl}^{(1,10)} &\equiv \langle e^{(1)} | BX | e_{kl}^{(10)} \rangle \\
C^{(1,\bar{5})n} &\equiv \langle e^{(1)} | BX | e^{(\bar{5})n} \rangle \\
C_{ij,kl}^{(10,10)} &\equiv \langle e_{ij}^{(10)} | BX | e_{kl}^{(10)} \rangle \\
C_{ij}^{(10,\bar{5})n} &\equiv \langle e_{ij}^{(10)} | BX | e^{(\bar{5})n} \rangle \\
C^{(\bar{5},\bar{5})mn} &\equiv \langle e^{(\bar{5})m} | BX | e^{(\bar{5})n} \rangle
\end{aligned} \tag{B.19}$$

Finally, using the explicit formulae for the basis vectors spanning the $SU(5)$ components of the 16 of $SO(10)$ and B and X and anticommuting the ladder operators one can infer the structure of these coefficients. Recalling the SM structure of the $SU(5)$ matter multiplets

$$\bar{5}_i \equiv \begin{pmatrix} d_1^c \\ d_2^c \\ d_3^c \\ e^- \\ -\nu \end{pmatrix}_L \quad 10^{[ij]} \equiv \begin{pmatrix} 0 & u_3^c & -u_2^c & u^1 & d^1 \\ \cdot & 0 & u_1^c & u^2 & d^2 \\ \cdot & \cdot & 0 & u^3 & d^3 \\ \cdot & \cdot & \cdot & 0 & e^c \\ \cdot & \cdot & \cdot & \cdot & 0 \end{pmatrix}_L \quad 1 \equiv (\nu^c)_L \tag{B.20}$$

it is easy to see that the weights of the Dirac mass terms of the MSSM matter fermions are encoded to the following matrix elements:

$$\begin{aligned}
w_u &\propto C_{ij,kl}^{(10,10)} \quad \text{for } i, j, k, l \in \{1, 2, 3\} \\
w_d &\propto C_{ij}^{(10,\bar{5})n} \quad \text{for } i \in \{1, 2, 3\}, j = 5 \text{ and } n \in \{1, 2, 3\} \\
w_l &\propto C_{ij}^{(10,\bar{5})n} \quad \text{for } i = 4, j = 5 \text{ and } n = 4 \\
w_\nu &\propto C^{(1,\bar{5})n} \quad \text{for } n = 5
\end{aligned} \tag{B.21}$$

Let us present the results for the Yukawa terms generated by the VEVs of $\overline{126}_H$. In such a case $X_{rstuv}^{(\overline{126})} \propto \Gamma_r \Gamma_s \Gamma_t \Gamma_u \Gamma_v$ and the structure of the vacuum that preserves the $SU(3)_c \otimes U(1)_Q$ symmetry is given by [69, 140]

$$\begin{aligned}
\langle X_{XY789}^{(\overline{126})} \rangle &\propto v_a \quad \text{for } XY = 12, 34, 56 \\
\langle X_{XY780}^{(\overline{126})} \rangle &\propto v_b \quad \text{for } XY = 12, 34, 56
\end{aligned}$$

The VEVs of all the other (doublet) components are 0. These relations also identify the index structure of the terms of interest in relations (B.19). Omitting overall normalization, after some tedium one obtains the results given in Table B.2. From this it

is already easy to infer the relative weights of the relevant terms stemming from the $Y_{126}16_F16_F\overline{126}_H$ piece of the Yukawa superpotential

$$\mathcal{L}_Y^{\overline{126}_H} \propto Y_{126}(w_\nu^a v_a + w_\nu^b v_b)(\psi^c)_L^T C^{-1} \psi_L + h.c. + \dots \quad (\text{no sum. over } a, b) \quad (\text{B.22})$$

that finally leads to

$$\begin{aligned} \mathcal{L}_Y \propto Y_{126} & \left[-(v_a + v_b)(u^c)_L^T C^{-1} u_L - (v_a - v_b)(d^c)_L^T C^{-1} d_L + \right. \\ & \left. + 3(v_a - v_b)(l^c)_L^T C^{-1} l_L + 3(v_a + v_b)(\nu^c)_L^T C^{-1} \nu_L \right] + h.c. + \dots \end{aligned} \quad (\text{B.23})$$

Denoting $v_u^{126} \propto -(v_a + v_b)$ and $v_d^{126} \propto -(v_a - v_b)$ and working out the spinorial products one recovers the sum-rules for the effective Dirac Yukawa matrices (3.2).

In the same manner one can obtain similar results also for the 10_H and 120_H Higgs representations. It is easy to see that in the case of 10_H the 6 different lines in Table B.2 shrink into just two (there are only two directions in the Hilbert space of 10_H annihilated by all the $SU(3)_c \otimes U(1)_Q$ generators corresponding to the pair of the MSSM Higgs doublets). Thus the numbers in the last two rows become identical (in absolute value) and the relevant quark and lepton Clebsches are therefore the same, c.f. relations (3.2).

B.5.2 Pati-Salam approach

An alternative and very elegant method that can be used to infer the result of the previous section in a kind of “back of the envelope” calculation stems from the embedding of the quark and lepton states into multiplets of the Pati-Salam $SU(4)_{PS} \otimes SU(2)_L \otimes SU(2)_R$ subgroup of $SO(10)$. Each family of the quark and lepton fields forms a reducible 16-dimensional representation of this group, in the traditional notation

$$\left(\begin{array}{cccc} u_L^{(1)} & u_L^{(2)} & u_L^{(3)} & \nu_L \\ d_L^{(1)} & d_L^{(2)} & d_L^{(3)} & l_L \end{array} \right) \oplus \left(\begin{array}{cc} u_L^{c(1)} & d_L^{c(1)} \\ u_L^{c(2)} & d_L^{c(2)} \\ u_L^{c(3)} & d_L^{c(3)} \\ \nu_L^c & l_L^c \end{array} \right) \quad (\text{B.24})$$

where the first component transforms as $(4, 2, 1)$ i.e. as a fundamental representation of $SU(4)_{PS}$ and a doublet with respect to $SU(2)_L$ while the second corresponds to $(\overline{4}, 1, 2)$ and transforms as a doublet under $SU(2)_R$.

Under the same subgroup the component of $\overline{126}$ containing the electroweak doublets transforms as $(15, 2, 2)$ i.e. as an adjoint of $SU(4)_{PS}$ and a bidoublet of $SU(2)_L \otimes SU(2)_R$. The adjoint representation of an $SU(4)$ can be viewed as a set of 15 *traceless* hermitean matrices. Therefore, the vacuum preserving the $SU(3)_c$ subgroup must have

the following $SU(4)_{PS}$ structure (up to a unitary transformation)

$$\langle \Phi_{(15,2,2)} \rangle \propto \begin{pmatrix} 1 & \cdot & \cdot & \cdot \\ \cdot & 1 & \cdot & \cdot \\ \cdot & \cdot & 1 & \cdot \\ \cdot & \cdot & \cdot & -3 \end{pmatrix} \otimes \begin{pmatrix} \cdot & v_1 \\ v_2 & \cdot \end{pmatrix} \quad (\text{B.25})$$

Indeed, all the $SU(3)$ generators spanning the first three indices commute with this structure, that is (up to the $SU(2)_L \otimes SU(2)_R$ components) nothing but the third Cartan operator of $SU(4)$, the Y_{B-L} . “Sandwiching” this structure between the vectors (B.24) brings the desired -3 factor for each lepton but only 1 for each quark.

On the other hand, the structure of the VEVs in the $(1,2,2)$ representation of $SU(4)_{PS} \otimes SU(2)_L \otimes SU(2)_R$ does not contain the “adjoint” factor proportional to the $\text{diag}(1,1,1,-3)$ matrix. This is easily traced back to the singlet $SU(4)_{PS}$ structure of this component of 10_H . Thus, the breaking is “isotropic” in the space of the spinorial components of 16_F . Thus, there is no such additional factor in case of the effective Yukawa couplings descending from the 10_H multiplet.

Table B.2: The Clebsch-Gordon coefficients (up to an overall normalization) in the decomposition of the $16_F \otimes \overline{126}_H \otimes 16_F$ Yukawa vertex giving rise to different contributions to the effective Yukawa couplings of SM matter fermions (i denotes the quark color index). There are only 6 directions in the space of $\overline{126}_H$ that acquire electroweak VEVs. Since the vacuum preserves $SU(3)_c$ gauge symmetry, all the color components of the quark fields receive the same contributions. Notice the overall relative -3 factors between the contributions of $\langle \overline{126}_H \rangle$ to the quarks and leptons respectively.

$$16_F^T C^{-1} B \langle X_{AB78C} \rangle 16_F \ni (w_\psi^a v_a + w_\psi^b v_b) (\psi^c)_L^T C^{-1} \psi_L + h.c. \quad (\text{no sum. over } a, b)$$

ABC	w_u^i			w_ν	w_d^i			w_l	
	$i = 1$	$i = 2$	$i = 3$		$i = 1$	$i = 2$	$i = 3$		
$\langle X_{AB78C} \rangle \propto v_a$	129	1	-1	-1	1	1	-1	-1	1
	349	-1	1	-1	1	-1	1	-1	1
	569	-1	-1	1	1	-1	-1	1	1
$\langle X_{AB78C} \rangle \propto v_b$	120	1	-1	-1	1	-1	1	1	-1
	340	-1	1	-1	1	1	-1	1	-1
	560	-1	-1	1	1	1	1	-1	-1
Σ_a		-1	-1	-1	3	-1	-1	-1	3
Σ_b		-1	-1	-1	3	1	1	1	-3

Appendix C

Antisymmetric perturbations of symmetric matrices

C.1 Real case

Consider a real symmetric matrix S normalized so that the magnitude of its largest eigenvalue is 1. There exists an orthogonal matrix U such that $S = US^dU^T$ where S^d is diagonal. If one adds a (real) antisymmetric matrix εA with $|A_{ij}| \leq 1$ and $\varepsilon \ll 1$, a pair of orthogonal matrices can be found such that $S + \varepsilon A = V_1(\varepsilon)X^d(\varepsilon)V_2(\varepsilon)^T$. Up to $\mathcal{O}(\varepsilon^2)$ terms one gets

$$V_1(\varepsilon) = (1 + \varepsilon Z)U, \quad V_2(\varepsilon) = (1 - \varepsilon Z)U, \quad X^d(\varepsilon) = S^d, \quad (\text{C.1})$$

where the antisymmetric matrix Z satisfies

$$\{S^d, U^T Z U\} = U^T A U.$$

Denoting $U^T Z U \equiv Z'$ and $U^T A U \equiv A'$, one obtains

$$Z'_{ij} = \frac{A'_{ij}}{S^d_{ii} + S^d_{jj}}.$$

Proof: from $(S + \varepsilon A)^T = S - \varepsilon A$ we get $V_1(-\varepsilon) = V_2(\varepsilon)$ and $X^d(-\varepsilon) = X^d(\varepsilon)$ which yields $X^d(\varepsilon) = S^d + \mathcal{O}(\varepsilon^2)$. Expanding now $S + \varepsilon A = V_1(\varepsilon)X^d(\varepsilon)V_1(-\varepsilon)^T$ with the ansatz $V_1(\varepsilon) \equiv (1 + \varepsilon Z)U$ (where Z is antisymmetric by orthogonality of V_1) one obtains, to the leading order in ε , $A = \{Z, S\}$. The last step is to rewrite this relation in the diagonal basis for S .

These results allow us to estimate the form of the right-handed quark mixing matrix W (4.14) in the presence of 120_H -perturbation. The quark mass matrices in eq. (4.8)

can be written as

$$\tilde{M}_u = \frac{1}{m_t} M_u^s + \varepsilon_u Y_{120} , \quad \tilde{M}_d = \frac{1}{m_b} M_d^s + \varepsilon_d Y_{120} .$$

Here $M_{u,d}^s$ are the minimal model symmetric mass matrices, *i.e.* the pieces $Y_{10} v_{u,d}^{10} + Y_{126} v_{u,d}^{126}$ in 3.2. If the antisymmetric pieces $\varepsilon_i Y_{120}$ are very small compared to the symmetric part, the eigenvalues of $M_{u,d}^s$ coincide with those of the full $M_{u,d}$ up to $\mathcal{O}(\varepsilon^2)$ terms (while such corrections can be relevant for first generation masses they are negligible for the estimate of mixing angles). This implies, up to $\mathcal{O}(\varepsilon^2)$ terms,

$$\tilde{M}_x = U_x \tilde{D}_x U_x^T + \varepsilon_x Y_{120} = V_x^R \tilde{D}_x V_x^{L^T} ,$$

for $x = u, d$. The orthogonal matrices $V_x^{R,L}$ are given by

$$V_x^L = (1 - \varepsilon_x Z_x) U_x , \quad V_x^R = (1 + \varepsilon_x Z_x) U_x .$$

and the antisymmetric Z_x satisfy

$$\{\tilde{D}_x, U_x^T Z_x U_x\} = U_x^T Y_{120} U_x .$$

Using eq. (4.14) and $Z'_x \equiv U_x^T Z_x U_x$, one obtains

$$W = (1 - \varepsilon_u Z'_u) U_u^T U_d (1 + \varepsilon_d Z'_d) \tag{C.2}$$

and

$$V_{CKM} = (1 + \varepsilon_u Z'_u) U_u^T U_d (1 - \varepsilon_d Z'_d) \tag{C.3}$$

This proves eq. (4.14).

C.2 Complex case

If both S and A matrices defined in the previous Appendix and a small parameter ε are in general complex, there are only few changes with respect to the real case.

First, without loss of generality one can always absorb the phase of ε into the definition of A so that ε becomes real:

$$S + \varepsilon A \rightarrow S + |\varepsilon| e^{i\phi} A \equiv S + |\varepsilon| \tilde{A}$$

Next, keeping the “real parametrization” of the *unitary* matrices $V_{1,2}$ in (C.1), the Z matrix in the expansion (C.1) must be antihermitean¹ and satisfy

$$ZUS^d U^T + US^d U^T Z^* = \tilde{A}$$

¹Alternatively, using the complex form of (C.1) with $V_1(\varepsilon) = (1 + i\varepsilon Z)U$ and $V_2(\varepsilon) = (1 - i\varepsilon Z)U$ the matrix Z should be hermitean.

Defining as before $U^\dagger Z U \equiv Z'$ and $U^\dagger \tilde{A} U \equiv B$ and using the antihermiticity of Z' , one arrives to

$$Z' S^d + S^d Z'^* = B \quad (\text{C.4})$$

To solve this system of equations notice that without loss of generality one can consider S^d real absorbing all the phases in the definition of U . Under this assumption the solution reads

$$\text{Re}(Z')_{ij} = \frac{\text{Re}(B)_{ij}}{(S^d)_{ii} + (S^d)_{jj}} \quad \text{Im}(Z')_{ij} = \frac{-\text{Im}(B)_{ij}}{(S^d)_{ii} - (S^d)_{jj}} \quad (\text{C.5})$$

Finally, let us derive the form of the right-handed quark mixing matrix W in this case. Decomposing the (normalized) quark mass matrices into the symmetric and antisymmetric parts

$$\tilde{M}_u = \tilde{M}_u^s + \varepsilon_u Y_{120} \quad \text{and} \quad \tilde{M}_d = \tilde{M}_d^s + \varepsilon_d Y_{120} \quad (\text{C.6})$$

one can write

$$\tilde{M}_u = V_u^R (|\varepsilon_u|) \tilde{D}_u V_u^L (|\varepsilon_u|)^T \quad \text{and} \quad \tilde{M}_d = V_d^R (|\varepsilon_d|) \tilde{D}_d V_d^L (|\varepsilon_d|)^T \quad (\text{C.7})$$

where $\tilde{D}_{u,d}$ are by definition real diagonal matrices and

$$V_u^{L^T} V_d^{L^*} \equiv V_{CKM}^0$$

is the CKM quark mixing matrix in the “raw form”, i.e. prior rotating out the 5 unphysical phases bringing it into the “standard” form denoted by V_{CKM} . The W matrix is then defined as

$$W^T \equiv V_d^{R\dagger} V_u^R \quad (\text{C.8})$$

After some tedium one concludes

$$W^T \doteq (1 - 2|\varepsilon_d| Z'_d) V_{CKM}^0{}^T (1 + 2|\varepsilon_u| Z'_u) \quad (\text{C.9})$$

with Z'_u and Z'_d given by the solution (C.5) of the formulae of the form (C.4):

$$\begin{aligned} Z'_u \tilde{D}_u + \tilde{D}_u Z'^*{}'_u &= e^{\phi_u} V_{CKM}^0{}^* Y'_{120} V_{CKM}^0{}^\dagger \\ Z'_d \tilde{D}_d + \tilde{D}_d Z'^*{}'_d &= e^{\phi_d} Y'_{120} \end{aligned} \quad (\text{C.10})$$

provided $\varepsilon_{u,d} \equiv |\varepsilon_{u,d}| e^{i\phi_{u,d}}$ and $Y'_{120} \equiv V_d^{R\dagger} Y_{120} V_d^{L^*}$ is an antisymmetric matrix up to $\mathcal{O}(\varepsilon)$ order.

Appendix D

Illustration of effects of 120_H on the leptonic mixing

In the minimal SUSY $SO(10)$ with type-II contribution dominating the seesaw formula, the rise of the atmospheric and decrease of the solar mixings (required to get into the experimental region) is prevented by the upper bound on $\Delta m_{\odot}^2/\Delta m_A^2$. As shown in section 4.6, this problem can be avoided in scenario with an additional quasidecoupled 120_H contribution in the Yukawa sector. We give a simple analytical argument to prove that the 120_H -correction to the neutrino mass matrix, eq. (4.19), can be used to reduce the predicted value of $\Delta m_{\odot}^2/\Delta m_A^2$ substantially.

The minimal model neutrino mass matrix M'_ν in eq. (3.13) can be written schematically as

$$M'_\nu = m_0\lambda \begin{pmatrix} X\lambda^2 & Y\lambda^3 & D\lambda \\ \dots & A & C \\ \dots & \dots & B \end{pmatrix}, \quad (\text{D.1})$$

where X, Y, A, B, C, D are $\mathcal{O}(1)$ parameters. This texture generates the following neutrino spectrum hierarchy: $m_1 \div m_2 \div m_3 \sim \lambda \div \lambda \div 1$, the sign of m_2 being opposite to that of m_3 and m_1 . Assuming the setup defined by eqs. (4.26) and (4.27), we can estimate the leading contribution to $\Delta M'_\nu$ using eq. (4.19):

$$\Delta M'_\nu \approx -\frac{m_0}{k} \varepsilon_d Y_{120}^s \sim -m_0\lambda^3 \begin{pmatrix} 0 & 1 & 1 \\ \dots & 0 & -1 \\ \dots & \dots & 0 \end{pmatrix}.$$

The three independent quantities $\text{Tr}M$, $\text{Tr}M^2$ and $\det M$ characterize completely the spectrum of a generic 3×3 real symmetric matrix M . Using the parametrization (D.1) one obtains

$$\text{Tr}M'_\nu = m_0\lambda[A + B + X\lambda^2],$$

$$\begin{aligned}
\text{Tr}(M'_\nu)^2 &= m_0^2 \lambda^2 [A^2 + B^2 + 2C^2 + 2D^2 \lambda^2 + X^2 \lambda^4 + 2Y^2 \lambda^6] , \\
\det M'_\nu &= m_0^3 \lambda^3 [XAB\lambda^2 - AD^2\lambda^2 - C^2X\lambda^2 + 2DCY\lambda^4 - BY^2\lambda^6] . \quad (\text{D.2})
\end{aligned}$$

The addition of $\Delta M'_\nu$ corresponds to

$$\begin{aligned}
Y &\rightarrow Y - \mathcal{O}(\lambda^{-1}) \\
D &\rightarrow D - \mathcal{O}(\lambda) \\
C &\rightarrow C + \mathcal{O}(\lambda^2)
\end{aligned} \quad (\text{D.3})$$

so that

$$\begin{aligned}
\delta \text{Tr} M'_\nu &= 0 , \\
\delta \text{Tr} (M'_\nu)^2 &\approx m_0^2 \lambda^2 (4C\lambda^2) < 0 , \\
\delta \det M'_\nu &\approx m_0^3 \lambda^3 \cdot 2D\lambda^3 (A - C) > 0 .
\end{aligned} \quad (\text{D.4})$$

Translated into relations for the eigenvalues this yields

$$\begin{aligned}
\delta(m_1 + m_2 + m_3) &= 0 \\
\delta(m_1^2 + m_2^2 + m_3^2) &\sim -m_0^2 \lambda^4 \\
\delta(m_1 m_2 m_3) &\sim m_0^3 \lambda^6
\end{aligned} \quad (\text{D.5})$$

Writing the neutrino masses m_i as the sum of the minimal model value m_i^0 plus the 120_H -correction δ_i , one obtains

$$\begin{aligned}
\delta_3(m_3^0 - m_1^0) + \delta_2(m_2^0 - m_1^0) &\sim -m_0^2 \lambda^4 , \\
\delta_3 m_2^0 (m_1^0 - m_3^0) + \delta_2 m_3^0 (m_1^0 - m_2^0) &\sim +m_0^3 \lambda^6 .
\end{aligned}$$

which after some algebra yields $\delta_2/m_2^0 \sim -\lambda$ and $\delta_3/m_3^0 \sim -\lambda^2$. The ratio of mass squared differences is then shifted as follows:

$$\frac{\Delta m_{\odot}^2}{\Delta m_A^2} \rightarrow \frac{\Delta m_{\odot}^2}{\Delta m_A^2} \left[1 + 2 \frac{\delta_2}{m_2^0} + \dots \right] . \quad (\text{D.6})$$

Therefore the predicted value of $\Delta m_{\odot}^2/\Delta m_A^2$ is reduced with respect to the minimal model by a factor $\sim (1 - 2\lambda)$.

Bibliography

- [1] S. L. Glashow, Nucl. Phys. **22**, 579 (1961).
- [2] A. Salam and J. C. Ward, Phys. Lett. **13**, 168 (1964).
- [3] S. Weinberg, Phys. Rev. Lett. **19**, 1264 (1967).
- [4] S. Weinberg, Eur. Phys. J. **C34**, 5 (2004), hep-ph/0401010.
- [5] E598, J. J. Aubert *et al.*, Phys. Rev. Lett. **33**, 1404 (1974).
- [6] SLAC-SP-017, J. E. Augustin *et al.*, Phys. Rev. Lett. **33**, 1406 (1974).
- [7] Gargamelle Neutrino, F. J. Hasert *et al.*, Phys. Lett. **B46**, 138 (1973).
- [8] B. Aubert *et al.*, Phys. Rev. Lett. **32**, 1454 (1974).
- [9] C. Y. Prescott *et al.*, Phys. Lett. **B77**, 347 (1978).
- [10] UA1, G. Arnison *et al.*, Phys. Lett. **B122**, 103 (1983).
- [11] UA2, M. Banner *et al.*, Phys. Lett. **B122**, 476 (1983).
- [12] G. Altarelli and M. W. Grunewald, Phys. Rept. **403-404**, 189 (2004), hep-ph/0404165.
- [13] LEP, L. Collaboration], (2003), hep-ex/0312023.
- [14] CDF, V. M. Abazov *et al.*, Phys. Rev. **D70**, 092008 (2004), hep-ex/0311039.
- [15] S. W. Herb *et al.*, Phys. Rev. Lett. **39**, 252 (1977).
- [16] CDF, F. Abe *et al.*, Phys. Rev. Lett. **74**, 2626 (1995), hep-ex/9503002.
- [17] D0, S. Abachi *et al.*, Phys. Rev. Lett. **74**, 2632 (1995), hep-ex/9503003.
- [18] R. P. Feynman and M. Gell-Mann, Phys. Rev. **109**, 193 (1958).

- [19] R. N. Mohapatra, Berlin, Germany: Springer (1986) 309 P. (Contemporary Physics).
- [20] S. M. Bilenky, (1999), hep-ph/9908335.
- [21] Super-Kamiokande, S. Fukuda *et al.*, Phys. Lett. **B539**, 179 (2002), hep-ex/0205075.
- [22] Super-Kamiokande, S. Fukuda *et al.*, Phys. Rev. Lett. **86**, 5651 (2001), hep-ex/0103032.
- [23] Super-Kamiokande, T. Toshito, (2001), hep-ex/0105023.
- [24] A. Strumia and F. Vissani, (2005), hep-ph/0503246.
- [25] H. V. Klapdor-Kleingrothaus, I. V. Krivosheina, A. Dietz, and O. Chkvorets, Phys. Lett. **B586**, 198 (2004), hep-ph/0404088.
- [26] L. Girardello and M. T. Grisaru, Nucl. Phys. **B194**, 65 (1982).
- [27] H. P. Nilles, Phys. Rept. **110**, 1 (1984).
- [28] J. Wess, Lectures given at Bonn Summer School, Int. Summer Inst. for Theoretical Physics, Jul 29 - Aug 9, 1974.
- [29] P. C. West, Singapore, Singapore: World Scientific (1986) 289p.
- [30] P. Langacker, Phys. Rept. **72**, 185 (1981).
- [31] T. Yanagida, Prog. Theor. Phys. **64**, 1103 (1980).
- [32] Z. G. Berezhiani, Phys. Lett. **B129**, 99 (1983).
- [33] A. Pomarol and D. Tommasini, Nucl. Phys. **B466**, 3 (1996), hep-ph/9507462.
- [34] C. S. Aulakh, B. Bajc, A. Melfo, G. Senjanovic, and F. Vissani, Phys. Lett. **B588**, 196 (2004), hep-ph/0306242.
- [35] B. Brahmachari and R. N. Mohapatra, Phys. Rev. **D58**, 015001 (1998), hep-ph/9710371.
- [36] K.-y. Oda, E. Takasugi, M. Tanaka, and M. Yoshimura, Phys. Rev. **D59**, 055001 (1999), hep-ph/9808241.
- [37] K. Matsuda, Y. Koide, and T. Fukuyama, Phys. Rev. **D64**, 053015 (2001), hep-ph/0010026.

- [38] K. Matsuda, Y. Koide, T. Fukuyama, and H. Nishiura, Phys. Rev. **D65**, 033008 (2002), hep-ph/0108202.
- [39] B. Bajc, G. Senjanovic, and F. Vissani, Phys. Rev. Lett. **90**, 051802 (2003), hep-ph/0210207.
- [40] H. S. Goh, R. N. Mohapatra, and S.-P. Ng, Phys. Lett. **B570**, 215 (2003), hep-ph/0303055.
- [41] H. S. Goh, R. N. Mohapatra, and S.-P. Ng, Phys. Rev. **D68**, 115008 (2003), hep-ph/0308197.
- [42] E. Witten, Phys. Lett. **B91**, 81 (1980).
- [43] B. Bajc and G. Senjanovic, Phys. Lett. **B610**, 80 (2005), hep-ph/0411193.
- [44] S. Bertolini, M. Frigerio, and M. Malinsky, Phys. Rev. **D70**, 095002 (2004), hep-ph/0406117.
- [45] S. Bertolini and M. Malinsky, (2005), hep-ph/0504241; to appear on Phys. Rev. D.
- [46] H. Georgi and S. L. Glashow, Phys. Rev. Lett. **32**, 438 (1974).
- [47] S. Dimopoulos and H. Georgi, Nucl. Phys. **B193**, 150 (1981).
- [48] N. Sakai, Zeit. Phys. **C11**, 153 (1981).
- [49] J. Hisano, T. Moroi, K. Tobe, and T. Yanagida, Phys. Lett. **B342**, 138 (1995), hep-ph/9406417.
- [50] M. T. Grisaru, W. Siegel, and M. Rocek, Nucl. Phys. **B159**, 429 (1979).
- [51] J. Banks and H. Georgi, Phys. Rev. **D14**, 1159 (1976).
- [52] J. Hisano, H. Murayama, and T. Yanagida, Nucl. Phys. **B402**, 46 (1993), hep-ph/9207279.
- [53] S. Wiesenfeldt, *Proton decay in supersymmetric grand unified theories*, PhD thesis, Universität Hamburg, 2004, DESY-THESIS-2004-009.
- [54] T. Goto and T. Nihei, Phys. Rev. **D59**, 115009 (1999), hep-ph/9808255.
- [55] Super-Kamiokande, K. S. Ganezer, Prepared for 26th International Cosmic Ray Conference (ICRC 99), Salt Lake City, Utah, 17-25 Aug 1999.

- [56] Y. Suzuki, M. Nakahata, I. Y., M. Shiozawa, and Y. Obayashi, Prepared for 4th Workshop on Neutrino Oscillations and their Origin (NOON2003), Kanazawa, Japan. 10-14 Feb 2003.
- [57] H. Murayama and A. Pierce, Phys. Rev. **D65**, 055009 (2002), hep-ph/0108104.
- [58] B. Bajc, P. Fileviez Perez, and G. Senjanovic, Phys. Rev. **D66**, 075005 (2002), hep-ph/0204311.
- [59] B. Bajc, P. Fileviez Perez, and G. Senjanovic, (2002), hep-ph/0210374.
- [60] D. Emmanuel-Costa and S. Wiesenfeldt, Nucl. Phys. **B661**, 62 (2003), hep-ph/0302272.
- [61] R. Slansky, Phys. Rept. **79**, 1 (1981).
- [62] C. S. Aulakh, B. Bajc, A. Melfo, A. Rasin, and G. Senjanovic, Nucl. Phys. **B597**, 89 (2001), hep-ph/0004031.
- [63] R. N. Mohapatra, (1993), hep-ph/9310265.
- [64] T. Fukuyama, A. Ilakovac, T. Kikuchi, S. Meljanac, and N. Okada, JHEP **09**, 052 (2004), hep-ph/0406068.
- [65] T. Fukuyama, A. Ilakovac, T. Kikuchi, S. Meljanac, and N. Okada, Eur. Phys. J. **C42**, 191 (2005), hep-ph/0401213.
- [66] B. Dutta, Y. Mimura, and R. N. Mohapatra, Phys. Rev. Lett. **94**, 091804 (2005), hep-ph/0412105.
- [67] T. E. Clark, T. K. Kuo, and N. Nakagawa, Phys. Lett. **B115**, 26 (1982).
- [68] C. S. Aulakh and R. N. Mohapatra, Phys. Rev. **D28**, 217 (1983).
- [69] B. Bajc, A. Melfo, G. Senjanovic, and F. Vissani, Phys. Rev. **D70**, 035007 (2004), hep-ph/0402122.
- [70] K. S. Babu and C. Macesanu, (2005), hep-ph/0505200.
- [71] H. S. Goh, R. N. Mohapatra, and S. Nasri, Phys. Rev. **D70**, 075022 (2004), hep-ph/0408139.
- [72] B. Bajc, G. Senjanovic, and F. Vissani, Phys. Rev. **D70**, 093002 (2004), hep-ph/0402140.

- [73] B. Dutta, Y. Mimura, and R. N. Mohapatra, Phys. Rev. **D69**, 115014 (2004), hep-ph/0402113.
- [74] B. Dutta, Y. Mimura, and R. N. Mohapatra, Phys. Lett. **B603**, 35 (2004), hep-ph/0406262.
- [75] E. Ma and U. Sarkar, Phys. Rev. Lett. **80**, 5716 (1998), hep-ph/9802445.
- [76] T. Hambye and G. Senjanovic, Phys. Lett. **B582**, 73 (2004), hep-ph/0307237.
- [77] J. C. Pati and A. Salam, Phys. Rev. **D10**, 275 (1974).
- [78] M. Gell-Mann, P. Ramond, and R. Slansky, Print-80-0576 (CERN).
- [79] S. L. Glashow, Based on lectures given at Cargese Summer Inst., Cargese, France, Jul 9-29, 1979.
- [80] R. N. Mohapatra and G. Senjanovic, Phys. Rev. Lett. **44**, 912 (1980).
- [81] T. Yanagida, In Proceedings of the Workshop on the Baryon Number of the Universe and Unified Theories, Tsukuba, Japan, 13-14 Feb 1979.
- [82] G. Lazarides, Q. Shafi, and C. Wetterich, Nucl. Phys. **B181**, 287 (1981).
- [83] R. N. Mohapatra and G. Senjanovic, Phys. Rev. **D23**, 165 (1981).
- [84] J. Schechter and J. W. F. Valle, Phys. Rev. **D22**, 2227 (1980).
- [85] M. Frigerio and A. Y. Smirnov, Nucl. Phys. **B640**, 233 (2002), hep-ph/0202247.
- [86] J. A. Casas, J. R. Espinosa, A. Ibarra, and I. Navarro, Nucl. Phys. **B573**, 652 (2000), hep-ph/9910420.
- [87] M. Frigerio and A. Y. Smirnov, JHEP **02**, 004 (2003), hep-ph/0212263.
- [88] S. Antusch, J. Kersten, M. Lindner, and M. Ratz, Nucl. Phys. **B674**, 401 (2003), hep-ph/0305273.
- [89] H. Arason *et al.*, Phys. Rev. **D46**, 3945 (1992).
- [90] H. Fusaoka and Y. Koide, Phys. Rev. **D57**, 3986 (1998), hep-ph/9712201.
- [91] Y. Koide and H. Fusaoka, Phys. Rev. **D64**, 053014 (2001), hep-ph/0011070.
- [92] C. R. Das and M. K. Parida, Eur. Phys. J. **C20**, 121 (2001), hep-ph/0010004.
- [93] Particle Data Group, S. Eidelman *et al.*, Phys. Lett. **B592**, 1 (2004).

- [94] S. Weinberg, Trans. New York Acad. Sci. **38**, 185 (1977).
- [95] D. B. Kaplan and A. V. Manohar, Phys. Rev. Lett. **56**, 2004 (1986).
- [96] H. Leutwyler, Phys. Lett. **B374**, 163 (1996), hep-ph/9601234.
- [97] CP-PACS, A. Ali Khan *et al.*, Phys. Rev. Lett. **85**, 4674 (2000), hep-lat/0004010.
- [98] QCDSF, D. Pleiter, Nucl. Phys. Proc. Suppl. **94**, 265 (2001), hep-lat/0010063.
- [99] Particle Data Group, K. Hagiwara *et al.*, Phys. Rev. **D66**, 010001 (2002).
- [100] SUPER-KAMIOKANDE, T. Nakaya, eConf **C020620**, SAAT01 (2002), hep-ex/0209036.
- [101] KamLAND, K. Eguchi *et al.*, Phys. Rev. Lett. **90**, 021802 (2003), hep-ex/0212021.
- [102] SNO, S. N. Ahmed *et al.*, Phys. Rev. Lett. **92**, 181301 (2004), nucl-ex/0309004.
- [103] C. Jarlskog, Phys. Rev. Lett. **55**, 1039 (1985).
- [104] S. Antusch, J. Kersten, M. Lindner, M. Ratz, and M. A. Schmidt, JHEP **03**, 024 (2005), hep-ph/0501272.
- [105] V. Barger *et al.*, NUMI-799 .
- [106] F. Wilczek and A. Zee, Phys. Rev. **D25**, 553 (1982).
- [107] F. del Aguila and L. E. Ibanez, Nucl. Phys. **B177**, 60 (1981).
- [108] H. Georgi, Nucl. Phys. **B156**, 126 (1979).
- [109] R. Barbieri, D. V. Nanopoulos, G. Morchio, and F. Strocchi, Phys. Lett. **B90**, 91 (1980).
- [110] A. Masiero, S. K. Vempati, and O. Vives, Nucl. Phys. **B649**, 189 (2003), hep-ph/0209303.
- [111] D. Bailin, A. Love, and S. Thomas, Phys. Lett. **B176**, 81 (1986).
- [112] J. C. Pati, (1996), hep-ph/9611371.
- [113] R. N. Mohapatra, M. K. Parida, and G. Rajasekaran, Phys. Rev. **D72**, 013002 (2005), hep-ph/0504236.
- [114] N. Arkani-Hamed and S. Dimopoulos, JHEP **06**, 073 (2005), hep-th/0405159.

- [115] N. Arkani-Hamed, S. Dimopoulos, G. F. Giudice, and A. Romanino, Nucl. Phys. **B709**, 3 (2005), hep-ph/0409232.
- [116] R. N. Mohapatra and J. W. F. Valle, Phys. Rev. **D34**, 1642 (1986).
- [117] R. N. Mohapatra, Phys. Rev. Lett. **56**, 561 (1986).
- [118] S. M. Barr, Phys. Rev. Lett. **92**, 101601 (2004), hep-ph/0309152.
- [119] J. Bernabeu, A. Santamaria, J. Vidal, A. Mendez, and J. W. F. Valle, Phys. Lett. **B187**, 303 (1987).
- [120] A. Ilakovac and A. Pilaftsis, Nucl. Phys. **B437**, 491 (1995), hep-ph/9403398.
- [121] G. 't Hooft, Lecture given at Cargese Summer Inst., Cargese, France, Aug 26 - Sep 8, 1979.
- [122] M. Malinsky, J. C. Romao, and J. W. F. Valle. (2005), hep-ph/0506296; to appear on Phys. Rev. Lett.
- [123] M. Maltoni, T. Schwetz, M. A. Tortola, and J. W. F. Valle, New J. Phys. **6**, 122 (2004), hep-ph/0405172.
- [124] C. S. Aulakh, B. Bajc, A. Melfo, A. Rasin, and G. Senjanovic, Phys. Lett. **B460**, 325 (1999), hep-ph/9904352.
- [125] D. Wyler and L. Wolfenstein, Nucl. Phys. **B218**, 205 (1983).
- [126] E. Akhmedov, M. Lindner, E. Schnapka, and J. W. F. Valle, Phys. Rev. **D53**, 2752 (1996), hep-ph/9509255.
- [127] N. G. Deshpande, E. Keith, and T. G. Rizzo, Phys. Rev. Lett. **70**, 3189 (1993), hep-ph/9211310.
- [128] R. N. Mohapatra and G. Senjanovic, Phys. Rev. **D27**, 1601 (1983).
- [129] D. Chang and A. Kumar, Phys. Rev. **D33**, 2695 (1986).
- [130] X. G. He and S. Meljanac, Phys. Rev. **D40**, 2098 (1989).
- [131] X. G. He and S. Meljanac, Phys. Rev. **D41**, 1620 (1990).
- [132] F. del Aguila, G. D. Coughlan, and M. Quiros, Nucl. Phys. **B307**, 633 (1988).
- [133] S. F. King and T. Yanagida, (2004), hep-ph/0411030.

- [134] F. Deppisch and J. W. F. Valle, Phys. Rev. **D72**, 036001 (2005), hep-ph/0406040.
- [135] L. Boubekur, T. Hambye, and G. Senjanovic, Phys. Rev. Lett. **93**, 111601 (2004), hep-ph/0404038.
- [136] E. J. Chun, (2005), hep-ph/0508050.
- [137] N. Sahu and U. A. Yajnik, Phys. Rev. **D71**, 023507 (2005), hep-ph/0410075.
- [138] C. S. Aulakh, (2005), hep-ph/0506291.
- [139] W. Greiner and B. Muller, Berlin, Germany: Springer (1989) 368 p.
- [140] R. N. Mohapatra and B. Sakita, Phys. Rev. **D21**, 1062 (1980).